Manufacturing and assessment of osteogenically enhanced hydroxyapatite/ calcium carbonate bone scaffolds

Emma Steijvers

Submitted to Swansea University in fulfilment of the requirements for the Degree of Master of Science

2023

Abstract

Bone grafts are essential for repairing large bone defects, but natural sources are scarce and alternatives are needed. Hydroxyapatite/calcium carbonate scaffolds are osteocompatible and resorbable and thus suitable for bone grafts, but lack the growth factors and related osteogenicity present in natural grafts. This study aimed to enhance the osteogenic capacity of these bone scaffolds through two methods: 1) culturing and osteogenically differentiating mesenchymal stem cells onto the scaffolds in vitro so that they generate and deposit growth factors, and adding retinoic acid to increase cell differentiation and bone morphogenic protein expression, and 2) adding bisphosphonates, anti-osteoporotic medication, to the scaffolds to inhibit bone resorption and maximize the initial bone growth. Cell growth on scaffolds in vitro was analysed using fluorescence and scanning electron microscopy and metabolic assays, and growth factors were quantified using ELISA. The results indicate that MSCs grow and deposit BMPs onto the scaffolds. Osteogenic differentiation increased the amount after 14, but not 7 or 21 days of culture, while the addition of RA is detrimental to growth factor production. The effect of bisphosphonates was determined by implanting scaffolds treated with OX-14 and Zoledronate in vivo in mice, then quantifying the bone growth through µCT scanning and the gene expression using qPCR. The addition of Zoledronate, but not OX-14, increased the bone callus size at all time points. In conclusion, both approaches are promising methods to improve bone scaffold osteogenicity. Culturing cells onto scaffolds can be done to add growth factors to them, though future research should aim to increase the amount deposited. The addition of Zoledronate increases bone callus size, and future research should determine the effectiveness of this approach in critical-sized bone defects.

Declaration

This work has not previously been accepted in substance for any degree and is not being concurrently submitted in candidature for any degree.

[redacted] _____ (candidate)

Date March 25th, 2023

STATEMENT 1

This thesis is the result of my own investigations, except where otherwise stated. Where correction services have been used, the extent and nature of the correction is clearly marked in a footnote(s).

Other sources are acknowledged by footnotes giving explicit references. A bibliography is appended.

[redacted] _____ (candidate)

Date March 25th, 2023

STATEMENT 2

I hereby give consent for my thesis, if accepted, to be available for photocopying and for inter-library loan, and for the title and summary to be made available to outside organisations.

[redacted] _____ (candidate)

Date March 25th, 2023

Table of contents

List of figures

List of abbreviations

Abbreviation	Full name
3D	Three-dimensional
ALP	alkaline phosphatase
ANOVA	Analysis of variance
BMP	Bone morphogenic protein
BV/TV	Bone volume / tissue volume
CC	Calcium carbonate
CCR-2	C-C chemokine receptor type 2
CD	Cluster of differentiation
Col1a1	Collagen type 1 alpha 1
CSK	C-terminal Src kinase
DBM	Demineralized bone matrix
DCC	Deleted in colorectal cancer
DNA	Deoxyribonucleic acid
EDX	Energy dispersive X-ray analysis
ELISA	Enzyme-linked immunoassay
FTIR	Fourier transform infra-red
HA	Hydroxyapatite
IGF-1	Insulin-like growth factor 1
M-CSF	Macrophage colony-stimulating factor
M-CSFR	Macrophage colony-stimulating factor receptor
ND	Not differentiated
OCN	Osteocalcin
OCSTAMP	Osteoclast Stimulatory Transmembrane Protein
OS	Osteogenically differentiated
OSTM-1	Osteopetrosis-associated transmembrane protein 1
OSX	Osterix
PBS	Phosphate buffered saline
PDGF-BB	Platelet-derived growth factor BB
PGA	Polyglycolic acid
PGP9.5	Ubiquitin C-Terminal Hydrolase L1
PLA	Polylactic acid
qPCR	Quantitative real-time polymerase chain reaction
RA	Retinoic acid
RANK	Receptor activator of nuclear factor κ B
RANKL	Receptor activator of nuclear factor kappa-B ligand
RNA	Ribonucleic acid
RunX2	Runt-related transcription factor 2
SDF-1	Stromal cell-derived factor 1
SEM	Scanning electron microscopy
TGF-β1	Transforming growth factor beta 1
TTCP	Tetracalcium phosphate
ZOL	Zoledronate

Acknowledgements

First and foremost I'd like to thank my primary supervisor, Dr Zhidao Xia, for his guidance and support throughout this project, and for going above and beyond in providing many more opportunities over the course of this degree.

I'd also like to thank my other supervisors, Davide Deganello and Ilyas Khan, for their contributions to our research, as well as Dr Xu Cao for generously providing lab space and mice for the in vivo experiments. I would also like to acknowledge the Royal Society, whose financial contribution facilitated the in vivo experiments.

Additionally, I am very grateful to my colleagues, in particular Hong Lu, for teaching me everything I needed to know to carry out the experiments and for always being willing to help. I am also thankful towards Armaan Ghei and Zhidao Xia for the collaboration in co-authoring our review paper that has been tremendously helpful in the writing of this thesis.

Finally, I want to express my appreciation for my parents and sister because they have endlessly supported me in so many ways over these past years.

Once again, thank you to everyone who has contributed to this work in one way or another. Your support and guidance have been invaluable.

1. Introduction

Bone defects can have many causes, including fractures, cancer, and obesity- and age-related stresses. Severe bone damage may be irreparable by natural processes alone(Dimitriou et al., 2011). In these cases, bone grafts are required for proper healing. The demand for bone grafts is expected to keep rising in future because of the increase in the geriatric population(Brydone et al., 2010).

The current gold standard for bone transplantation is autografts, for which bone is taken from the patient and re-implanted at the trauma site. Taking bone directly from the patient has great advantages: it provides a mechanically-matched scaffold with osteogenic cells that can help grow new bone, is full of growth factors and other signalling molecules, and is fully biocompatible, osteoconductive(Daniel et al., 2019) and osteoinductive(T & C, 2001). Osteoconductivity is bone formation along the surface of an implanted bone graft scaffold by bone-forming cells, specifically osteoblasts and their progenitors, that migrate from nearby bone tissue, whereas osteoinductivity is bone formation through the recruitment and stimulation of immature cells(Weber, 2019). Despite this, autografts have significant drawbacks. Because the bone is taken from the patient, only a limited quantity is available, which may not be enough to fill the defect. It also adds an extra surgical site, and patients are likely to suffer from severe pain(Qi et al., 2014), increased recovery time, and donor site morbidity(Matsuura et al., 2019). One study found that 20% of patients were left with chronic pain at the donor site(Friedlaender et al., 2001a).

Different bone graft substitutes have been developed to replace autografts. Allografts, bone taken from living human or cadaveric donors, are a widely used alternative(Lomas et al., 2013). Being derived from human bone, they are highly osteoconductive as well as biocompatible and osteoinductive(Brink, 2021). Unlike autografts, however, allografts are freeze-dried, decellularised and sterilised to reduce the risk of rejection and infection, respectively. These procedures remove cells, proteins, and potentially even collagen, lowering the bone-forming ability of the allograft(Brink, 2021; Dimitriou et al., 2011). Thus, some vital growth factors are removed, resulting in little to no osteoinductivity. The mechanical strength of bone

allografts is also reduced, and their bone integration is slower than that of bone autografts. Allografts have success rates similar to autografts(McNamara, 2010) but occasionally fail, usually at the allograft–host junction point. New bone formation does not extend into the allograft very well, usually less than 5 mm even in the second year after implantation(Enneking & Campanacci, 2001). There are also still other drawbacks, such as the risk of rejection and disease transmission(Conrad et al., 1995; Simonds et al., 1992). Additionally, while much more abundant than autografts, the supply remains limited(Campana et al., 2014; Steijvers et al., 2022).

Demineralized bone matrix (DBM) is a subset of allograft, essentially consisting of allografts that have been demineralized in addition to the normal decellularisation and sterilisation process. Having lost their calcium matrix, DBM scaffolds consist primarily of collagen, proteins and growth factors(Gruskin et al., 2012; Servin-Trujillo et al., 2011). As an allograft-derived product, it carries identical risks and is subject to the same scarcity concerns.

Xenografts are produced from animal bones and carry similar risks to allografts, with the extra risk of animal-borne diseases. Commercial xenografts are commonly subjected to sterilisation by heat treatment(Perić Kačarević et al., 2018) because of the prion risk. Bio-Oss™ xenografts are treated at a relatively low 300°C, while Cerabone® products are calcinated at temperatures of up to 1,250°C. Both treatments damage bone constituents, harm osteoinductivity, and change the scaffold structure by increasing the hydroxyapatite (HA) crystal size(Perić Kačarević et al., 2018). The severe heat treatment of Cerabone® destroys all organic compounds and even partially degrades HA into other compounds(Herliansyah et al., 2009). Some research has shown that xenografts perform poorly, finding evidence of graft loosening and a lack of incorporation(Charalambides et al., 2005). These results are controversial, as other researchers have found good results with xenografts(Savolainen et al., 1994; Siqueira & Kranzler, 1982). In practice, however, xenografts are rarely used(Campana et al., 2014).

1.1 Artificial bone grafts

These issues create a demand for other alternatives, and artificial grafts could be the

solution. Many materials have already been clinically used in bone grafts, each with advantages and disadvantages. Autografts and allografts are both osteoconductive and osteoinductive. An artificial graft should aim to mimic both of these properties to achieve the best results. As scaffolds are intended as a bone replacement, it makes sense to mimic natural bone as much as possible in terms of hardness, structure, and compounds. The hardness of scaffolds is very important for their functioning. Bones have a structural function in the body, and soft or injectable scaffolds may not be able to bear the loads required. Conversely, a high rigidity is also undesired as bone actively responds to mechanical stimulation and can become weak and brittle when over-supported(Niinomi et al., 2016). Thus, the stiffness of a scaffold should approach that of natural bone, which has a young's modulus of 10-30 GPa(Niinomi et al., 2016).

Another highly desired quality of scaffolds is resorbability, the ability to biodegrade in order to be replaced by natural bone. A low biodegradation rate is suboptimal, since the scaffold should ideally be broken down and replaced by natural bone to avoid unexpected risks such as infection leading to biofilm formation(Westas et al., 2014) or scaffolds weakening the surrounding bone(Niinomi et al., 2016). However, rapid biodegradation is also undesirable as new bone growth may not be able to keep up, leaving open areas and lowering the mechanical strength of the scaffold. This is especially important due to the supportive functions of the skeleton.

Material requirements for bone scaffolds are often somewhat paradoxical. It is advantageous for materials to be strong in order to provide mechanical support, but the scaffold also has to be porous and resorbable, both of which lower the strength of the scaffold, and neither can it be too rigid, as it may then weaken the bone. Because of this, single materials are rarely the most suitable option available. Instead, composite materials allow for the fine-tuning of properties required to optimize bone grafts(Koons et al., 2020).

Many types of materials are available on the market, each with advantages and disadvantages. Table 1 details a number of common materials and their advantages and disadvantages. Metals, particularly titanium, are a common material for bone

implants and scaffolds. Titanium is used extensively in bone surgery due to its light weight, high mechanical strength and biocompatible properties(Takizawa et al., 2018), but it is not a suitable material for bone scaffolds. The material is very rigid, has a high mechanical strength, and is completely non-resorbable. In addition, unlike screws and plates scaffolds cannot be removed post-implantation. The combination of these traits can be problematic (Niinomi et al., 2016) because bone requires mechanical stimulation to grow, and over-support will weaken the surrounding bone. Other metals, such as iron, magnesium and zinc, are gaining popularity due to their resorbability(Ray et al., 2018) and osteogenic properties(Li et al., 2008; Moonga & Dempster, 2009). Furthermore, metals are increasingly used in alloyed forms to balance properties such as mechanical strength, osteogenicity and resorbability (Jia et al., 2022)(Takizawa et al., 2018). While immensely useful, the alloying of metals can cause unforeseen problems as well. As an example, the combination of Co/Cr/Ti nanoparticles released by metal hip implants was proven to be more cytotoxic than nanoparticles from either of the metals alone(Liu et al., 2023). The inclusion of non-metal compounds for scaffold enhancement is rare, as the high temperatures required for metal scaffold production tend to preclude the inclusion of other materials.

Table 1. A Comparison of materials used in bone scaffold research

	Graft	Advantages	Disadvantages
Natural grafts	Autograft	Live cells and growth factors	Extra surgery causes pain Very limited quantity available
	Allograft	Contains growth factors	Risk of infection/rejection Somewhat scarce
	Xenograft	Very abundant	Risk of infection/rejection Controversial effectivity No growth factors
	CHACC	Naturally porous Adjustable speed of resorption	Derived from endangered animals No (human) growth factors
Metals	Titanium (alloys)	Can be 3D printed	Excessive mechanical strength Non-resorbable No growth factors Limited possibility for additives
	Zinc/ Iron/ Magnesium	Can be 3D printed Osteogenic properties	No growth factors Limited possibility for additives

Polymers	Collagen /Alginate	Can be mixed with fragile additives such as proteins or living cells Can be 3D printed	Very low mechanical strength
	Synthetic polymers	Can be 3D printed	Risk of foreign body response and inflammation
Ceramics	Calcium Carbonate	Component of natural bone	Resorbs very quickly No growth factors
	HA	Component of natural bone	Resorbs very slowly No growth factors
	HA/CC	Component of natural bone Can be 3D printed Adjustable speed of resorption	No growth factors

Polymers are another highly popular choice for bone implant research and can be divided into natural and synthetic polymers. Collagen and alginate are examples of natural proteins. Both are most commonly used for bone implant research in the form of hydrogels. Collagen, being a main component of bone, is used especially often in bone implant research. Due to their low mechanical strength, collagen hydrogels are most commonly used as a delivery agent for other compounds, such as growth factors.

Synthetic polymers have fewer limitations as their properties can be carefully fine-tuned. Many synthetic polymers are available for bone scaffold production, including polyglycolic acid (PGA), multiple variants of polylactic acid (PLA), and co-polymers of the two. These polymers are resorbable by the body. PLA is resorbed through the tricarboxylic acid cycle, while PGA can be converted to other metabolites or otherwise be degraded through normal body functions(Rezwan et al., 2006). Their resorbability and the ease of fine-tuning material properties makes them a popular material for bone scaffold research, with their ease of 3D-printing being an especially important selling point. Despite their degradation into non-cytotoxic compounds, foreign-body response resulting in incomplete scaffold resorption and intermittent inflammation can occur(Bergsma et al., 1993). Much like other materials, polymers are commonly used in conjunction with additives to improve their properties. Examples of this are the addition of fish scales, which were shown to improve the

mechanical properties and bone-forming capacity(Kara et al., 2020), and the addition of ceramics to increase the mechanical strength(J. Zhang et al., 2016). Synthetic polymers can also be used as a binder to allow for the 3D-printing of materials that have better osteogenicity and osteoinductivity but can normally not be shaped with high accuracy(Distler et al., 2020).

Finally, ceramics are very frequently used in bone implants. Ceramics are normally defined as solid materials that consist of either two or more nonmetal elemental solids or a combination of a metallic elemental solid with at least one nonmetal elemental solid. Bones are famously high in calcium phosphate, which fits the latter definition. Various ceramics, often involving calcium phosphates, are therefore used in bone implant research.

Hydroxyapatite is a crystalline calcium apatite compound that makes up about 65% of the non-organic bone matrix(Shi et al., 2020), making it an obvious choice for use in bone implants. Its chemical structure is Ca5(PO4)3(OH), sometimes written as Ca10(PO4)6(OH)2 to denote its crystallised form as a dimer. It has a high compressive strength with a Young's modulus of up to 117 GPa, which in the case of sintered scaffolds decreases linearly as the porosity increases(Panda et al., 2021). Being very similar to bone, HA is both biocompatible and osteoconductive. HA was also shown to be osteoinductive in vivo in primates(Ripamonti, 1996), though the mechanism behind this is unclear. The authors suggest the absorption of osteoinductive compounds post-implantation as a possible cause. Cowan et al. also hypothesize that apatites may encourage osteogenic differentiation(Cowan et al., 2005). The main disadvantages are its brittleness and very low biodegradation rate(Campana et al., 2014; Shi et al., 2020). The latter renders HA somewhat unsuitable for use on its own.

β-tricalcium phosphate, its amorphous form, and calcium carbonate (CC), another main component of bone, are much more easily resorbed by the body than HA. They can be resorbed in as little as six weeks and have lower mechanical strength, and are therefore also unsuitable as the primary component of a scaffold(Campana et al., 2014). It would be resorbed long before new bone can be formed and compromise the skeletal strength. A mixture of HA and CC can be used instead. This creates a

much more suitable material that, depending on the ratio used, can have a biodegradation rate compatible with the growth rate of new bone(Fu et al., 2013; Shi et al., 2020; Yang et al., 2016).

Such a mixture can be obtained using many different methods. For powder-based methods, such as when used in combination with polymers, it could be as easy as mixing purchased reagents. CC can also be hydrothermally converted to HA, a process that can be partially completed to reach the desired HA/CC ratio. This technique has been used to make scaffolds out of corals, some of which naturally have a structure similar to human trabecular bone(Koëter et al., 2008; Ripamonti et al., 2009). Despite their otherwise suitable properties, corals are a poor choice for the production of artificial bone grafts due to their endangered status. Instead, scaffolds intended to be mass-produced as medical devices should be made from scratch.

Hydrothermal conversion has also been used on calcium microspheres, which were partially converted to HA by microwaving them in solution(Yang et al., 2016). This is a useful and functional method but is somewhat limited by the difficulty in obtaining porous calcium carbonate scaffolds. Alternatively, to obtain HA/CC scaffolds with a porous structure HA/CC can be produced as a 3D-printable cement. This can be done by combining tetracalcium phosphate (TTCP), calcium hydrogen phosphate ($CaHPO_4$) and calcium carbonate ($CaCO_3$). The former two compounds can react together to form HA in a 1:1 molar ratio, while the latter is added according to the desired HA/CC ratio(Shi et al., 2020). The cement is easily produced and suited to extrusion printing, a fairly cheap and simple production method that allows for fine pore-size regulation(Xia et al., 2018).

Aside from TTCP, $CaHPO_4$ and $CaCO_3$, the cement described in previous papers contains gelatine. The gelatine has three functions in the scaffold. The first function is to give the cement a paste-like structure, suspending the powdered components homogenously and allowing for the cement to be 3D-printed. The second function is to form a matrix keeping the powdered components together after printing but before the HA-forming reaction takes place. This is performed through gelatine crosslinking, which forms bridges between the gelatine polymers and entraps the

powdered scaffold components. The third function is as an organic component of the scaffold. Natural bone contains around 30% of collagen, another organic polymer. Many other organic compounds, including bone morphogenic proteins (BMPs), bind to the collagen more so than to the calcium matrix(Nguyen et al., 2007), and the inclusion of gelatine in the scaffolds may therefore improve their ability to bind proteins. HA/CC cement is therefore expected to be a very suitable base material for the production of bone scaffolds.

1.2 Enhancing the osteogenic capacity of artificial grafts

Various combinations of materials can be used to make a suitable base for the production of bone implants, and HA/CC scaffolds are particularly interesting due to their similarity to bone. Still, there are improvements to be made. HA/CC is suitable for bone implants due to its non-cytotoxic and osteogenic properties as well as its resorbability, but like most raw materials it is not actively osteoinductive as it lacks the growth factors and organic materials present in natural scaffolds. The osteogenic and osteoinductive abilities of HA/CC scaffolds can be improved by controlling a number of variables.

The structure of the scaffold can make a large difference. Trabecular human bone has an interconnected porous and vascularised structure ranging from 50% to 90% porosity(Hart et al., 2017). It is highly beneficial for grafts to mimic this structure, as it allows for nutrients and cells to reach every part of the scaffold. The structure of the scaffold can also greatly influence its mechanical strength(Pobloth et al., 2018). The structure of the scaffold even directly influences osteogenic capacity(Yuan et al., 1999), influenced by the fluid dynamics affecting the nutrient flow through the scaffold(Deng et al., 2021).

The pore size of grafts is critical as well. Small pores will reduce cell migration and nutrient flow, but pores too big result in a smaller surface area for cells to attach to and may compromise the scaffold's structural integrity(Murphy & O'Brien, 2010). The right balance needs to be found. It was found that the presence of pores ~300 µm and larger is essential as this encourages vascularisation(Tsuruga et al., 1997). Smaller pores can encourage ossification (Tsuruga et al., 1997), but pores too small (85-120

µm) prevent cells from migrating into the scaffold, causing aggregates on the surface, further inhibiting nutrient flow (Murphy & O'Brien, 2010). A pore size of at least 300-400 µm was shown to be ideal in hydroxyapatite scaffolds; increasing the pore size beyond 300 µm was shown to have a more limited effect on bone regeneration(Roosa et al., 2010; Tsuruga et al., 1997). Another study suggests that larger pores are helpful to prevent cell detachment, showing that a smaller growth channel radius can cause cells to detach from the surface and create bridges (Yamashita et al., 2016). While the channel sizes recommended in this study cannot be directly translated to bone scaffolds – the study used smooth muscle cells, whose contractile nature plays a direct role in their detaching – other studies confirm that the surface curvature affects cell behaviour, including migration and attachment (Werner et al., 2019). Thus, aside from preventing cell aggregates and allowing for vascular growth, the lower surface curvature of larger pores could positively affect cell attachment.

Furthermore, the outside shape of scaffolds is important: Allografts have been shown to gain increased stability and osteoinductivity when given a textured surface before implantation(Ford et al., 2003). Particle-based scaffolds were found to encourage bone growth with particle sizes between 100-250µm and 250- 500µm(Mankani et al., 2001).

The final structure is highly dependent on the production method used. Examples include gas foaming, sintering, fibre bonding, solvent casting and particulate leaching, membrane lamination, melt moulding and 3D-printing (Xia et al., 2018). Many of these methods have significant drawbacks, such as a lack of pore interconnectivity, high temperature requirements, or difficulty regulating pore size. 3D-printing is the most promising among them, being suited to a wide range of materials and allowing for the regulation of pore size and structure(Deng et al., 2021; Xia et al., 2018).

While the structure of bone grafts is undoubtedly a crucial part of their effectivity, graft osteogenicity can be enhanced further. Bone autografts and allografts contain osteogenic compounds, including BMPs, Runt-related transcription factor 2 (RUNX2), Transforming growth factor beta 1 (TGF-β1), stromal cell-derived factor 1 (SDF-1),

insulin-like growth factor 1 (IGF-1), and many others(Garg et al., 2017). These compounds have long been proven to be beneficial: bovine collagen scaffolds enhanced with BMP-7 and implanted in humans were shown to reduce the incidence of postoperative osteomyelitis compared to autografts(Friedlaender et al., 2001b), seeding of DBM scaffolds with TGF-β1 before implantation in dogs was shown to accelerate bone repair(Servin-Trujillo et al., 2011), and collagen and DBM scaffolds seeded with BMP-9 were significantly more osteoinductive than controls when implanted in rabbits(Fujioka-Kobayashi et al., 2017). Thus, enhancing scaffolds by adding compounds directly to the scaffold is a popular and effective choice.

The delivery method depends on the scaffold material, preparation method, and the compound added: In gently-prepared scaffolds such as hydrogels, proteins and even cells can be directly added to the material before forming the scaffold. This is impossible in scaffolds produced using high temperatures or harsh chemicals, such as titanium or 3D-printed polymer scaffolds, as the proteins would be destroyed. Other methods of adding compounds to scaffolds are necessary to improve their osteogenicity.

Coating scaffolds in various materials is an option that can be used to achieve diverse applications. Scaffold coatings are often used to combine multiple materials and obtain the advantageous properties from both. As an example, titanium is a strong and biocompatible material, but its lack of osteogenic capacity and subsequent poor bone integration can lead to complications (Zuo et al., 2021). To resolve this, titanium scaffolds are sometimes coated with calcium phosphates(Geesink et al., 1988; Pereira et al., 2020) or bioactive glasses(Pereira et al., 2020) in order to improve their bone-binding capacity, and thus improve scaffold integration into the body. Conversely, phosphate glass/HA scaffolds have been coated with polymers to increase their compressive strength(Govindan et al., 2015).

Another advantage of coating is the ability to make use of materials that are otherwise unsuitable to make scaffolds out of. For instance, gypsum is not a suitable structural component for scaffolds as it cannot be made into a porous shape. It does, however, have the osteoinductive property of creating a weakly acidic environment,

thereby stimulating inflammation and recruiting cells to improve bone regeneration. To get around this issue, β-tricalcium phosphate scaffolds were coated with gypsum to obtain porous scaffolds with enhanced osteoinductivity(He et al., 2021). Other improvements made through the coating of scaffolds include antibacterial properties(Calabrese et al., 2021) and a slower release of added compounds(Tenkumo et al., 2018). A great number of materials and compounds have been used for scaffold coating: phosphates, bioglasses, polymers, metals, and even medications(Ray et al., 2018) have been used to enhance scaffolds. The possibilities are endless.

A similar method is to soak scaffolds in liquid containing the compound of interest. The effectivity of this method is very dependent on the scaffold material: any material that does not soak up liquid, such as titanium or certain polymers, would not benefit much from soaking. It is, however, cheap, fast, and easy to do even in sterile conditions, making it a great method for certain scaffold materials and compounds. The combination of HA/CC scaffold and bisphosphonates is one such example. Bisphosphonates are a widely used anti-osteoporotic medication, and their anti-resorptive properties could be useful for use in bone grafts. Though bisphosphonates can be applied to scaffolds as a coating (Ray et al., 2018), their calcium-binding properties make them uniquely suitable for soaking in combination with any calcium-containing scaffolds.

Many different bisphosphonates are available on the market, such as alendronate, risedronate, zoledronate (ZOL) and OX14. Bisphosphonates generally consist of two phosphonate ($PO(OH)_2$) groups with varying side chains. As they bind very strongly to calcium, they bind to hydroxyapatite and prevent its breakdown by osteoclasts. The side chain's makeup determines several factors, including the binding capacity to bone and the required dose to meet a certain effect(Lawson et al., 2017). Notably, bisphosphonates with nitrogen-containing side chains inhibit the mevalonate pathway inside osteoclasts, thereby inhibiting their functioning. The same is not true for other bisphosphonates, which have a cytotoxic effect on osteoclasts by inducing caspase-3-mediated apoptosis(Rogers et al., 2020). Nitrogen-containing bisphosphonates generally provide stronger effects compared to their nitrogen-free

counterparts.

OX14 and Zoledronate are both nitrogen-containing bisphosphonates but have differences in both side chains (Figure 1). Specifically, ZOL contains an -OH group at one side chain and a nitrogen ring in another. In OX14 these are exchanged for a fluoride atom and a double nitrogen ring. The result of this is that their effect on bone resorption is similarly strong, but ZOL has a stronger binding capacity than OX-14, being retained by the skeleton for longer periods. Because of this, the required dosage of ZOL is lower than that of OX-14(Lawson et al., 2017).

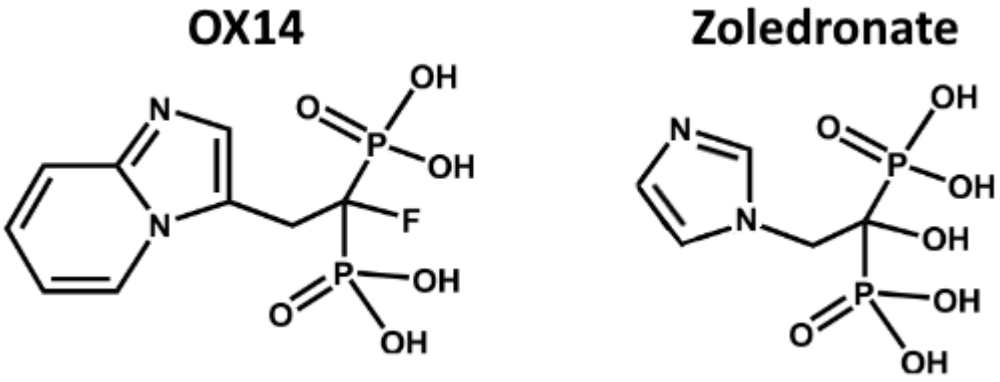

Figure 1. The structures of OX14 and Zoledronate. *OX-14 has a double nitrogen ring on one side chain and a fluoride atom on another, whereas Zoledronate has a single nitrogen ring and an -OH group(Lawson et al., 2017). This is an open access article under the CC BY license (https://creativecommons.org/licenses/by/4.0/). The right image was edited by Emma Steijvers using Paint.net 5.0.2, 2023.*

As bisphosphonates bind strongly to bone they are rapidly taken out of the bloodstream, providing a very localised effect specific to osteoclasts. Despite this, the soft-tissue toxicity of bisphosphonates may cause jaw osteonecrosis, the risk of which is thought to increase with longer use and at higher doses(Gupta & Gupta, 2022). Other risk factors include the mode of administration(Cartsos et al., 2008), co-morbidities such as cancer and infections, extensive dental work, medication interactions and even genetic predisposition(Gupta & Gupta, 2022; Hess et al., 2008). Much like with other compounds used for scaffold soaking, the dosage should be carefully controlled. Which bisphosphonate to use has some relevance as well: As various bisphosphonates have different potencies and even function through

different pathways, both the minimum amount needed for an effect and the maximum safe amount are likely to vary between bisphosphonates.

Another reason why more or stronger bisphosphonates are not necessarily beneficial is that while they inhibit bone resorption, bone resorption is a natural and important part of bone remodelling. An ideal outcome of bisphosphonate use would be to maximize the initial bone formation to repair the damaged bone while not inhibiting the subsequent bone remodelling. Considering that high concentrations and long-term use of bisphosphonates may be detrimental with regards to the risk of jaw osteonecrosis, and taking into account that certain bisphosphonates bind the bone so strongly they can remain inside the body for years, a stronger bisphosphonate is not necessarily advantageous. Instead, weaker bisphosphonates may aid the initial bone formation process and be removed before interfering with bone remodelling.

Proteins, such as growth factors TGF- β and BMPs, are also commonly added to scaffolds(Friedlaender et al., 2001b; Fujioka-Kobayashi et al., 2017; Gao et al., 1997; Servin-Trujillo et al., 2011). This commonly happens either through soaking, as it is a very gentle delivery method, or by direct addition into the scaffold. BMPs are very commonly used to induce or enhance bone growth and regeneration. There are over 20 BMPs that, with the exception of BMP-1, are all part of the larger TGF-β superfamily(Schmitt et al., 1999). BMP-2, 4, 7 and 9 are all able to induce osteogenic differentiation of cells(Luther et al., 2011; Myllylä et al., 2014), and thus have potential for use as a growth factor included in bone scaffolds. Among them, BMP-2 and BMP-7 are particularly popular in scientific bone implant studies, likely in large part due to their FDA approval for medical use, though the approval of BMP-7 was later revoked, and it is currently on a strict human device exemption label(Gillman & Jayasuriya, 2021).

BMP-2 is an essential part of the natural bone repair process(Chappuis et al., 2012; Tsuji et al., 2006) and has been used for many different approaches to induce bone healing. It is a highly osteoinductive compound and is often used in conjunction with a collagen scaffold carrier to control the BMP-2 release rate, as a long-term release is more beneficial than a single dose(Hollinger et al., 1998; Kim et al., 2005; Nevins et

al., 1996). It has also been added to other types of scaffolds, including titanium scaffolds, where its addition was shown to be beneficial during bone repair(Hall et al., 2007).

BMP-7, also known as osteogenic protein 1 (OP-1), is involved in kidney formation, eye development, and skeletal patterning(Luo et al., 1995). Much like BMP-2, it has been used with collagen carriers and internal fixation to encourage the healing of non-junctions. Its use was shown to be effective(Friedlaender et al., 2001a), though the use of BMP-2 is more effective in comparison(Conway et al., 2014). BMP-2 and BMP-7 are known to colocalize and even form heterodimers with a distinct function from the original proteins(Lyons et al., 1995), the presence of which was shown to be beneficial for bone formation(Loozen et al., 2018). As such, adding BMP-2 and BMP-7 into a scaffold could further increase the scaffold osteoinductivity.

BMPs are consistently shown to function dose-dependently, with a larger amount of BMPs leading to a decrease in non-unions in both clinical trials(Govender et al., 2002) and in vivo research(Harada et al., 2012). As such, it would be easy to think that higher doses are better. At least in spinal surgeries, however, the use of BMPs has been linked to adverse events(Mroz et al., 2010), including glial scarring and radiculitis, characterised by inflammation and nerve pain(Dmitriev et al., 2011), when implanted near the spinal cord. In-vitro, high concentrations of BMP-2 (~2 mg/ml) are also linked to an inhibition of cell proliferation and increased cell apoptosis, despite similarly high concentrations (~1.5mg/ml) being common in clinical use(Kim et al., 2013). These results indicate that the overuse of BMP-2 is possible and should be avoided.

Likewise, BMP-7 is often used in very high amounts for clinical use, with previous studies having used dosages of up to 3.5mg(Friedlaender et al., 2001a). The concentrations at which BMPs are clinically used to induce bone growth are significantly higher than the natural body concentration, which has been linked to adverse effects. The use of high concentrations of BMPs is even thought to link to cancer incidence, though the consensus is that this effect, if present, is too rare to be clinically relevant(Cahill et al., 2015). All in all, these extreme dosages are risky.

Moreover, bone grafts should not contain extreme dosages as the size of both the bone defects and the patients receiving grafts can differ significantly.

Not only the BMP content but also its release rate is relevant for bone graft effectivity. BMP-2, 4 and 7 can induce bone formation even in non-native areas of the body even when the growth factor is injected into the area directly(Groeneveld & Burger, 2000), but a carrier may be used to provide mechanical support and to finetune the release rate. This allows for the tissue to be affected by the BMPs for a longer time while being able to significantly lower the initial concentration. It has been shown that bone induction can be achieved with doses as low as 8µg/mL in hydrogel scaffolds, provided that the scaffold is formulated in order to optimize its release pattern. The amounts of BMP-2 added to scaffolds that provided osteogenic capacity could be as low as 51 ng BMP-2 per mm^2 of defect area in hydrogel scaffolds, 79 ng/mm^2 in synthetic polymer scaffolds, and 191 ng/mm^2 in silk polymer scaffolds. It is clear that the BMP-2 retaining capacity of the scaffold is relevant: Titanium, a non-absorbent scaffold material, requires 1 µg /mm^2 to gain bone-forming capacity(Ben-David et al., 2013), a much larger amount.

The amount of BMPs present in DBM is much lower despite its osteoinductive capabilities. An exact amount cannot be determined as the amount of BMPs measured in DBM differed significantly between studies: One measured 2.11 ± 1.26ng/g BMP-2, another measured 21.4 ± 12.0ng/g BMP-2 and 84.1 ± 34.4 ng/g BMP-7. Yet another measured 20.2–120.6 ng/g of BMP-2 and 54.2–226.8 ng/g of BMP-7. BMP-4 was entirely undetectable according to one set of authors, while another study proved that there is a donor-age-related decrease in BMP-4(Bae et al., 2006; Honsawek et al., 2005; Pietrzak et al., 2006). This makes it hard to gauge an accurate BMP-content from literature, which is exacerbated by the BMP-content of DBM having significant lot-to-lot variation. Donor age and gender may affect the BMP content as well, though this is controversial as multiple studies report opposite results(Honsawek et al., 2005; Pietrzak et al., 2006).

Furthermore, there may be discrepancies in the amount of active BMPs, which is not always apparent through BMP-2 measurement. BMPs, being proteins, are folded in a

specific manner that is necessary for their functioning. Various environmental changes, such as temperature or pH changes, can cause denaturation or other conformational changes in these proteins. This is unavoidable to some extent during the sterilisation, transport and storage of grafts(El Bialy et al., 2017). Allografts, DBM and xenografts will lose more BMPs during the decellularisation process. In synthetic grafts, the inactivation of BMPs is heavily dependent on the material and the method of addition. One study using scaffolds consisting of collagen-1, propiolactone and live cells found that half the BMP-2 was inactivated after mixing with the scaffold(Kisiel et al., 2012). This percentage will undoubtedly change for different materials and between different methods of addition. Denatured proteins can still be detected through methods such as enzyme-linked immunoassay (ELISA) assays, depending on the extraction method used(Lechtzier et al., 2002), and western blots. Thus, protein quantifications are likely to detect higher amounts of BMPs in the sample than are actually active. Native western blots may be an exception, as a protein in its tertiary structure will move through the agarose at a different speed compared to its denatured form.

Scaffold materials were also shown to differ in their BMP-2 retention capacity, an effect that is undoubtedly present for other growth factors as well. Collagen implants release BMP-2 more quickly than hydroxyapatite implants(Babensee et al., 2000), indicating that the suitable concentrations found in research using collagen implants may not be ideal for use in other types of scaffolds. Considering that a too-low-level release was not shown to be beneficial(Li & Wozney, 2001), the amounts of BMP-2 may need to be higher in hydroxyapatite scaffolds compared to collagen implants.

1.3 Enhancing bone grafts through cell-seeding

Soaking scaffolds is an effective manner of adding osteoinductive compounds to scaffolds but has several drawbacks. Purified proteins are difficult to produce in large numbers, for one, so to add natural osteogenic compounds to scaffold on a mass scale would be prohibitively expensive. Additionally, mimicking the exact number and concentration of compounds found in allografts would be highly expensive and very difficult, if not impossible, as there are many different compounds with their own ideal concentrations. Instead, this could be done by creating scaffolds that are then

seeded with stem cells. When stem cells undergo osteogenic differentiation they can produce osteogenic compounds that stay in the scaffold even after decellularization, enhancing the osteoinductive capacity of the artificial allografts and increasing their similarity to natural allografts. This method has even been used to improve allografts(Shi, 2017).

There are a number of requirements for the selection of cells for the mass production of allografts. The cells need to be able to osteogenically differentiate, and cells that have great proliferation capacity and are suitable for multiple subpassages are desired. Osteoprogenitors are therefore an obvious choice. Bone marrow stromal stem cells, also termed mesenchymal stem cells (MSC), are a group of pluripotent, heterogenous cells that may differentiate into different lineages, including bone(Liang & Song, 2020). They are reasonably popular in bone research, (Mankani et al., 2001; Zhou et al., 2006), being relatively accessible. Autologous bone marrow MSCs are the most used stem cells for in vitro bone tissue engineering(Adamzyk et al., 2016). They are considered an accessible source (Caterson et al., 2002), are known to express osteogenic markers (Day et al., 2018), and can differentiate into osteocytes(Squillaro et al., 2016). A disadvantage is the process of obtaining them for the purpose of artificial allograft, which requires bone marrow aspiration (Caterson et al., 2002).

Ideally, cells should be derived from medical waste so as to be both abundant and ethical. Mesenchymal stem cells can be isolated from umbilical cord matrix, umbilical cord blood, and adipose tissue, all sources that are more suitable from an ethics perspective compared to their marrow-derived counterparts. MSCs isolated from different sources behave somewhat differently, and their osteogenic capacity should ideally at least match that of bone marrow MSCs.

Comparative studies between bone marrow MSCs, umbilical cord blood MSCs and adipose tissue MSCs found that all three types are able to osteogenically differentiate(Kern et al., 2006) and that the osteogenic differentiation capacity was similar between the three(Rebelatto et al., 2008). In the case of adipose tissue MSCs this is not entirely uncontroversial; at least one study did find that their osteogenic

capacity is lower than that of bone marrow MSCs (Mohamed-Ahmed et al., 2018). Differences were found in the expression of mesenchymal stem cell markers, with umbilical cord blood MSCs showing lower expression of CD105 and adipose tissue MSCs having reduced CD106 expression (Kern et al., 2006).

Umbilical cord blood MSCs were shown to have the highest expansion potential, allowing subculture for at least ten passages, while adipose tissue MSCs showed much lower senescence in earlier passages(Kern et al., 2006). A disadvantage of umbilical cord blood MSCs is that they are difficult to isolate compared to alternatives, with many studies failing to isolate MSCs from a large percentage of their samples(Rebelatto et al., 2008; Zeddou et al., 2010). A solution relying on only umbilical cord blood MSCs may therefore be less suitable, though there may be merit in using them in conjunction with umbilical cord matrix MSCs to avoid waste.

Both umbilical cord matrix and adipose tissue MSCs are suitable for scaffold seeding despite being less osteogenic than bone marrow MSCs (Day et al., 2018; Mennan et al., 2019). Ideally, their osteogenic capacity should be enhanced to at least match bone marrow MSCs. The osteogenic differentiation capacity of umbilical cord MSCs was shown to be retained better in monolayer cultures(Zhang et al., 2009) and is affected by which parts of the cord are used for MSC isolation(Mennan et al., 2013), with a mixture of cells outperforming any single tissue. The proliferation rate of adipose tissue MSCs was shown to be affected by the tissue harvesting method(Schneider et al., 2017), and their osteogenic capacity is affected by the harvesting method(Markarian et al., 2014) and donor age(Choudhery et al., 2014). The osteogenicity could be further enhanced by optimising other culture conditions, such as altering the chemical concentrations in osteogenic medium.

Many compounds have a positive effect on bone growth or maintenance, including tomatine, testosterone, icariin and retinoic acid (RA). These positive effects are realised through a variety of different pathways, and various administration methods are therefore used in research. Tomatine, for example, was added to the diet of osteoporotic mice and was shown to prevent bone loss(Nirmala et al., 2020). Scaffolds loaded with testosterone proved to be as effective as those loaded with

BMP-2 through a pathway initiated through androgen receptors(Cheng et al., 2013). The direct addition of TGF-β1 to bone injuries in rabbits stimulates osteoblast recruitment and proliferation at the bone defect site(Beck et al., 1993). Icariin activates cell proliferation and differentiation in vitro through the activation of BMPs and RunX2, and is able to increase MC3T3-E1 cell proliferation and differentiation through these pathways(Cao et al., 2012; Zhao et al., 2008).

Retinoic acid, a metabolite of vitamin A, is particularly interesting for bone research. It is involved in many processes in the body, including vision and embryonic limb patterning. As a result, much research has already been done into its effects on various tissues. Many studies report that RA regulates osteogenic differentiation, which happens through a variety of pathways. For example, in vitro research shows that RA induces osteogenic differentiation in MSCs through Wnt/β-catenin signalling as RA activates the PI3K/AKT/GSK3β signalling pathway(S. Zhang et al., 2016). BMPs are often involved: RA also increases the rate of BMP-9 induced osteogenic differentiation of mesenchymal progenitor cells when added to cell culture medium (Zhang et al., 2010) and can regulate osteogenesis through the BMP2-Smad-Runx2/Msx2 pathway(Hisada et al., 2013).

Overall, the addition of RA to bone defects in vivo was shown to enhance bone healing(Weng et al., 2019). RA affects various cell types differently, as confirmed by in vitro studies. For instance, it downregulates receptor activator of nuclear factor kappa-B ligand (RANKL)-mediated osteoclast differentiation (Balkan et al., 2011) and upregulates the osteogenic differentiation of hypertrophic chondrocytes(Descalzi Cancedda et al., 1992). Even for MSC-lineage cells the results are somewhat controversial: The addition of RA to preadipocytes induces osteogenesis through induction of Wnt/β-catenin signalling, but in preosteoblasts osteogenesis is reduced through inhibition of the very same pathway(Liu et al., 2014; Roa et al., 2019; Skillington et al., 2002; S. Zhang et al., 2016).

Inconsistencies remain even within studies using MSCs. Many studies conclude that overall, the addition of RA benefits osteogenic differentiation(Cowan et al., 2005; Hisada et al., 2013; Malladi et al., 2006; Zhang et al., 2010), but a number of studies

instead determine that osteogenic differentiation is inhibited(Ahmed et al., 2019; Wang et al., 2008). Despite the opposing conclusions there is a consensus between these studies that the expression of alkaline phosphatase (ALP) is induced by RA, indicating some level of osteogenic function even in studies that ultimately conclude RA inhibits osteogenic differentiation. Previous unpublished research by this group corroborates the positive effect of RA on osteogenic differentiation of MSCs seeded onto HA/CC scaffolds: When 20µM of RA was added to cell culture medium the expression of ALP and BMP-9 was increased after 7 and 14 days. As the results in literature are so varied, however, and many factors, such as the scaffold structure and material, could affect the osteogenic differentiation capacity, it remains important to research the real effect of RA addition on cell-seeded scaffolds.

The cell seeding method an important factor as well. During the bulk production of cell-seeded scaffolds they are commonly seeded with cells first and transferred to a bioreactor afterwards. Common cell seeding methods are either pipetting a cell suspension directly onto the graft or soaking the graft in a cell suspension(Zhou et al., 2006). For larger grafts where liquid penetration into the centre is a concern the graft may be placed in liquid under a vacuum to remove the air from the graft before cell seeding. One study compared various methods by seeding porous β-TCP scaffolds using four different methods, before moving the scaffolds to a static culture in osteogenic medium. It was found that vacuum-based methods perform the best in terms of bone growth after in-vivo implantation, especially when the resorption of bubbles adhering to the scaffolds is prevented. The soaking method was shown to be less effective than any other(Hasegawa et al., 2010). Another method that can be opted for is dynamic cell seeding, in which the cells are added to the scaffolds inside the bioreactor. This method is compatible with most, if not all bioreactor types, including spinner flasks, rotating wall vessel bioreactors, and perfusion bioreactors. Dynamic seeding has various advantages. In spinner flasks, it can promote the formation of cell aggregates, the presence of which encourages cell deposition onto the scaffolds (Vunjak-Novakovic et al., 1998). In perfusion bioreactors dynamic seeding can improve cell distribution throughout the scaffold as the cells are

encouraged to move further throughout, instead of stopping at the first obstacle they encounter (Marín et al., 2018). Additionally, multiple studies suggest that the added shear stresses and increased nutrient supply can enhance osteogenic differentiation and mineral deposition onto the scaffolds (Marin et al., 2017; Melke et al., 2020).

The number of cells to seed onto a scaffold is also of interest, but is fairly controversial. Various studies suggest that seeding more cells onto scaffolds is not necessarily beneficial as it leads to reduced proliferation(Wilson et al., 2002; Zhou et al., 2006), while others found that collagen and glycosaminoglycan production were increased in samples seeded with a higher number of cells (Vunjak-Novakovic et al., 1998). At the same time, very low cell numbers can discourage cell penetration into the scaffold(Lode et al., 2008). While many different papers have tried to find optimal seeding methods, their results are difficult to compare as the ideal amount depends on many parameters, including the scaffold material, structure, and the cell type used for seeding. Different cell materials can add many variables, such as the ease with which cells adhere to the scaffold. The structure is important as it affects the nutrient flow into the scaffold, which becomes especially important in larger scaffolds. The cell type will also affect factors such as the adherence and proliferation rate, all of which will affect the final results.

Lastly, the physical environment is a factor. Bioreactors come in many shapes, sizes and perfusion methods. A reactor with a flow mechanism is essential for larger grafts: the nutrient flow in static cultures has been shown to halt even as low as 1 millimetre deep into grafts(Grayson et al., 2011) and oxygen and carbon dioxide in the medium is quickly depleted in static cultures(Gooch et al., 2001). Perfusion bioreactors are among the most used in scaffold research. Some studies even go as far as to say they are essential for grafts of clinically relevant size(Temple et al., 2013). These bioreactors use pressure to force a flow of medium through the grafts. This has two large advantages. For one, this provides the scaffolds with an even amount of wall shear stress, which is beneficial for bone growth(Marijanovic et al., 2016; O'Dea et al., 2012). It also allows nutrient to reach the centre of grafts more easily. Despite these advantages, perfusion bioreactors are not very suitable for mass production because of their extremely low capacity.

Another method, compression bioreactors, use a piston to press down onto the scaffold and directly apply mechanical loads. This is intended to mimic the compressive load of bones in vivo and is commonly combined with perfusion. The scaffold structure is highly important in these types of bioreactors, even more so than in others, because when not fully uniform, the scaffold structure will cause an unequal distribution of mechanical shear stress throughout the scaffolds (Vetsch et al., 2015).

Rotating wall vessel (RWV) bioreactors make use of upwards hydrodynamic force so that the scaffolds remain in suspension forever, never touching the edges. This movement allows for sufficient nutrient flow while reducing shear stresses(O'Dea et al., 2012). Constructs cultured in RWV bioreactors showed improved chemical and mechanical properties compared to those cultured in spinning flasks(Martin et al., 2004). While generally suitable, commercially available RWV bioreactors still have very low maximum capacities.

Spinning bioreactors are generally better suited to bulk production, being easy to scale up and produced in many sizes. Scaffolds either lie on the bottom or are suspended, and flow is created by a stirring or rocking motion. Spinning bioreactors significantly surpass static bioreactors when measuring collagen and glycosaminoglycan synthesis and can perform comparably to RWV bioreactors(Burova et al., 2019). They are, therefore, a promising tool.

Not just the type of bioreactor but also its settings are important. For spinning bioreactors specifically, an increased mixing intensity was shown to lead to higher collagen and glycosaminoglycan production by the scaffolds, likely because of the increased nutrient flow and/or increased mechanical stress(Gooch et al., 2001), though the increased shear stress caused most of these to be leached into the medium(Gooch et al., 2001; O'Dea et al., 2012). In other words, a high flow rate has the advantages of adding extra nutrient flow and mechanical pressure but also has drawbacks in the form of disturbing the scaffolds, causing cell and protein loss. A balance, which is undoubtedly dependent on scaffold size and structure, must be found.

1.4 Assessment of enhanced scaffolds

To summarize, scaffolds can be enhanced through structural changes, directly adding osteoinductive compounds, or adding them indirectly by co-culturing scaffolds with cells. Regardless of which method is used, the resulting scaffolds need to be tested in order to confirm both their chemical make-up and their real effects in-vivo.

The macro-structure of the scaffold is often visible by eye. Scanning electron microscopy can be used to visualize microstructures or take accurate measurements, such as for pore sizes. Methods for measuring scaffold composition vary and highly depend on the scaffold material. Fourier transform infra-red (FTIR) spectroscopy is a suitable method for many materials. This technique measures the infra-red light refraction of materials on a spectrum of wavelengths. Different materials have different refractive indexes that display as peaks at different wavelengths, thereby making it possible to distinguish separate components within a mixture. For larger scaffolds the mechanical strength can be of interest as well.

The osteogenic and osteoinductive capacity of the scaffolds needs to be assessed as well. Multiple qualities of the scaffolds influence their bone-forming capacity, which can be assessed through either in vitro or in vivo experiments. For either method it is important to know whether the scaffold supports cell growth and to confirm that it is not cytotoxic. In cell-seeded scaffolds, microscopy can be used to confirm the presence of cells growing on the scaffolds in vitro. Due to the non-transparent nature of ceramic scaffolds brightfield microscopy has limited use, only clearly showing thick plaques of cells. Fluorescence microscopy can be used to more clearly visualise small numbers of cells, as well as to distinguish them, such as through live-dead staining. Confocal microscopy is especially useful for this purpose, as the cells are growing on a 3D structure.

Scanning electron microscopy (SEM) also provides a very high-quality 3D view of the outside structure and can be used to show cells growing on the scaffolds, though unlike fluorescent microscopy it cannot be used to assess their vitality or perform immunohistochemistry. SEM can be combined with energy-dispersive X-ray analysis (EDX) to label chemical elements on the image.

Aside from live-dead staining, which is more of a visualisation method, the number of living cells can be measured through their metabolic activity using an Alamar Blue assay. This assay involves a blue dye that cells metabolise into a fluorescent red dye, which can then be measured using spectrophotometry. Measuring the amounts of growth factors deposited onto a scaffold is fairly straightforward and can be performed using ELISA. These assays allow for the quantification of a specific protein of interest in a sample, including BMP-2 and BMP-7.

Assessing the effect scaffolds have in vivo is a more complicated process, as many variables exist that can be looked into. In the first place, in vivo bone implantation can be done using a number of methods. Many researchers papers use critical-sized bone defects, a term used to describe a bone defect that is too large for the body to naturally repair it. This allows the researchers to obtain a real idea of whether the scaffold can repair the type of severe bone defects they are meant for, with accurate results since it happens in the natural bone environment. Disadvantages of this method, however, are that fewer defects can be placed per animal and the surgeries involved are often complicated as well as very painful for the animals. Most other techniques involving bone defects, such as distraction osteogenesis models, have similar issues.

Subcutaneous implantation is a common alternative method to assess scaffold osteoinductivity. It has the advantage of being able to place many implants on one animal, thereby reducing the number of animals required, and it can give insight into the bone-forming capacity of a material. It is limited, however, in that it requires scaffolds to contain compounds that can actively induce bone formation, since otherwise no bone will form near the skin, and in that the natural bone environment is not used. That is to say, the body's natural bone healing mechanisms are not present due to the distance from the natural bone environment.

We propose a hybrid method, where scaffolds are placed in-between the tibia and anterior tibialis muscle. This method does not require bone damage, making for an easy-to-perform procedure that causes the animals less pain. Unlike with the subcutaneous method, the scaffold is near the natural bone environment and can be

affected by migrating bone marrow MSCs, periosteal stem cells and osteoblasts/osteoclasts, the same factors that would normally affect the healing bone. It is expected that callus formation will be caused by the presence of the scaffold, though unlike the subcutaneous method, it may not require the presence of osteoinductive compounds like BMP-2 due to the bone-adjacent implant location. Much like with the subcutaneous method, bone formation can then be quantified and compared between groups in order to assess the osteogenic capacity of the scaffolds.

Histological analysis is a common technique used to look at the scaffold, callus and natural bone in detail. It usually involves the tissue being sliced into 7-50 µm slices through the use of either cryo- or paraffin sectioning. The tissue can then be stained, mounted, and imaged using either brightfield or fluorescence microscopy. While immensely useful, it is somewhat limited by its 2D nature and the limited amount of bone material. µCT scans, or regular CT scanning for research involving large animals, can be used to quantify new bone growth as well as measure scaffold resorption, two of the most important factors looked at when judging scaffold effectivity. This technique can also be used to measure much more detailed structural features, such as the trabecular structure and number, in order to assess bone quality.

Additionally, the expression of genes of interest can be measured using quantitative real-time polymerase chain reaction (qPCR). When the right genes are selected, this can give interesting insights as to which genes are up or downregulated due to scaffolds or their enhancements. For bone research, a number of factors are of particular interest. One of these factors are osteoblasts, the cells that produce the bone mineral matrix. They are essential to the bone formation process, and genes related to their differentiation or functioning can tell much about the osteogenicity and osteoinductivity of an implanted scaffold or its enhancements. TGFβ1 and BMPs are both osteogenic growth factors secreted by osteoblasts(Huang, 2007) and are thus associated with osteoblast activity.

Osteoblast differentiation can be assessed as well, and osterix (OSX), osteocalcin (OCN), and collagen type 1 alpha 1 (Col1a1) are commonly used as markers for this

purpose(Huang, 2007). OSX is a BMP-2 inducible compound necessary for osteoblast differentiation(Nakashima et al., 2002) that remains necessary throughout life for bone generation, homeostasis and fracture repair(Sinha & Zhou, 2013). OCN is a hormone that regulates insulin secretion and sensitivity as well as muscle function, among others, that is synthesized and mainly expressed in osteoblasts(Shao et al., 2015). It also has a relation to osteoclasts, as it is γ-carboxylated to exist in an inactive form and is indirectly decarboxylated, and thus activated, by osteoclasts during bone resorption (Mera et al., 2018). Col1a1 is well-known for its expression in chondrocytes, cartilage-producing cells, and its relation to collagen production. Together with ALP it serves as an early marker for bone formation(Dacic et al., 2001).

Osteoclasts are another obvious factor to investigate. Together with osteoblasts, they mediate bone formation, maintenance and remodelling by removing the mineral matrix. The presence of C-terminal Src kinase (CSK) is essential for osteoclast activity since bone resorption is prevented by its absence. It is also involved in the mediation of cell adhesion, proliferation and movement(Miyazaki et al., 2006). Macrophage colony-stimulating factor (M-CSF) and it's receptor, M-CSFR, enhance monocyte differentiation into osteoclasts by inducing Receptor activator of nuclear factor κ B (RANK) expression, thereby enhancing osteoclast formation. It also enhances osteoclast survival by preventing apoptosis(Boyce, 2013). Osteoclasts can also be created through macrophage fusion, a complex process mediated by many different genes. Osteoclast Stimulatory Transmembrane Protein (OCSTAMP), for one, promotes osteoclast fusion through the mediation of fusogen Cluster of Differentiation (CD)-9 (Ishii et al., 2018). CD47 promotes macrophage-macrophage fusion by binding to SHPS-1, leading to its tyrosine phosphorylation and the subsequent pathway activation causing macrophage fusion(Maile et al., 2011). C-C chemokine receptor type 2 (CCR2) is the receptor for CCL-2 and mediates osteoclast fusion through this pathway(Khan et al., 2016). It is also involved in skeletal muscle regeneration(Warren et al., 2005). Osteopetrosis-associated transmembrane protein 1 (OSTM1) mediates osteoclast maturation and also plays a role in the intracellular lysosomal trafficking in mature osteoclasts(Pata & Vacher, 2018).

There are also a number of important functions that do not directly relate to bone cells but are still highly important during the bone formation process. One such process is vascularisation. Platelet-derived growth factor BB (PDGF-BB) and angiogenin are both commonly associated with vascularisation. PDGF-BB's involvement in vascularisation is twofold: It stimulates the genesis of new blood vessels(Lange et al., 2009), as well as the maintenance of existing blood vessels through the recruitment of mural cells and differentiation of skeletal myoblasts to pericytes(Betsholtz et al., 2005; Cappellari et al., 2013). PDGF-BB also protects multiple cell lineages, including MSCs, against apoptosis(Vantler et al., 2010; J. M. Zhang et al., 2016) and is known to be involved in the regulation of MSC immunosuppressive capacity(J. M. Zhang et al., 2016). In addition to vascularisation, it is linked to skeletal effects: PDGF-BB can be produced by pre-osteoclasts, was shown to mediate arterial stiffening (Santhanam et al., 2021), and its addition to poly-L-lactide membranes was shown to increase their osteogenicity when implanted(Park et al., 1998). Angiogenin is another strong promoter of angiogenesis, mediating nearly every step of the vascularisation process(Shestenko et al., 2001). It does so by acting through many pathways, including receptor binding on endothelial cells, nuclear transport, and cascade activation(Pyatibratov & Kostyukova, 2012). Angiogenin is also involved in endothelial cell-cell interactions necessary for endothelial cell proliferation, smooth muscle cell and actin interaction(Tello-Montoliu et al., 2006), and has microbicidal functions against bacteria and fungi(Hooper et al., 2003).

Innervation is another essential process during bone regeneration. Ubiquitin C-Terminal Hydrolase L1 (PGP9.5) expresses in osteoblasts, and it is thought that nerve impulses affect osteoblasts(Kjaer & Nolting, 2008). Netrin-1 is involved in nerve regeneration (Dun & Parkinson, 2017) and has a strong effect on the skeleton, being a negative mediator of BMP signalling(Abdullah et al., 2021). Despite inhibiting osteoblast differentiation(Sato et al., 2017) and encouraging osteoclast differentiation(Mediero et al., 2015), it has a bone-retaining effect due to its inhibition of osteoclast fusion(Maruyama et al., 2016). The 'deleted in colorectal cancer' (DCC) gene is most well-known for its tumour-suppressive function but is also

a Netrin-1 receptor. Together, they determine whether the cell survives or initiates apoptosis(Mehlen & Furne, 2005). Thus, Netrin-1 and DCC regulate cell viability.

While the up- or downregulation of a single gene doesn't say much due to most genes regulating many different pathways, taken together they can provide an overview and give an indication of what effect the scaffold or its additions have on their environment. It is, therefore, an important step in the final assessment of scaffolds.

In summary, while scaffolds can be made out of many base materials and can be enhanced using many methods, HA/CC ceramic scaffolds enhanced through the addition of either natural growth factors or bisphosphonates are likely to be particularly useful for bone repair. HA/CC scaffolds are chemically similar to natural bone, are resorbable, and can be produced with a suitable structure. It has even been suggested to have osteogenic properties. Improvements to the scaffold osteogenicity can be made by adding growth factors, preferably through cell seeding or the addition of bisphosphonates.

The aims of this study are to determine in how far the osteogenic capacity of HA/CC scaffolds can be enhanced through cell seeding, and to assess whether the addition of bisphosphonates to HA/CC scaffolds is a suitable method for their osteogenienhancement.

The first objective set to accomplish these goals is to reliably produce HA/CC scaffolds by making them from cement. FTIR spectroscopy will be used to analyse its composition and confirm the presence of HA.

The second objective is to culture cells onto these scaffolds, differentiate them, and finally to measure the growth factors produced in vitro. Fluorescence microscopy and SEM will be used to confirm cell growth on the scaffolds, and the viability of said cells will be assessed through Alamar Blue assays and live-dead staining using CalceinAM. Growth factor deposition will be measured through BMP-2 and BMP-7 ELISA assays.

The third objective is to determine the effect of bisphosphonate treatment on the osteogenicity of HA/CC scaffolds in vivo. The bone formation will be quantified using

techniques such as histology and µCT scanning, and the gene expression will be quantified using qPCR.

2. Materials & Methods

2.1 Materials

The suppliers of all chemical reagents and instruments used are listed in appendix 1.

2.2 HA/CC scaffold production

To create HA/CC scaffolds, tetracalcium phosphate (TTCP, Matexcel) and Emprove Essential $CaHPO_4$(Sigma-Aldrich) were mixed 1:1 in molar ratio and then mixed with 1:1 $CaCO_3$(Sigma-Aldrich) in weight. The three powders were ground using a mortar and pestle for five minutes, then mixed with 15% EMPROVE Essential Gelatine powder (Sigma-Aldrich) in water to create a paste. This paste was then left to dry at room temperature. To ensure the HA-forming reaction was completed, the scaffolds were first submerged in 0.1% glutaraldehyde (Sigma-Aldrich) to crosslink for 10 minutes to prevent the scaffold from dissolving, then washed with water and soaked in phosphate-buffered saline (PBS) (Gibco) overnight at 37°C. Scaffolds were then air-dried and autoclaved.

2.3 FTIR spectroscopy

FTIR spectroscopy was used to determine the final concentrations of compounds present in the scaffolds. The four main components, TTCP, $CaHPO_4$, $CaCO_3$ and HA, were each ground by hand using a mortar and pestle for five minutes. Scaffold was then made as described above and either left untreated or soaked in 0.1% glutaraldehyde for 10 minutes, then soaked in PBS overnight for 24, 48 or 128 hours before being air-dried and powdered. In order to test whether bisphosphonates impede HA/CC formation, 7.5µg OX14 and 1.6µg of Zoledronate (both kindly provided by Prof. Graham Russell, Botnar Research Centre, Oxford University) were added to a small amount of scaffold cement per mg of dry weight. These amounts were chosen to match the bisphosphonate concentrations desired during in vivo implantation, which vary between Zoledronate and OX14 due to their different potencies. The scaffold was then processed as usual and soaked for 24 hours. All powders were processed on a Perkin Elmer Spectrum 100 FTIR spectrophotometer. All spectra were normalised from 1-100 using OriginPro software.

2.4 MSC isolation from human umbilical cords

Human umbilical cords were sourced from Singleton Hospital, and cords were taken only with fully informed consent of the anonymised donors(West Wales Research Ethics Committee REC11/WA/0040). The umbilical cords were stored in PBS during transport. The veins and artery were removed, and the cords were cut until paste-like. This paste was then spread onto T25 culture flasks and incubated at 37°C for 10 minutes to improve surface adherence. 0.5ml of FBS (Gibco) was added to the culture flasks, after which the flasks were incubated at 37°C overnight. The next day, 1.5ml culture medium (1:1 DMEM: F12(Gibco) with 10% FBS(Gibco) and 1% penicillin/streptomycin(Gibco)) was added to the plates. After one more day, the medium was topped up to 5ml, and the medium was exchanged every 2-3 days. MSCs started adhering to the surface after approximately one week and were subcultured when making up about 50% of the plate surface area. Cell subculture was performed by washing the flasks with PBS (Gibco), detaching the cells with 0.25% Trypsin-EDTA (Gibco), and then adding cell culture medium to inactivate the Trypsin-EDTA. Cells were centrifuged at 1200rpm(Eppendorf 5810 R) for 5 minutes and either seeded in new flasks for subculture, frozen in FBS (Gibco) with 10% DMSO (Sigma-Aldrich), or used in experiments. In-between subcultures, the medium was changed every 2-3 days.

2.5 Cell adherence to scaffolds

It is essential to find a method to successfully seed cells onto scaffolds and create a 3D culture. Considerations are the seeding- and culturing method, the number of cells seeded, and the amount of scaffold seeded per batch. In order to find an optimal amount, several millions of umbilical cord MSCs were seeded on 10g of scaffold in a spinning bioreactor, which was only turned on after allowing cells to attach overnight. The scaffolds were re-seeded every 3-4 days in order to improve cell attachment to the scaffolds. These tests were largely unsuccessful; hence, a small-scale approach was chosen in which approximately 0.017g of scaffold was seeded with the MSCs in 48-well plates. This approach yielded clumps of scaffold held together by cells after culturing, hereafter referred to as nodules. To find a suitable cell seeding amount for nodule creation, cells were seeded onto 0.017g of scaffold powder in 48 well plates

at 31,250, 62,500, 125,000, 250,000 or 500,000 cells per well. Alamar Blue assays and confocal fluorescent microscopy were performed at 3, 7, 14 and 21 days after seeding.

2.6 Confocal microscopy

Before confocal microscopy, samples were stained with a dye solution containing 50 µg/mL Hoechst (Invitrogen) and usually also 4 µM of CalceinAM (Invitrogen) in PBS. The samples were then incubated at 37˚C for approximately five minutes. Confocal microscopy was performed on a Zeiss LSM710 imaging system.

2.7 SEM

Any samples destined for SEM were fixed in 4% glutaraldehyde (Sigma-Aldrich) and then dehydrated through immersion in a series of ethanol dilutions: 40%, 70%, 80%, 90%, 95% and 100% ethanol for one hour each, then 50:50 ethanol/hexamethyldisilane. Samples were then immersed in 100% hexamethyldisilane, followed by another soak in 100% hexamethyldisilane and overnight evaporation. Dried samples were coated with chromium using a chromium coater (Quorum Q150T ES) until sufficiently conductive. The samples were then imaged on a Hitachi S-4800 SEM.

2.8 Cell differentiation on HA/CC scaffold

Cells were seeded at 250,000 cells/well in a 48-well plate on approximately 0.18g of HA/CC scaffold granules and cultured in medium. The medium was refreshed every 2-3 days. After one week, the nodules were strong enough to hold their shape even if picked up. At this stage, the nodules were divided into three groups and treated with normal medium, osteogenic medium (medium with added 50µg/ml L-ascorbic acid(Sigma-Aldrich), 10mM β-glycerophosphate(Sigma-Aldrich) and 1µM dexamethasone(Sigma-Aldrich)) and retinoic acid medium (osteogenic medium with 20uM retinoic acid (Sigma-Aldrich)). The nodules were then cultured for 1, 7, 14 or 28 days before being harvested for confocal fluorescent microscopy and SEM. ELISA assays were performed using BMP-2 and BMP-7 ELISA kits (ABClonal) according to the manufacturer's instructions. A number of samples were kept for 14 days and treated with Alamar Blue on days 1, 7 and 14.

2.9 Scaffold production for in-vivo implantation

The scaffolds used were produced as previously described(Xia et al., 2018). The prepared HA/CC scaffold was cut into pieces of approximately 1.5 mg in weight, and then autoclaved. The autoclaved scaffolds were divided into three groups and soaked in 200 µL 2.45µg/mL Zoledronate in PBS, 11.35µg/mL OX14 in PBS, or in PBS only for 90 minutes at RT. The liquid was then aspirated, and the scaffolds were dried at 37°C overnight.

2.10 In-vivo implantation of materials in mice

All in vivo experiments were performed at Johns Hopkins University in accordance with local and university regulations. The animal protocols were approved by the Institutional Animal Care and Use Committee of Johns Hopkins University, Baltimore, MD, USA (MO21M276). Three- to four-month-old male C57BL/6 (wt) mice were obtained through Jackson Laboratory (strain number: 000664). 54 C57BL/6 mice were injected with 0.18-0.25 mL anesthetic (13mg/mL ketamine hydrochloride (Ketalar) and 1.2ng/mL Xylazine Hydrochloride (Sigma-Aldrich) in PBS) and sheared. An incision was made in the leg, and one scaffold piece was implanted with tweezers in-between the tibia and fibula. The wounds were then sutured. The mice were placed back into their cages and left to wake up naturally. After 1, 14 or 28 days, the mice were anesthetized using FORANE (isoflurane USP, Baxter) gas. Four mice per experimental group were used for the day 1 timepoint, and five mice per group were used at days 14 and 28. The right limbs were harvested, after which the mice were perfused with PBS (Corning) and 10% formalin (Thermo Fisher Scientific) consecutively. The left limbs were then harvested as well and processed to remove the gastrocnemius muscles, any femur-adherent muscles, and the foot. The remaining muscle was then carefully trimmed to decrease the limb size. Processed left limbs were stored in 10% formalin at 4°C.

2.11 qPCR

The right limbs were processed immediately after harvesting. The gastrocnemius muscles and fibula were removed, and the tibia and remaining muscle were trimmed to include only the area around the scaffold. At this stage, the tissue from all mice in the same group was mixed. The tissue pieces were frozen using liquid nitrogen and

crushed in a mortar, then homogenized using a sonifier. Ribonucleic acid (RNA) was isolated from the tissue using the QIAGEN RNeasy mini kit. Reverse transcription was initiated by adding PrimeScript RT Mastermix (TaKaRa) to the RNA and holding the tubes at 37°C for 15 minutes, then at 85°C for five seconds before cooling. The Deoxyribonucleic acid (DNA), along with water and primers, was added to SYBR green PCR Master Mix (Qiagen) and run for 40 cycles. A list of the primers used and their sequences can be found in appendix 2.

2.12 µCT

Left limbs were taken from the formalin and wrapped in parafilm, then scanned in a Skyscan X-ray microtomography system (Bruker) at a voltage of 65kV and current of 153uA. A resolution of approximately 6.5 µm, pixel size of 6, rotation of 0.3 and high-resolution exposure time of 218ms were used for scanning. After scanning, the limbs were unwrapped and placed back in 10% formalin at 4°C. A consistent area of 0.096 mm^3 was selected and used for calculation of the bone volume/tissue volume (BV/TV) value.

2.13 Bone imaging

Fixed samples were embedded in London Resin Gold (Agar Scientific) with 1% w/v benzoyl peroxide (Agar Scientific) according to the manufacturer's protocol. Aluminium foil was used to position the blocks correctly and was embedded into the blocks, after which the resin was cured at room temperature. The resulting blocks were sanded at 600 and 1200 grit, then polished to 6 and 3 microns. The bones were photographed using a Tomlov TM-DM10 imaging system. SEM-EDX scanning of the samples was outsourced.

2.14 Statistical analysis

Statistical analyses were performed in IBM SPSS Statistics and GraphPad Prism. All data is presented as mean ± standard deviation. T-tests were used when comparing two groups, and 2-way analysis of variance (ANOVA) analysis was performed for comparisons between multiple groups. A p-value < 0.05 was considered statistically significant.

3. Results

3.1 HA/CC scaffold can be successfully produced

The scaffold was made by combining three powders, of which two react together to form hydroxyapatite. In order to confirm whether TTCP and $CaHPO_4$ react to form hydroxyapatite, scaffolds were prepared with and without a soaking step and then analysed using FTIR spectroscopy. Analysing pure hydroxyapatite and the other three main compounds of the scaffold revealed that $CaCO_3$ forms three clearly distinguishable peaks. HA and TTCP both have an absorption peak around 1000nm, though with distinct shapes. The former has a smooth and pointy peak, while the latter has a broader, jagged peak (Figure 2). CaHPO4 shows weaker absorption at a wider range.

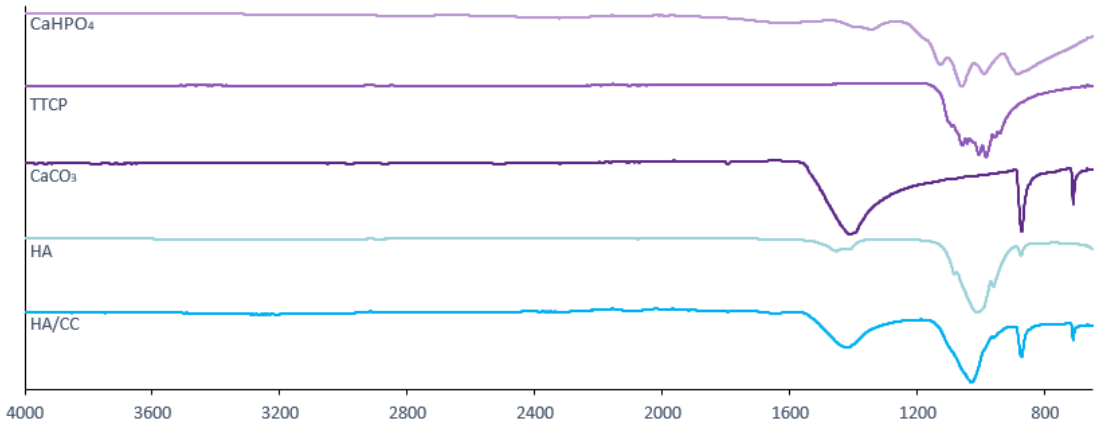

Figure 2. Infrared spectra of scaffold compounds and hydroxyapatite. *Calcium carbonate forms clear peaks at 700, 875 and 1400nm. Both HA and TTCP form peaks around 1000nm, though with clearly distinguishable shape. CaHPO4 absorbs a wider range of infrared radiation. Graph generated by Emma Steijvers using Microsoft Excel, 2022.*

After scanning unsoaked HA/CC scaffolds and scaffolds that had been soaked for 24, 48 and 128 hours, there is a distinct difference in the shape of the 1000nm peak between the unsoaked and soaked groups (Figure 3). Thus, it could be determined that while untreated HACC still consists of its three main compounds, HA was formed in all samples soaked in PBS. As the scaffold is soaked for a longer period of time, the HA peak becomes comparatively larger than the $CaCO_3$ peaks. This indicates a

possibility that HA formation is a slow process, and more HA has formed in the samples that were soaked longer. However, as the HA peak completely obscures the TTCP and $CaHPO_4$ peaks, an exact quantification is impossible.

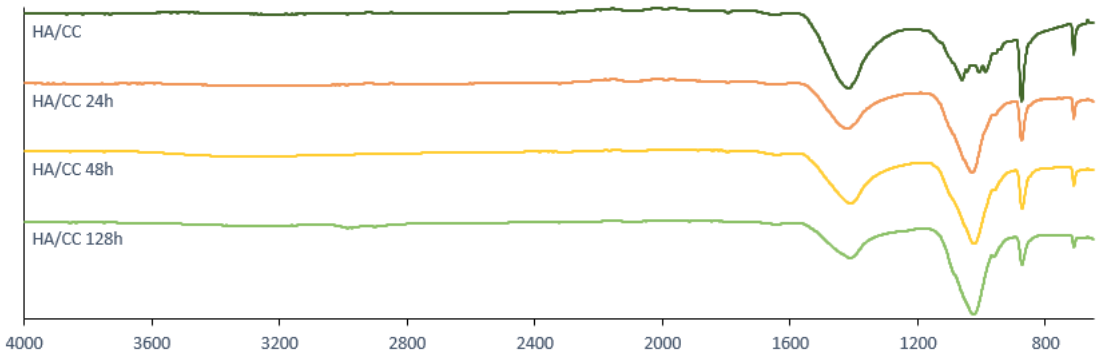

Figure 3. Infrared spectra of HA/CC scaffolds with different preparation methods. *The graph shows the infrared spectra of scaffolds that are left untreated and soaked in PBS for 24, 48 and 128 hours. The peak at around 1000nm is clearly distinguishable as mainly TTCP in the untreated HACC sample, while the shape corresponds to HA in all soaked samples. Graph generated by Emma Steijvers using Microsoft Excel, 2022.*

3.2 Bisphosphonates inhibit HA formation during scaffold production

Bisphosphonates strongly bind to calcium, which is present in the scaffold compounds required to form hydroxyapatite. In order to confirm whether the presence of bisphosphonates disturbs this reaction, scaffolds were made with OX14 and ZOL, which were then compared to unsoaked and soaked control scaffolds. The infrared spectra of bisphosphonate-scaffolds were distinctly similar to the unsoaked controls, having the rough peak that corresponds to the presence of TTCP, indicating that HA formation did not take place in measurable amounts (Figure 4). Scaffolds should therefore be prepared before adding bisphosphonates.

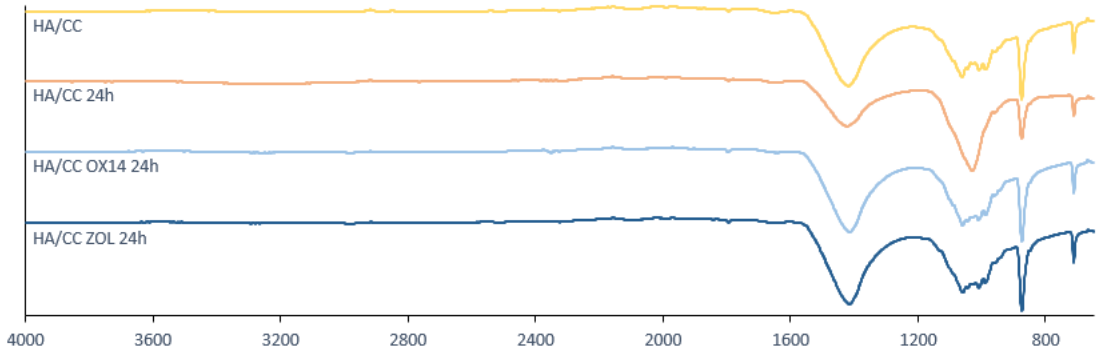

Figure 4. Infrared spectra of scaffolds with and without bisphosphonates. *The graph shows the infrared spectra of normal soaked scaffolds, unsoaked scaffolds and scaffolds made with bisphosphonates, then soaked. The peak around 1000nm indicates the presence of HA in the normally prepared scaffold, but only TTCP in all other groups. Graph generated by Emma Steijvers using Microsoft Excel, 2022.*

3.3 MSCs are able to adhere to HA/CC scaffolds

Cells were seeded onto scaffold granules and co-cultured in order to confirm whether MSCs can adhere to HA/CC scaffolds. After culturing in a bioreactor it was observed that cells do, in fact, adhere to and grow on the scaffold (Figure 5A). However, the cells do not jump from one HA/CC granule to another, and so while some granules ended up covered, others remained near empty. This problem could not be fixed by culturing for longer periods and/or re-seeding. In order to attain improved scaffold coverage, smaller quantities of cells and scaffolds were combined in 12-well plates (Figure 5B). In the 12-well plates, cell coverage of the scaffolds remained mediocre, ranging from ‘none’ to ‘low’ depending on the number of cells seeded. In addition, when seeding higher amounts of cells (2,500,000 on 0.085g of scaffold) the cells occasionally formed organoids instead of attaching to the scaffold (Figure 5C).

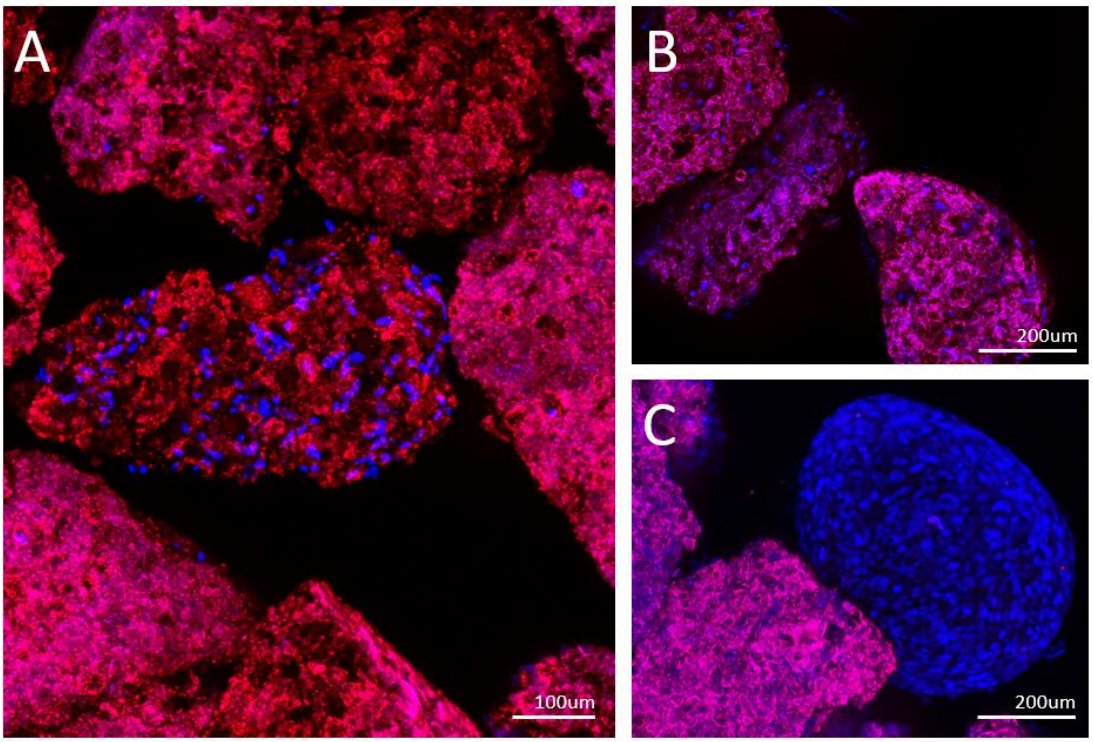

10x | DAPI Autofluorescence

Figure 5. Cells growing on HA/CC scaffold in a bioreactor (A) and 12-well plates (B, C). *In the bioreactor, cell coverage is high on some granules but very low on others. In 12-well plates, cell coverage is generally mediocre (B), and occasionally cell organoids are formed. (C) Images taken by Emma Steijvers, 2021.*

Reducing the amount further, and seeding cells on 0.017g of scaffold in 48 well plates, was comparatively much more successful. Cells attaching to the scaffolds were observed with confocal microscopy (Figure 6A). The cell coverage can be so high that the cells stitch the scaffold granules together, forming nodules strong enough to be gently picked up with tweezers (Figure 6B). Cell growth on the surface of these nodules was confirmed by SEM (Figure 6C, D).

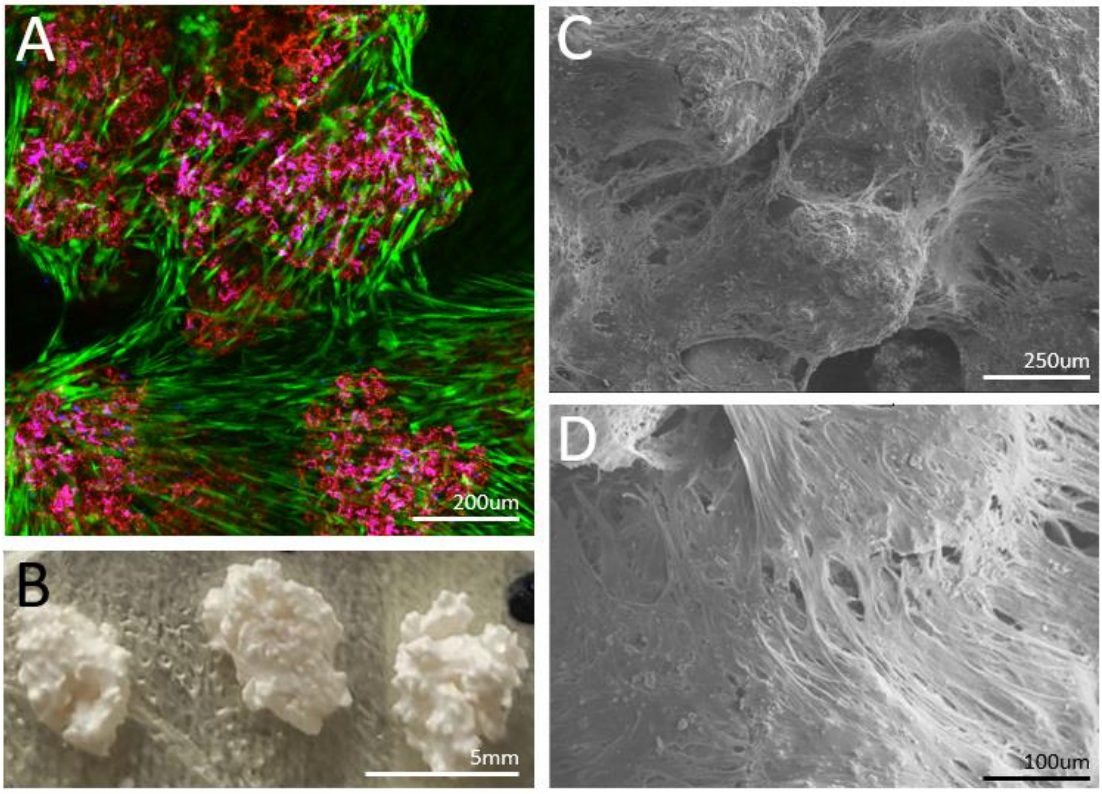

Figure 6. Nodules resulting from culturing cells and scaffold in 48 well plates. *These images show the cells attaching to the scaffold and forming larger nodules seen through confocal (A), by eye (B), and through SEM (C, D.) Images taken by Emma Steijvers, 2021.*

When seeding scaffolds, a question that comes to mind is the required seeding density. Larger amounts of cells require more resources; minimizing the number of cells seeded is therefore important. To assess the minimum required cell number, cells were seeded onto scaffolds in varying numbers and grown, after which the number of cells was assessed using confocal imaging and Alamar Blue testing. Confocal imaging of the scaffolds (Figure 7) shows that there is a balance to be found between cells seeded and time.

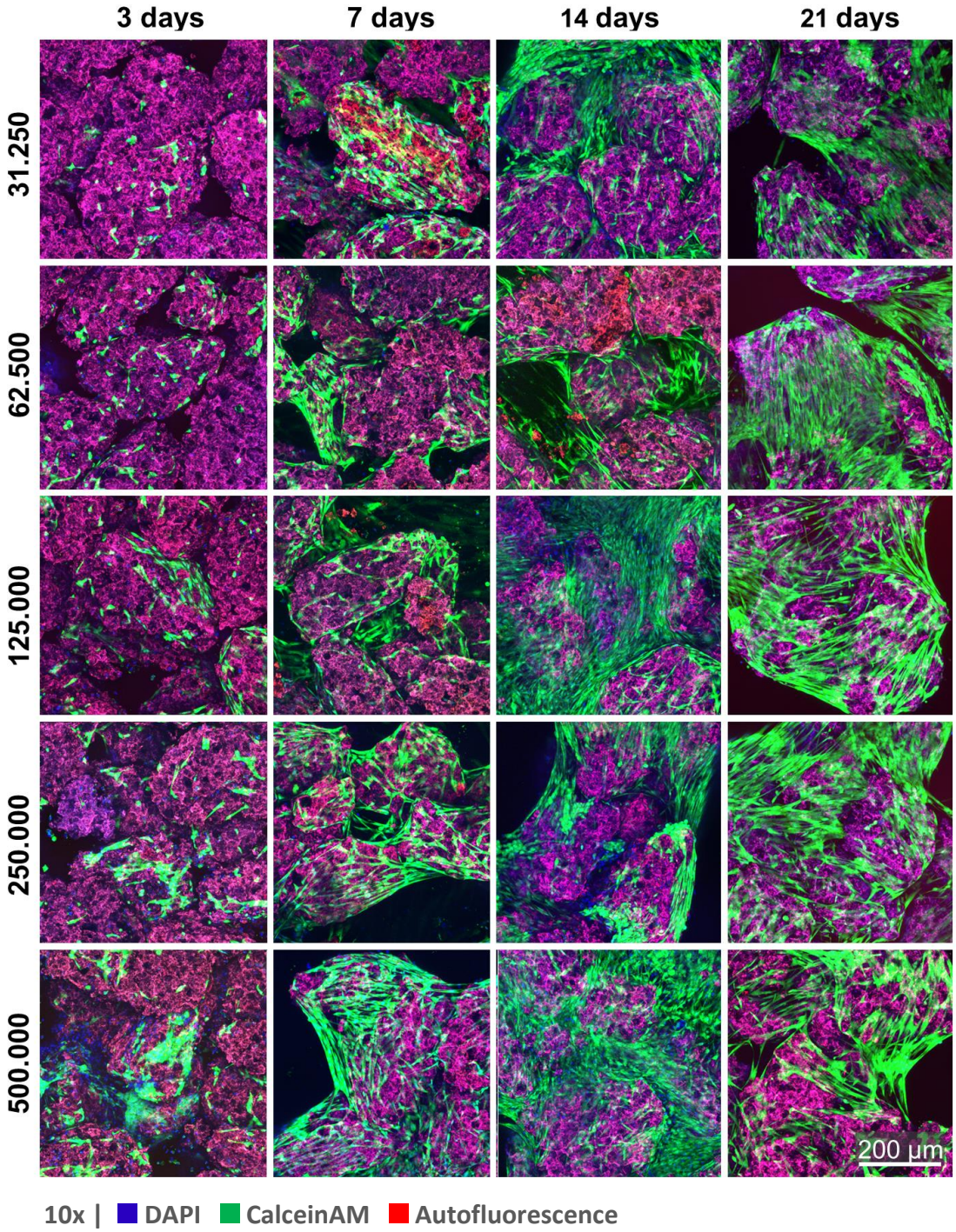

Figure 7. Cell coverage of HA/CC scaffold granules with different cell seeding amounts over time. *The image shows cells adhering to the scaffold in different amounts, with the amount increasing over time and when seeding more cells. Stained with DAPI in blue and CalceinAM in green. Scaffold autofluorescence is shown in red. Images taken by Emma Steijvers, 2021.*

Three days after seeding cells had attached to the scaffolds, but none of the scaffolds were fully covered, regardless of the number of seeded cells. After one week, the scaffolds where 250,000 cells or more were seeded were fully covered and ready for use. In scaffolds seeded with 31,250-125,000 cells, cell coverage had increased, but not to a usable degree. After fourteen days, all scaffolds were covered with cells regardless of seeding amount, and little difference could be seen between fourteen and twenty-one days of cell culture.

Alamar Blue testing of nodules with identical treatments also showed that while at earlier timepoints the metabolic activity roughly corresponded to the number of cells seeded, this effect diminished with time. At day 3 post-seeding there is a very large difference between the groups seeded with 31,250 and 500,000 cells, with the latter showing an approximately 3.5-fold increase in metabolic activity compared to the former. By day 7 the increase has become less than two-fold, and by day 14 there is significant overlap between the groups. The other groups behave similarly: At day 3 post-seeding each doubling in cell number leads to an 1.5-fold increase in metabolism with an exception for the 500,000 group seemingly hitting a ceiling.By day 7 this effect has largely been reduced, with doubled cell numbers only leading to a 1 – 1.25 fold increase, and by 14 days post-seeding there is no more linear relation between the amount of cells seeded and the metabolic activity(Figure 8).

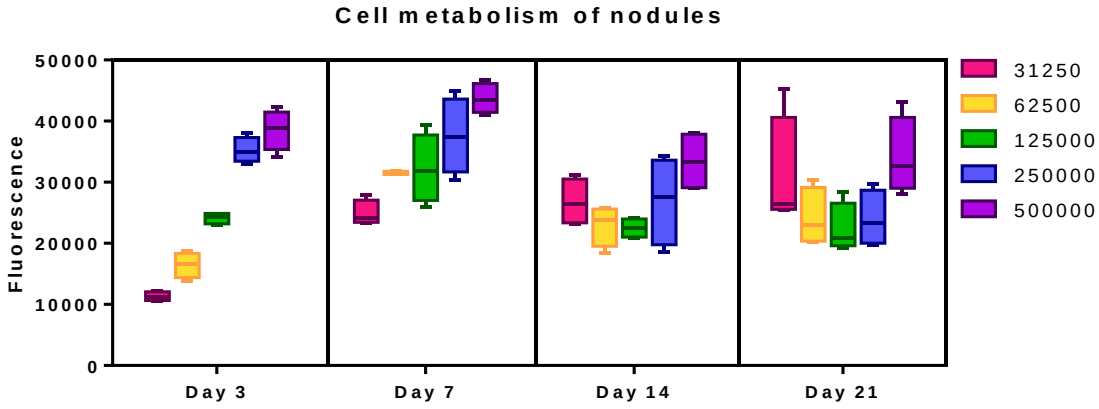

Figure 8. The metabolic activity of nodules seeded with different amounts of cells. *These graphs show the relative metabolic activity of nodules seeded with 31250, 62500, 125000, 250000 or 500000 cells, as measured by Alamar Blue assay. Graph generated by Emma Steijvers in GraphPad Prism, 2022.*

3.4 USMSCs can be differentiated on HA/CC scaffolds but require more enhancement

It has been proven that cells can be cultured onto HA/CC scaffold granules. The next step is then to osteogenically differentiate these cells in order to seed the scaffolds with osteoinductive compounds. To assess this, scaffolds were seeded with cells. After confluence was achieved the nodules were divided into three groups: a non-differentiated (ND) group, an osteogenically differentiated (OS) group, and an osteogenically differentiated group with retinoic acid (RA) added in an attempt to improve osteogenic enhancement. Cell morphology was assessed with fluorescent confocal microscopy and scanning electron microscopy. Fluorescent images show changes in cell morphology of differentiated cells compared to non-differentiated cells (Figure 9). Specifically, the ND group shows no morphological changes during the entire 21 days, retaining the clearly segmented elongated phenotype. For both the OS and RA groups, the cells change from elongated and separate entities to a more irregular-appearing mass of cells. These changes in cell morphology indicate that cell differentiation was successfully induced.

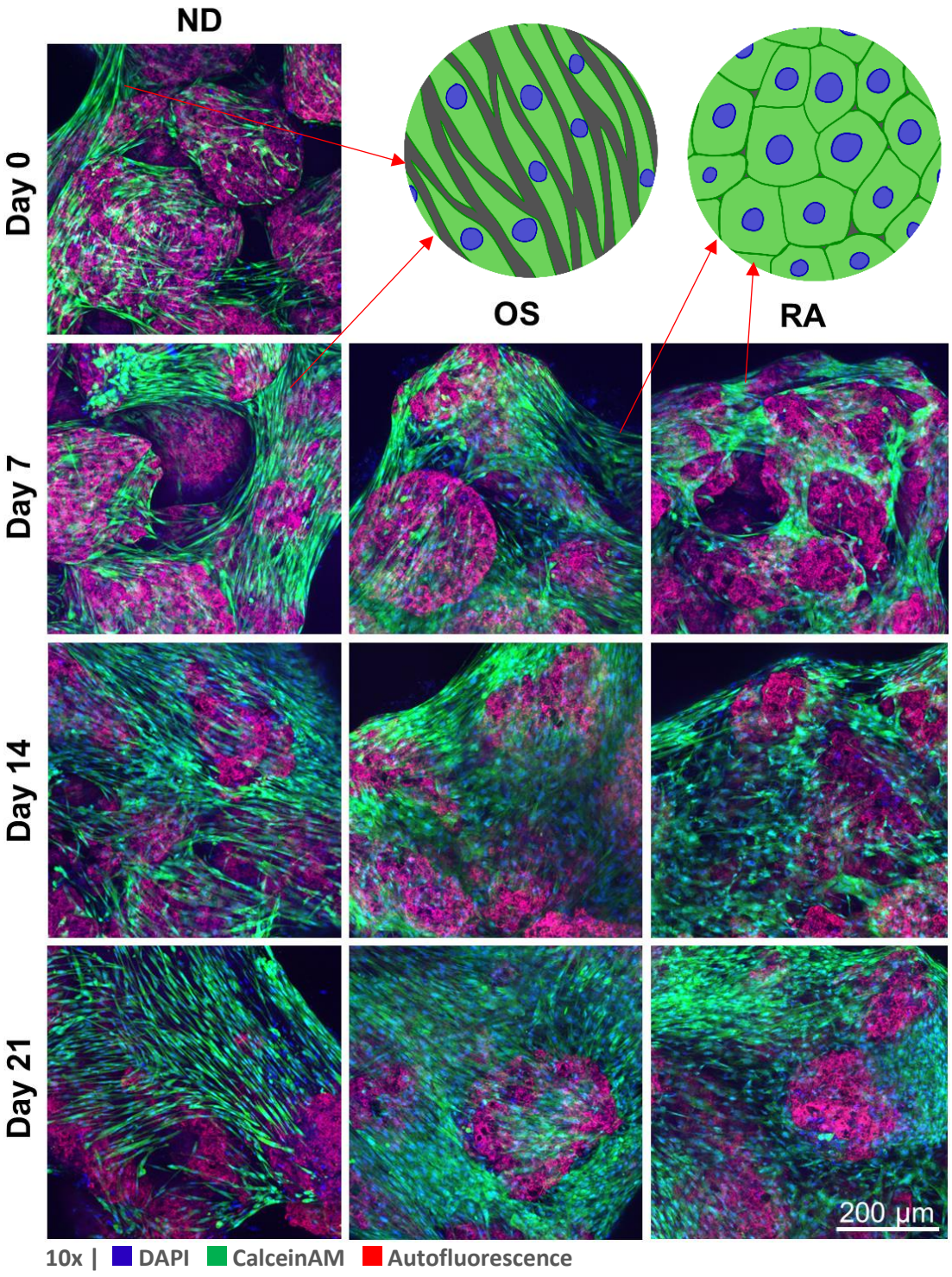

Figure 9. Morphological changes of MSCs adhering to scaffolds during differentiation. *The figure shows the cell morphology of MSCs cultured on scaffold in normal medium (ND), osteogenic medium (OS), and osteogenic medium enhanced with retinoic acid (RA) after 1, 7, 14 and 21 days. Cells cultured in osteogenic media change shape to be less elongated and increasingly disorganised. Stained with DAPI in blue and CalceinAM in green. Scaffold autofluorescence is shown in red. Pictures taken and schematic images created using Paint.net 5.0.2 by Emma Steijvers, 2022.*

SEM was used to image the cell surface in more detail. The morphological differences between cells are much less obvious due to the lack of colour, causing difficulty in distinguishing cells from each other. On a smaller scale, however, the SEM images show the generation of fibres and ball-like structures in higher numbers in the OS and RA groups compared to the ND group (Figures 10, 11). The fibres and spheres are likely to be collagen and bone-formation, respectively, though this cannot be said with certainty.

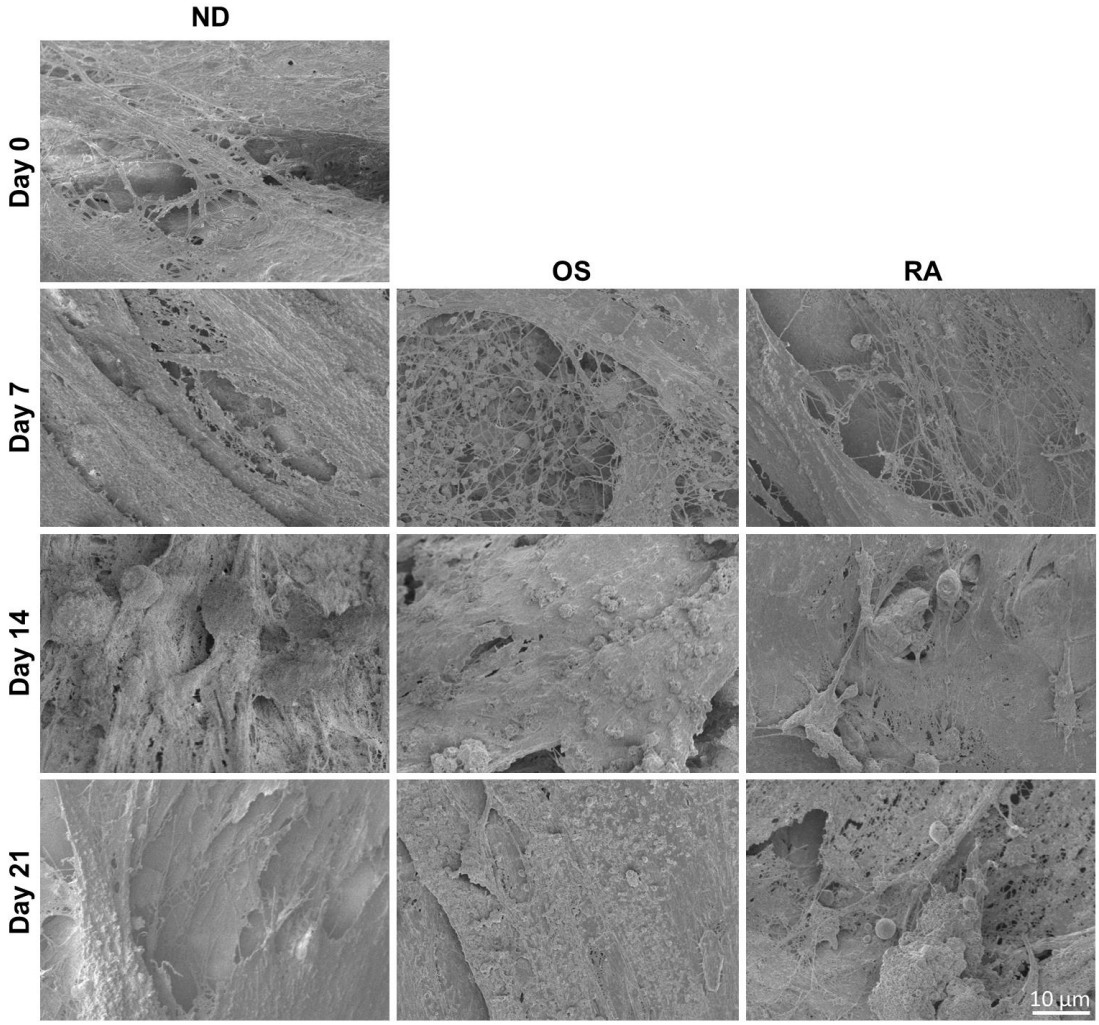

Figure 10. Morphological changes on the surface of MSC-seeded scaffolds imaged with SEM. *The figure shows a 2000x enlarged surface of nodules with cells attached in a non-differentiated group (ND), osteogenically differentiated group(OS), and osteogenically differentiated group with retinoic acid added to the medium (RA). 2000x enlarged. Images taken by Emma Steijvers, 2021.*

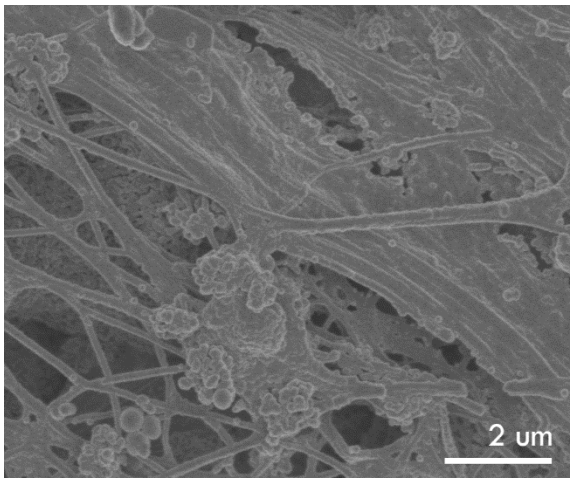

Figure 11. Close-up of the surface deposits on cell nodules. *This figure shows a 10,000x enlarged view of the fibres and ball-like structures that appear in higher numbers on the surface of differentiated nodules. The image shows a sample 7 days post-osteogenic differentiation. Image taken by Emma Steijvers, 2021.*

To assess the amount of cell activity on the scaffolds, an Alamar Blue assay was performed. Over time, the number of cells in the ND group increases a lot, then decreases again. The OS group shows a slow increase in cell activity, and the RA group a slow decrease (Figure 12A). At day 1 there was no significant difference between groups. After 7 days both the OS and RA groups had significantly less metabolic activity compared to the ND group. ($p<0.001$, N=6, one-way ANOVA) After 14 days the OS group showed less metabolic activity compared to the ND group ($p=0.024$, N=4-6), and the RA group had lower activity than both the ND ($p<0.001$, N=4-6) and OS groups. ($p<0.001$, N=6) Cells dying during osteogenic differentiation is common and these results are expected.

ELISA assays were used to quantify the BMP-2 and BMP-7 protein levels in cell-scaffold nodules (Figure 12B, C). There was no significance in BMP-2 content after 7 days. After 14 days the OS group had a significantly higher BMP-2 content compared to the two others ($p=0.003$, 1-way ANOVA, N=3). By day 21 this effect has been lost, and only the RA group is significantly lower than the two others ($p=0.04$, N=3). At day 7 the BMP-7 content was significantly lower in the RA group than the ND group($p=0.014$, N=3), with no significant difference between the others. After 14 days, much like BMP-2, the BMP-7 content was significantly heightened in the OS

group compared to the two others (p=0.001, N=3). After 21 days this effect lowered to a non-significant level, and only the RA-group was significantly lower than the OS group (p=0.015, N=3), though not different from the NS group. In short, the OS group performs slightly better than the ND group at day 14, but there is little effect at other time points. The RA group consistently performs worse than other groups throughout all time points. One possible explanation for this phenomenon is the decreased cell count: Fewer cells will naturally secrete fewer proteins.

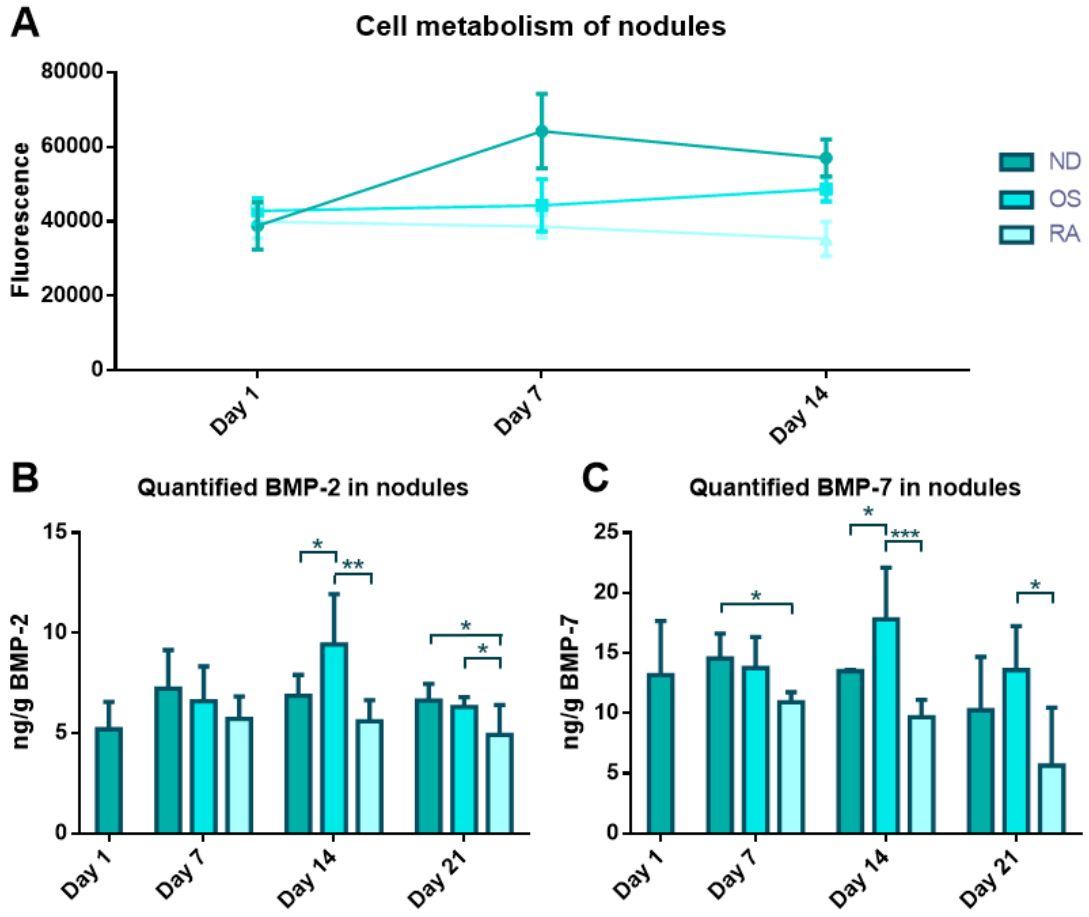

Figure 12. Quantification of cells (A) and BMPs (B, C) in nodules. *These graphs show the fluorescence units measured by Alamar Blue assay (A), and BMP-2 (B) and BMP-7 (C) quantified with ELISA in undifferentiated (ND), differentiated (OS), and differentiated with RA (RA) nodules. Graphs generated by Emma Steijvers in GraphPad Prism, 2022.*

3.5 Implanting HA/CC in mice leads to bone callus formation

HA/CC granules treated with PBS, OX14 or Zoledronate were implanted in-between the tibia and anterior tibialis muscle of 3 month old mice in order to assess the osteogenic capacity of these scaffolds. Limbs were harvested, embedded in resin, and then used for 2D imaging. Images were taken using a light microscope as well as using SEM-EDX technology. The pictures taken using a light microscope show a clear view of the implanted scaffolds as well as the calluses, showing that the calluses are much bigger at day 14 compared to day 28, and much bigger in all HA/CC groups compared to the sham control (Figure 13).

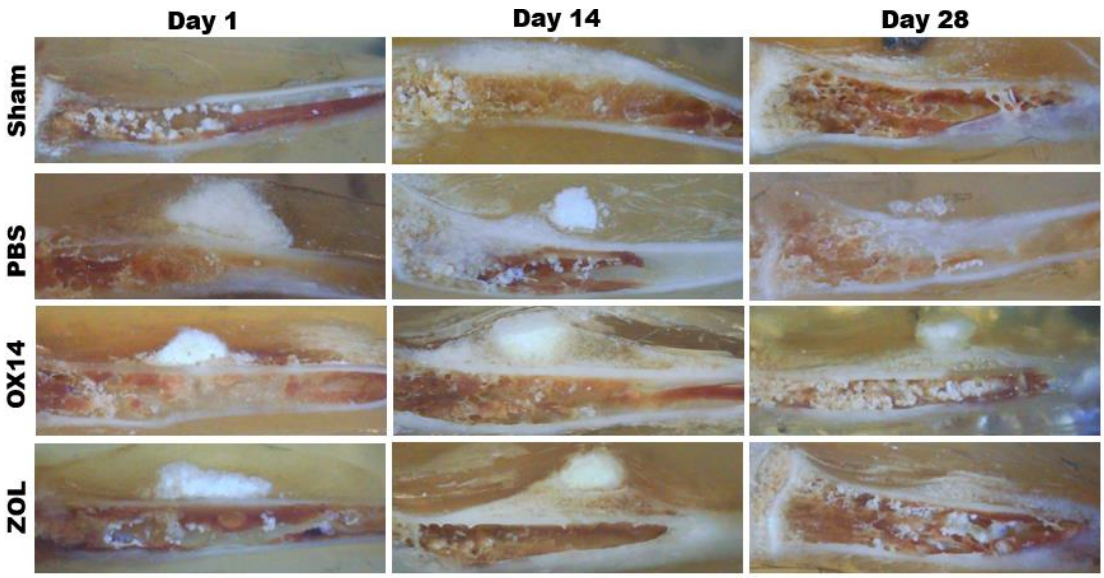

Figure 13. Pictures taken of the resin-embedded bones. *These pictures show the bones after resin-embedding and polishing. The scaffold is clearly visible, as are the calluses formed after 14 and 28 days in all non-sham groups. Images taken by Emma Steijvers, 2022.*

The pictures taken with SEM-EDX corroborate these findings. No group has any callus formation on day 1. The Sham group grew a small, dense callus on day 14 that had completely disappeared by day 28. The other groups had grown large calluses of new bone formation after 14 days, that by day 28 were all remodelled into smaller calluses with a clear distinction between cortical bone and bone marrow (Figure 14).

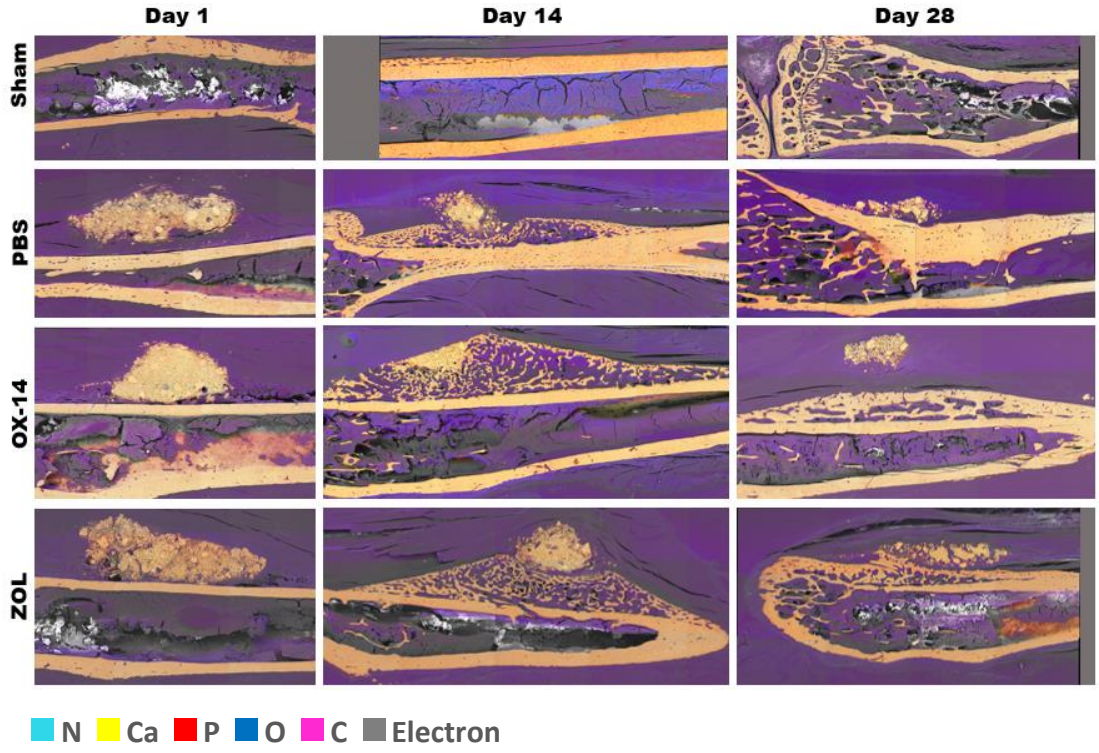

Figure 14. EDX-SEM pictures of the bone calluses. *Element analysis shows the difference between soft tissues (N, O, C, in cyan, blue and magenta, respectively) and bone (Ca, P, yellow and red, respectively.) Images were taken by Zhidao Xia in collaboration with Open University, and used with permission.*

3.6 The addition of Zoledronate leads to larger bone callus formations

To obtain an accurate volume measurement of the callus, limbs were scanned using high-resolution µCT. The scaffolds were then measured and quantified using cTAN software. The callus visibly changes over time: After one day no callus has formed yet, while after 14 days there is a large, uniform new bone formation and after 28 days cortical bone and bone marrow have distinctly formed (Figure 15A). The exception is the Sham group, where the callus formed after 14 days has disappeared completely after two more weeks. 3D analysis showed that 14 days post-implantation the zoledronate group has significantly more bone formation than the sham group ($p=0.014$, $n=5$, 1-way ANOVA) while the HA/CC and OX14 groups are not significantly distinct from any other (Figure 15B). 28 days post-surgery the HA/CC and OX14 groups have significantly more bone formation than the Sham group, and the ZOL group has significantly more bone than every other group. OX14 treatment did not lead to more bone formation compared to the bisphosphonate-free control scaffolds

(p<0.001, n=4-5, 1-way ANOVA)(Figure 15C). This indicates that implantation of HA/CC in-between the tibia and anterior tibialis muscle encourages bone formation, and that this effect may be enhanced by adding Zoledronate to the scaffolds.

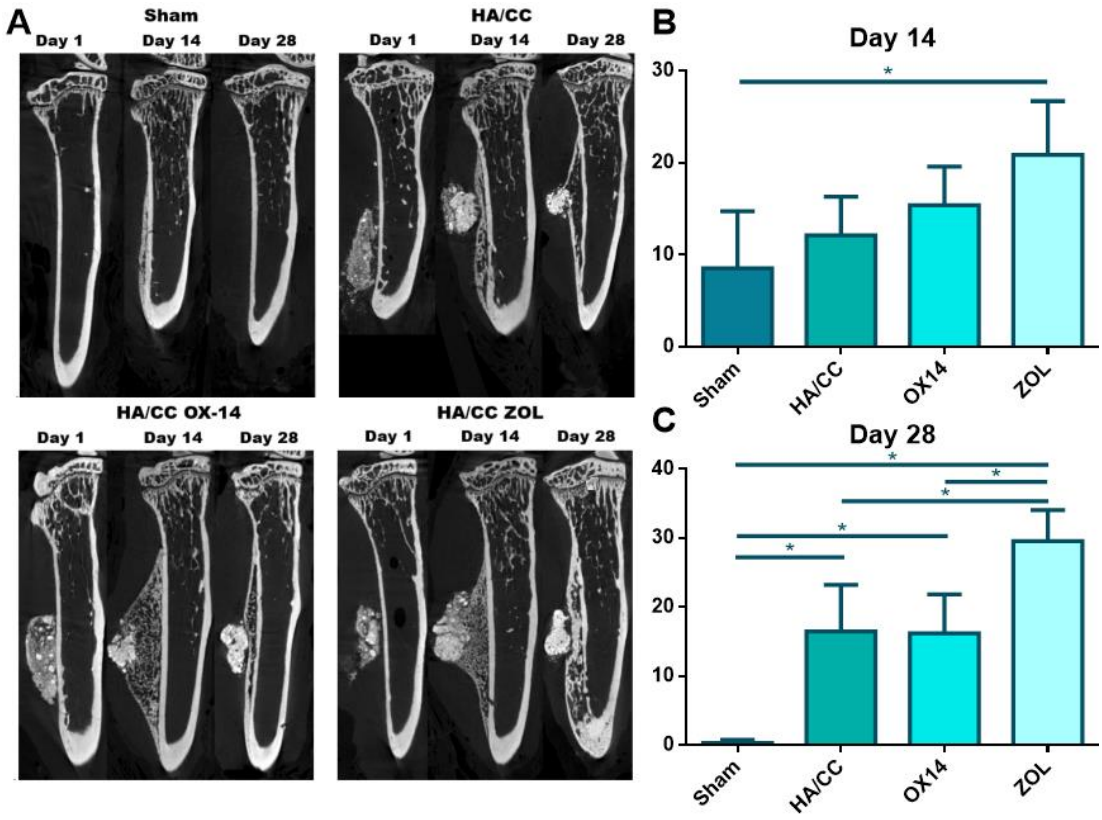

Figure 15. Bone calluses as scanned by µCT (A) and their BV/TV values (B, C). *(A)Representative images of the bones 1, 14 and 28 days post-surgery. (B, C) The BV/TV values of the bones at day 14 and day 28. (N=4-5) Images taken from DataViewer reconstruction and graphs generated in GraphPad Prism by Emma Steijvers, 2022.*

3.7 Gene expression analysis

qPCR was performed on bone calluses and their surrounding areas to assess changes in the expression levels of genes associated with callus formation. One day post-implantation there was an increase in osteoblast related genes in all groups compared to sham, both those relating to osteoblast activity (TGF-B1, BMP-2) and osteoblast differentiation(OSX, OCN, Col1a1.) Conversely, most genes relating to osteoclast differention and fusion were downregulated or unchanged in all HA/CC groups. Osteoclast differentiation gene CSK is the main exception, being

upregulated in all groups compared to Sham (Figure 16). Innervation genes Netrin1 and DCC are very downregulated in all groups compared to Sham, but PGP9.5 is very strongly upregulated in the HA/CC and ZOL groups. Likewise, the vascularisation is inconsistent: Angiogenin is very upregulated in all three HA/CC groups, but PdgfBB is downregulated for HA/CC and ZOL, yet upregulated for OX14 (Figure 17).

After 14 days the osteoblast genes had mostly neutralised in the HA/CC group. The osteoblast activity genes are only upregulated in the ZOL group, while the osteoblast differentiation genes appear most upregulated in the OX14 group, though some data is missing for the ZOL group. The osteoclast genes were mostly neutralised by this point as well, with the exception of ZOL being upregulated in osteoclast differentiation genes CSK and CSFR, as well as fusion gene CD47. Vascularisation and innervation had, likewise, mostly neutralised, though OX14 showed a reduction in PdgfBB (Figures 16, 17).

By day 28 the osteoblast activity genes were highest in the HA/CC group, neutral in the OX14 group and slightly lowered in the ZOL group. The differentiation genes, however, are extremely high in both bisphosphonate groups compared to the HA/CC and sham groups. The osteoclast genes are neutral at this point, with the exception of CSFR being strongly heightened in the bisphosphonate groups. Likewise, vascularisation and innervation were mostly neutralised with the exception of extremely high ZOL in PdgfBB and PGP9.5 (Figures 16, 17).

Figure 16. ***The expression levels of gene markers for osteoblast activity and differentiation, and osteoclast differentiation and fusion.*** *The expression levels are compared in the sham, HA/CC, HA/CC OX14 and HA/CC ZOL groups. Graphs generated by Emma Steijvers in GraphPad Prism, 2023.*

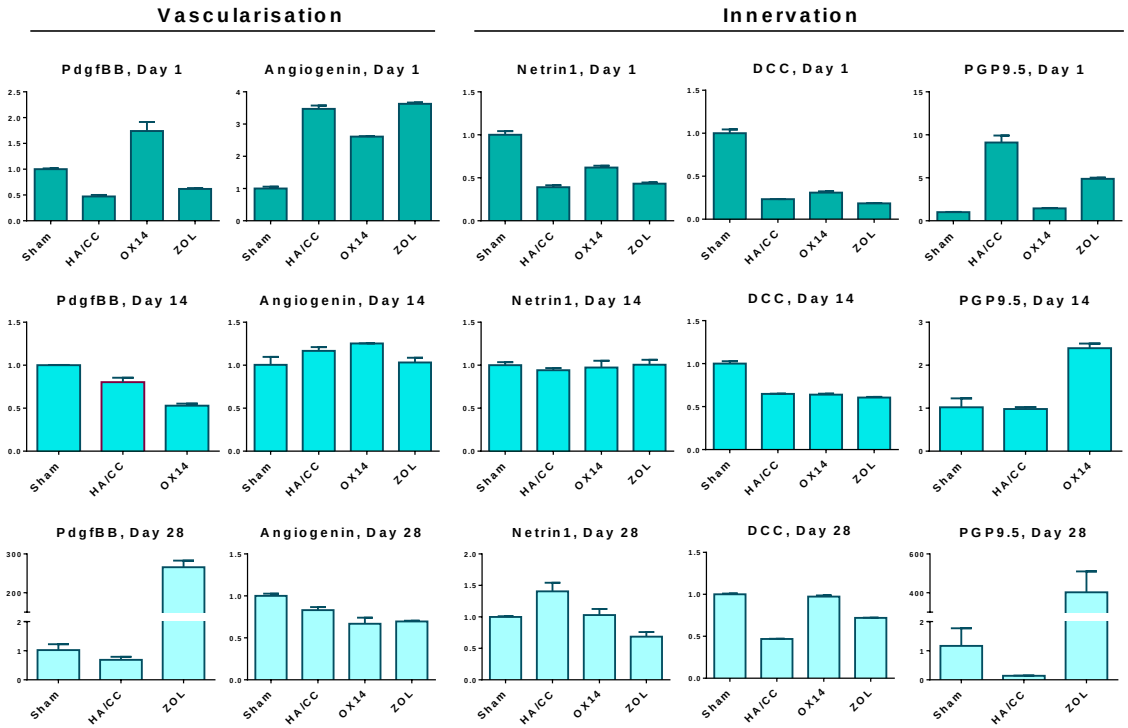

Figure 17. ***The expression levels of gene markers for vascularisation and innervation.*** *The expression levels are compared in the sham, HA/CC, HA/CC-OX14 and HA/CC-ZOL groups. Graphs generated by Emma Steijvers in GraphPad Prism, 2023.*

4. Discussion & Conclusion

The aim of this study was to find a suitable method to produce HA/CC scaffolds with enhanced osteoinductive capacity to improve patient outcomes and healing time. The HA/CC scaffolds themselves were produced as described in previous research(Xia et al., 2018) with some minor alterations. HA/CC was successfully created, as evidenced by FTIR spectroscopy: The 1000nm peak, corresponding to TTCP when flat with multiple spikes and to HA when presenting as one large spike, clearly changes shape after 24 hours of soaking the scaffold in PBS.

It has also been proven that adding bisphosphonates to the scaffold during production inhibits HA formation. Therefore, they can not be added directly to the cement but have to be added later through either soaking or coating. Soaking theoretically works through the bisphosphonate calcium bonding together and was shown to be a viable option, seeing as the zoledronate-soaked scaffolds yielded significantly higher callus formation. This method of soaking HA/CC scaffolds in bisphosphonates has previously been used as well(Fu et al., 2013). A disadvantage of soaking is that the exact amount of bisphosphonate that ends up in the scaffolds is hard to determine: Attempts to use UV-VIS spectroscopy on the remaining liquid were foiled by dissolving gelatine in the HA/CC scaffolds. The varying binding capacity between different bisphosphonates could be a factor here as well. Ray et al. avoided this problem by coating their scaffolds rather than soaking them(Ray et al., 2018) and were able to determine the amount of bisphosphonates on the scaffolds even after washing; such a method may prove useful when comparing different bisphosphonates or determining a clinically relevant amount of bisphosphonates to add.

4.1 Scaffold improvement through cell culture and differentiation

Another main goal was to subsequently enhance the bone formation of these scaffolds. The enhancement was attempted through two methods: 1) seeding cells onto the scaffolds so that they deposit growth factors onto the scaffold, and 2) adding bisphosphonates to the scaffold for their anti-resorptive function. The first method has been widely used in research. Scaffolds of varying base materials are produced,

then seeded with cells and cultured, usually in bioreactors. Bioreactors are very commonly used in bone scaffold development, with variations occurring in the type and the settings used. Spinning and perfusion bioreactors are the most common types used, being found in many bone scaffold seeding and culturing studies(Gooch et al., 2001; Grayson et al., 2011; Temple et al., 2013; Vunjak-Novakovic et al., 1998). Many studies use static culture of the scaffolds(Hasegawa et al., 2010; Lode et al., 2008; Wilson et al., 2002; Zhou et al., 2006) despite others claiming that it is ineffective, halting nutrient flow inside the grafts and depleting the oxygen in the medium(Gooch et al., 2001).

Despite many studies finding success with bioreactors, and bioreactors theoretically being the preferable option due to their improved nutrient flow, the use of a bioreactor to seed umbilical cord MSCs onto HA/CC scaffold granules was largely unsuccessful. While some MSCs attached to the scaffolds, there was little proliferation before they ultimately died. The granule shape of the scaffolds forms a problem in spinning bioreactors. As the granules float around, some are crushed by the spinning mechanism, releasing fine particles that increase the pH of the medium.

Small-scale static cultures were much more successful. Adding 0.017±0.02 g dry weight of 300-400µm scaffold granules to 48 well plates, along with varying amounts of MSCs, reliably produced nodules consisting of HA/CC granules held together by cells. Attempts to scale up this process failed. The surface area to scaffold ratio may well be a factor: During nodule formation, the networks of MSCs and HA/CC granules were attached to both the HA/CC granules and the plate surface before being manually disturbed. One possibility is that this small-scale method works best because the plastic adherent MSCs proliferate and then migrate onto the scaffold. In future research, this could be determined by testing larger areas of ‘monolayer HA/CC granule’ culture.

The seeding method is unlikely to be a cause of the poor performance in scaling up. A comparative study showed that some seeding methods perform better than others, but every method was able to deposit cells onto the scaffolds. Pipetting cells onto the scaffold directly, the method used during our experiments, even performed well

compared to others(Hasegawa et al., 2010). Many more studies were able to seed cells directly on scaffolds, even in the case of scaffolds suspended in medium(Seebach et al., 2010; Vunjak-Novakovic et al., 1998; Zhou et al., 2006). Furthermore, the same seeding method was used for the successful small-scale nodule formation and the unsuccessful larger-scale and bioreactor culture attempts.

Likewise, the number of MSCs seeded onto the scaffolds is not a large factor in the success rate. Literature is inconsistent on this subject, with some articles claiming that seeding few cells onto the scaffold leads to poor cell migration into the scaffold (Lode et al., 2008) while seeding many cells can lead to reduced cell proliferation(Wilson et al., 2002; Zhou et al., 2006), and yet others find that seeding high numbers of cells is beneficial as it leads to an increase in the production of osteogenic compounds(Vunjak-Novakovic et al., 1998). For the production of MSC-HA/CC nodules, the number of cells seeded did not have a large effect on the end result. Using very large amounts of MSCs – 250,000 to 500,000 per 0.017±0.02 g dry weight of scaffold – did lead to faster nodule formation. In this case the nodules were ready for use after only one week of culture, whereas equal amounts of scaffold seeded with 31,250, 62,500, or 125,000 MSCs took two weeks to be covered in cells to the point of nodule formation.

Alamar Blue testing confirmed that while the 500,000 MSC seeded group had the highest metabolic activity throughout every time point, the difference diminished over time. Additionally, the group with the lowest number of MSCs seeded (31,250) had a higher total metabolic activity than any of the middle groups, rivalling that of the 500,000 MSC group by day 28. A cost-benefit analysis between the expense of obtaining MSCs versus the expense of culturing the nodules for another week before further use would be essential to determine which method is more economical: Culturing MSCs for seeding requires medium and flasks, but scaffold culture requires frequent medium changes as well. Thus, the correct amount of cells to seed remains controversial, especially since the optimal amounts may very well differ between granules and 3D-shaped scaffolds, the intended end product.

The cells seeded onto grafts are usually some variant of osteoprogenitor. This is not necessarily the case, and a number of studies have seeded scaffolds with osteoblasts and chondrocytes(Vunjak-Novakovic et al., 1998; Zhou et al., 2006). Still, mesenchymal stem cells, usually from bone marrow origin, are preferred due to the relative difficulty in sourcing and culturing osteoblasts and chondrocytes. In order to maximize the deposition of osteogenic factors, the next step is usually to osteogenically differentiate the MSCs. This is done by culturing the seeded scaffolds in cell culture medium supplemented with dexamethasone, β-glycerophosphate, and often also ascorbic acid(Ahmed et al., 2019; Hasegawa et al., 2010; Lode et al., 2008; Malladi et al., 2006; Wilson et al., 2002).

The osteogenic differentiation of MSCs using a combination of dexamethasone, β-glycerophosphate, and ascorbic acid is a very common technique. This study also found that it was successful in inducing osteogenic differentiation. Confocal fluorescent microscopy showed a clear morphological difference between cells that had been differentiated and those that had not, with undifferentiated MSCs retaining their elongated spindle shape and differentiated cells taking on a more round shape. This finding was also noted by other studies(Ahmed et al., 2019). Images taken using SEM appear to show more bone and collagen deposits on differentiated samples, though a quantitative analysis was not performed.

Overall, studies that osteogenically differentiate MSCs tend to find an increase in osteogenic compounds, such as BMPs and ALP, post-differentiation. The current study corroborates this to an extent. ELISA assays revealed that the nodules with osteogenically differentiated MSCs had higher amounts of BMP-2 and BMP-7 compared to the undifferentiated group after 14 days of culture, but not after 7 or 21 days. A partial explanation for this, especially at day 7, may be the cell death linked with osteogenic differentiation. At day 7 the number of cells was, on average, 30% lower in osteogenically differentiated nodules compared to undifferentiated nodules. The difference in BMP-2 and BMP-7 expression was much smaller, indicating that the amount of BMPs expressed by each cell is higher. The decrease after three weeks of culture could potentially be explained by negative feedback loops: BMP-2 can induce the expression of BMP antagonists such as GREM-2, which

may inhibit its expression at later time points(Luo et al., 2021). Alternatively, over-culturing the cells for too long could cause other changes in the cells, such as the induction of senescence, changing their gene expression patterns.

4.2 Enhancement of cell differentiation

The addition of retinoic acid to osteogenic differentiation medium is controversial even in literature. Many studies report that its addition induces the osteogenic differentiation capability of MSCs(Cowan et al., 2005; Hisada et al., 2013; Malladi et al., 2006; Zhang et al., 2010), while a smaller number present opposing results(Ahmed et al., 2019; Wang et al., 2008). In this study, the group treated with retinoic acid in addition to osteogenic differentiation medium showed either equal or significantly lower BMP-2 and BMP-7 expression compared to the other groups in all time points. This is unexpected despite the controversy in literature, as previous research in this group has corroborated the findings that RA is osteogenic. There may be multiple causes at play. The osteogenic differentiation of MSCs reduces their proliferation, an effect mirrored by several studies. Notably, the addition of RA reduces MSC proliferation even further and reduces it even without the presence of other osteogenic compounds(Cowan et al., 2005; Malladi et al., 2006; Wang et al., 2008). Alamar blue testing confirmed that the number of cells was lowest in the RA group at every time point. This has likely played a part in reducing the BMP-content.

Another possibility is the duration of RA exposure. Interestingly, RA appears to have opposite effects on preadipocytes and preosteoblasts, both MSC-derived lineages. In vitro studies found that the addition of RA to preadipocytes or MSCs leads to the upregulation of Wnt signalling and, subsequently, the induction of osteogenic differentiation(Liu et al., 2014; Skillington et al., 2002; S. Zhang et al., 2016), but that its addition to preosteoblasts led to the downregulation of Wnt signalling as well as reduced osteogenic differentiation(Roa et al., 2019).

Hisada et al. suggest that RA may have opposing roles in early- and late-stage osteoblastogenesis. This would explain why RA has a positive influence on preadipocytes and a negative effect on preosteocytes, which are further into the osteogenic differentiation process. It is also consistent with a number of studies that

show an RA-induced increase in ALP expression after 7 days but not at later time points(Ahmed et al., 2019; Zhang et al., 2010). This suggests that the addition of RA may be time-sensitive. Perhaps an initial short-term exposure to RA is more beneficial for MSC osteogenic differentiation compared to the continuous exposure used over the course of this study.

The amount of growth factors required to make a scaffold osteoinductive is highly dependent on the nature of the scaffold. It is dependent on both the dosage and the release rate, the latter of which is influenced by scaffold material and the method of BMP-addition. In general, the physical entrapment of BMPs inside the scaffold slows the release rate and reduces the required amount of BMPs. Many studies have added BMPs to scaffolds, but not all are concerned with attempting to reduce the amount as far as possible. Osteoinductive concentrations of BMP-2 range from 51 ng/mm mm^2 of defect area in hydrogel scaffolds to 1 $\mu g/mm^2$ in titanium scaffolds, a 20-fold difference. Other materials require amounts somewhere in between, namely 79 ng/mm^2 in synthetic polymer scaffolds and 191 ng/mm^2 in silk polymer scaffolds(Ben-David et al., 2013). These differences can in large part be ascribed to the scaffold material and method of BMP-addition: BMPs are often directly incorporated in hydrogel scaffolds and become physically entrapped by the polymer strands, while on a titanium scaffold they are necessarily present only on the outside.

The amount of BMPs present in natural grafts is, again, different. Many scientists have attempted to determine the BMP contents in DBM and have measured wildly different amounts. The measured BMP-2 content ranged from as low as 2.11 ± 1.26ng/g in one study to 21.4 ± 12.0 and 20.2–120.6 ng/g in others. BMP-7 showed slightly more consistent measurements, those being 84.1 ± 34.4 ng/g in one study and 54.2–226.8 ng/g in another(Bae et al., 2006; Pietrzak et al., 2006). DBM is a natural product and the BMP content varies. While the exact cause of these variations is controversial, with some studies claiming that age made a significant difference but gender did not and vice-versa, there is a definite lot-to-lot variability that has been shown to influence its osteoinductive potential(Honsawek et al., 2005; Schwartz et al., 1998). Auto- and allografts, being less processed compared to

DBM, are expected to contain higher amounts of growth factors on average. Still, the BMP content of DBM influencing its osteoinductive potential is a clear indication that the relatively low amounts of BMPs present in DBM can nevertheless be high enough to enhance their osteogenicity.

The amounts of BMPs found in this study were fairly low, even compared to the amounts found in DBM. Assuming that the cell remains add negligible dry weight, the amounts of BMP-2 measured in nodules ranged from approximately 3.8 to 8.9 ng per gram dry weight of scaffold in undifferentiated samples, and 5.1 to 12.3 ng/g in osteogenically differentiated samples, disregarding the RA group. Likewise, for BMP-7, the measurements were 7-17.8 and 10-21 ng/g, respectively. The BMP-content is somewhat similar to that measured in DBM, though still on the low end.

Both the scaffolds produced in this study and DBM have a very low BMP-content compared to the studies performed on artificial grafts, but DBM is still osteogenic. A number of reasons could explain the higher BMP-concentrations required in artificial grafts compared to DBM. For one, the base materials are different. The release rate of BMPs remains a concern, and optimised BMP-contents cannot be freely translated between different materials. DBM is a complex material consisting mainly of collagen, the exact part of bone that BMPs attach well to(Nguyen et al., 2007). As natural bone consists of cells entrapped in a matrix, and these cells produce BMPs, the manner in which BMPs are physically entrapped into the scaffold is likely different compared to artificial scaffolds.

Another possible explanation is the variety of growth factors present in the scaffolds. The studies seeding scaffolds with BMPs or other growth factors generally seed them with a single compound or, at best, a combination of interest. On the contrary, DBM, allografts and autografts all contain a mixture of growth factors. Aside from various BMPs this includes compounds like TGF-B, RunX2, osteocalcin and osteonectin(John Martin et al., 1988). In other words, while the total BMP-2 or BMP-7 content may be much lower, the total amount of osteoinductive factors may not be. Additionally, certain factors, notably BMP-2/6 and BMP-2/7, form heterodimers with different functions to the original proteins that further enhance the osteoinductivity of the

DBM(Loozen et al., 2018; Lyons et al., 1995). The method used in this study, where cells are cultured onto HA/CC scaffolds and differentiated, is expected to generate a similar profile of osteoinductive compounds compared to allografts and DBM.

The latter explanation is especially relevant for the nodules produced in this study, as the cells that produced BMP-2 and BMP-7 have undoubtedly expressed many proteins, various growth factors being among them. The former may have influence to a lesser extent as the cells are expected to produce some extracellular matrix, though this cannot be said with certainty as collagen production was neither visualised nor quantified. Because of the natural variety of growth factors deposited in the cell-cultured nodules it may be reasonable to compare them to natural grafts such as DBM and allografts instead of artificial grafts, even though they themselves are artificially produced.

Still, the BMP content should be somewhat higher than it is now. The amount of BMPs cultured in these nodules is on the low side even compared to DBM, and the osteoinductivity of DBM is proportional to its BMP-content(Honsawek et al., 2005). Furthermore, auto- and allografts are expected to have higher growth factor contents than DBM as they are derived from the same source but less heavily processed. Lastly, the decellularisation process, a necessity to reduce immunogenic compounds, is expected to remove some of the BMPs present in the scaffold. Follow-up research is necessary to both further enhance the growth factor content of these scaffolds and to more accurately determined its growth factor contents. At least one study noted that the residual calcium content in DBM interfered with BMP extraction(Honsawek et al., 2005). The scaffolds used in this study consist nearly entirely of calcium compounds, which may have interfered with BMP extraction and the subsequent measurement. A small comparative experiment could determine whether modifications to the protocol, such as taking care to keep the scaffold mostly intact or decalcifying the nodules post-fixing, are necessary. Further research into enhancing the growth factor content could take the form of using a single dose of RA only, trying other compounds, or looking into the physical environment: differentiating the nodules inside a bioreactor could encourage osteogenic differentiation through providing an environment with wall shear stresses. Later,

the loss of BMPs post-decellularization and sterilisation should be determined and the scaffolds can be tested in vivo to determine their osteogenic capacity.

4.3 Scaffold improvement through bisphosphonate addition

The second method of scaffold enhancement was to treat the scaffolds with bisphosphonates before use, intending to use their anti-resorptive function to maximize the initial bone formation. In vivo implantation was used to assess the bone-forming capacity of these scaffolds. Bisphosphonates are most commonly used as anti-osteoporotic medications, but their use in scaffolds is not unprecedented. Ray et al. have coated iron foam scaffolds with zoledronate and found that this increased bone formation at the implantation site(Ray et al., 2018).

Two bisphosphonates, OX14 and Zoledronate, were used in this study. Both are nitrogen-containing bisphosphonates and thus function through the same pathway. Specifically, both bisphosphonates prevent osteoclast function through inhibition of the mevalonate pathway(Rogers et al., 2000). As such, the addition of OX14 and ZOL to HA/CC scaffolds was expected to have a similar effect post-implantation. The main difference is their binding capacity, which is much lower in OX14 compared to ZOL. Lawson et al. proved that the skeletal retention capacity of OX14 is much lower compared to that of ZOL. They did so by administering various bisphosphonates to rats by intraperitoneal injection and measuring the urinary excretion, showing that 47.15±3.85% of OX14 was retained by the skeleton, as opposed to 72.05±3.18% of ZOL. They also showed that OX14 required a dose over three times larger than ZOL to reach a similar bone mass density increase (0.3 and 0.08 µg/kg, respectively)(Lawson et al., 2017). This information led to the hypothesis that OX14 may, in the right dosage, have an equally strong initial effect as ZOL while tapering off more quickly. This could be desirable in order to maximize initial bone formation while lessening the inhibition of remodelling.

While the bisphosphonates were expected to perform similarly at least initially, this was not found to be the case: Bone formation was significantly increased in scaffolds treated with ZOL compared to all other groups, while those treated with OX14 did not differ from PBS-treated control scaffolds. All groups showed significantly larger

callus formation compared to the sham group, which only generated small calluses at day 14 that had completely resorbed by day 28. This confirms the findings by Ray et al. that the addition of zoledronate to bone scaffolds can enhance bone formation. Despite ZOL and OX14 being added in similar proportions as used by Lawson et al., the addition of OX14 had no effect on the amount of bone formation. There are a number of causes for why this concentration may not have been sufficient. The lower calcium binding capacity of OX14 may have caused less of the bisphosphonate to bind through the scaffold, causing the real concentration in the scaffolds to be lower than intended. Alternatively, the lower binding capacity could have made the OX14 be released from the scaffolds too quickly, leading to its effect being lost before the analysis on day 14 post-implantation.

Ideally, multiple concentrations of OX14 and Zoledronate should have been tested. Currently, it cannot be ruled out that a higher concentration of OX14 may have the desired effect, namely increasing the initial bone formation while reducing the effect on bone remodelling compared to ZOL treatment. While treatment with ZOL was successful and increased the bone callus size its concentration may still not have been optimal, though the concentration used is similar to the concentration used by Roy et al. to coat iron scaffolds: Whereas they added 0.61 µg ZOL per mm^3 of scaffold, the concentration used in this study, assuming 100% adsorption of the ZOL by the scaffold, was approximately 0.49 µg/mm^3. Common dosages of ZOL used for osteoporosis treatment are 4-5 mg, roughly equivalent to 6.5-8 cm^3 of Roy et al.'s coated iron scaffold or 8-10 cm^3 of the soaked HA/CC scaffold prepared in this study. Thus, for human-sized critical bone defects the ZOL content may be on the high side, noting that these 4-5 mg are meant to sustain the entire skeleton for extended periods. Other reasons to keep the dosage to a minimum are to prevent the risk of jaw necrosis and undesired inhibition of bone remodelling at later stages of healing. More mouse research should be performed to optimize the concentration of ZOL and test higher concentrations of OX14 to assess whether it can be effective.

Another improvement to the current study would be to determine the medication uptake and release curve for both OX14 and ZOL. Both can be measured in vitro by using UV-VIS spectroscopy. The scaffold adsorption can be determined by measuring

the bisphosphonate solution before and after scaffold soaking. Likewise, the release curve is normally determined by soaking the scaffold in PBS and measuring its absorbance at set time points. Lawson et al. have also tested urine to determine the bisphosphonate excretion. In the present study, neither the uptake nor curve could be determined as the gelatine in the HA/CC interfered with the UV measurements, while urine collection requires catheterisation, which is notoriously difficult in mice. More advanced methods, such as mass spectroscopy, are necessary to determine the true BMP content.

Nevertheless, it was proven that the addition of ZOL to scaffolds can enhance the initial bone formation and will slow down the resorption by day 28. Nitrogen-containing bisphosphonates are known to function through inhibition of the mevalonate pathway in osteoclasts, inhibiting their functioning, which is likely to play a large role in these results. Bisphosphonates have also been shown to affect osteoclasts in other ways, such as the disruption of their cytoskeleton or by initiation of apoptosis (Rogers et al., 2000). Enhancing the bone-forming capacity through an inhibition of bone resorption, Zoledronate may well be a viable addition to scaffolds. Further research is needed to determine optimal concentrations. Another limitation of the current study is the gap between day 1 post-implantation, when there is no callus formation, and day 14, when a large callus has already formed. More insight into the speed with which these calluses form, and the earliest time at which ZOL significantly affects bone formation, would be a useful next step.

A somewhat unusual method of scaffold implantation was chosen for this experiment with the purpose of determining whether this method is viable for the assessment of rapid scaffold osteogenesis. In published research, scaffolds are most commonly implanted either subcutaneously or in a critical-sized bone defect. The former has the disadvantage of the scaffold being far away from the bone and thus far from natural healing mechanisms such as MSC migration. The latter requires surgeries that are often complex and always painful for the animals. It was hypothesized that this new method offers the best of both worlds, as the scaffold is in near proximity to the bone but the bone is not significantly damaged.

There was a significant difference between the Sham group and all other groups. The sham group had little to no callus formation, while all HA/CC-containing groups grew large calluses around the scaffold. As the callus size changed depending on the scaffold properties, in this case the presence of ZOL, the method appears to be suitable for determining the scaffold osteogenicity. Furthermore, the calluses consisted of new bone growth by day 14 but had already been remodelled by day 28, now consisting of cortical bone and bone marrow. This confirms that the implantation method can be used to assess not only the initial bone formation capacity but also the effect of a scaffold on bone remodelling. While not performed over the course of this study, the scaffold size can also be analysed to measure its resorption. It is, therefore, a promising method, involving a procedure that is both easier to perform and less painful for the animals and only requiring a short time period for callus formation. A limitation of this study is that only HA/CC was tested. Thus, in how far the callus formation is caused by the presence of a scaffold versus the HA/CC material remains unclear. A follow-up study with a non-osteoinductive material for comparison, such as titanium or polymer scaffolds, would be valuable in determining the usefulness of this method under different circumstances.

Gene expression analysis was performed in order to assess the effect of HA/CC and bisphosphonates on the expression of osteoblast, osteoclast, and vascular- and nerve-related genes. The expectation is that the presence of HA/CC increases the expression of osteoblast and osteoclast genes, as multiple studies suggest that apatites can attract these cells(Cowan et al., 2005; Ripamonti, 1996). This study found an upregulation of all osteoblast-related genes at days 1 and 28, confirming the findings of literature.

Previous research suggests that bisphosphonates enhance both osteoblast activity and differentiation but have an inhibitory effect on osteoclastogenesis(Maruotti et al., 2012). Contrary to literature, our findings suggest that most of these genes are downregulated on day 1 compared to the HA/CC group, though not always the Sham group, with the exception of OX14 upregulating osteoblast differentiation. 14 days post-implantation, the results start to match literature more closely: The addition of ZOL was shown to activate osteoblast activity as well as osteoclast

differentiation and fusion. OX14 upregulates only osteoblast differentiation at this time point. After 28 days both bisphosphonates upregulate osteoblast differentiation extremely strongly, but they lower the expression of osteoblast activity genes and have little effect on osteoclasts, slightly upregulating some genes and downregulating others.

The effect of HA/CC on vascularisation and innervation is less clear-cut, with many genes that share functions having opposing results at day 1 and 28. It is notable that the HA/CC control and the ZOL group behave very similarly, suggesting that, for the most part, ZOL doesn't strongly affect these genes. By comparison, the OX14 group upregulates PdgfBB and only slightly upregulates PGP9.5. At day 14 there is little effect in most genes and groups. The exceptions are DCC, which is downregulated in all groups, and the OX14 group, which shows downregulation of Pdgfbb and upregulation of PGP9.5. At day 28 the PdgfBB and PGP9.5 are extremely upregulated by ZOL, suggesting that it may activate vascularisation and innervation.

There are a number of general limitations to the study. For one, the materials have been used in a granular form. While this provided some interesting insight, in that the cells can tie together the granules to form a scaffold, these resulting scaffolds are too fragile to use as-is during bone surgeries. The end goal of this research remains to produce 3D-printed porous scaffolds for implantation in humans. 3D-printing the cement has been proven possible in previous research(Shi et al., 2020), but as the shape and size change, many factors will be affected. This includes cell adherence to the scaffold, which would change the ideal cell seeding number. This will both solve problems – large scaffold chunks are less likely to be destroyed by a spinning bioreactor – and add new challenges, such as maintaining cell and nutrient penetration into the scaffold. A number of findings in this study are unlikely to translate well to the culture of 3D scaffolds. This includes the number of cells to seed, the finding that static culture is better for granule culture, and the speed at which cells sufficiently cover the scaffold. A recommendation for future research is, therefore, to focus on 3D-printing the HA/CC scaffolds before determining parameters for decellularization and sterilisation, as both are undoubtedly also affected by the porosity and size of 3D-printed scaffolds.

Further limitations of the study lie in its potential translation to clinical studies in the future. For one, the ratio between HA and CC has been set at 50% for the duration of this study. The HA/CC ratio is yet to be optimised for use in human critical-sized bone defects. The enormous size difference between humans and mice makes mice a suboptimal test animal for these purposes. Large animal testing would be more useful, but due to the expense and animal suffering involved, the scaffolds need to be well-tested before such an experiment. For use in humans, two things must be kept in mind. For one, bones repair themselves at different rates, ranging from 3-4 weeks for the distal radius to 12-24 weeks for the neck of the femur(Prasad, 2021). This likely means that there is not one singular scaffold resorption rate ideal for the human body but that the perfect resorption rate varies based on the injury location. Second, the healing process slows down with age(Clark et al., 2017), which suggests that elderly recipients may need slower-resorbing scaffolds compared to adults and especially children. Further research is necessary to resolve these issues at later stages, and in human clinical trials the location and donor age should be closely monitored.

Despite these limitations, we conclude that HA/CC is a suitable material for bone repair. HA/CC is osteocompatible and bioresorbable, and qPCR results even suggest some innate osteoinductivity. It is suited to mass production by 3D-printing as well, alleviating any scarcity concerns. Furthermore, its osteogenic capacity can be increased through various methods. In future research it would be useful to focus on the structural design of the scaffolds. Both the pore size and structure are highly important for the nutrient flow throughout the scaffolds. In HA/CC scaffolds made from cement there are a number of limitations to this process. For one, the cement is suited to extrusion 3D printing, which generates a continuous line of filament with a minimum practical thickness. Thus, the shapes that can be generated are less complex compared to what can be achieved using metal sintering and certain shapes that have proven beneficial in titanium scaffolds, such as a diamond lattice (Deng et al., 2021), may not be achievable. Additionally, for HA/CC scaffolds it is imperative that any air bubbles can be very reliably removed, as air bubbles can prevent glutaraldehyde from reaching the scaffolds, causing them to be damaged

later on. Nevertheless, there are likely improvements that can be made over the standard square grid lattice, such as a round or honeycomb shape, or a non-uniform scaffold with multiple pore sizes (Roohani-Esfahani et al., 2016), either spread over the entire scaffold or in a directional manner. A scaffold with a structure optimized for both nutrient flow and mechanical strength could make a large difference for the subsequent cell culture and differentiation.

During this study, it was shown that growing umbilical cord MSCs on HA/CC scaffolds led to thick cell growths, strong enough to bind scaffold granules together, that expressed BMPs and possibly created extracellular matrix. The amount of BMPs can be increased through osteogenic differentiation, and while the addition of RA proved detrimental, a short-term exposure or the use of a different compound may still heighten the expression of BMPs and other growth factors. The use of bioreactors, as opposed to static culture, may also prove beneficial as shear stresses have been shown to encourage osteogenic differentiation and mineral deposition onto scaffolds. The amount of growth factors measured may also have been lower than its actual content because of calcium-related interference during BMP extraction, and any future studies into increasing BMP-expression, decellularisation or sterilisation methods should take this into account. Finally, in vivo research would be highly interesting to assess the effect of these growth factors on new bone formation.

Enhancing the scaffolds through the addition of zoledronate was also shown to be a viable pathway for enhancing the bone-forming capacity of HA/CC. Zoledronate increases the callus size both initially and after bone remodelling and thus may lead to accelerated bone repair in patients. In order to confirm this, future research should use a critical-sized defect model to assess the effect of bisphosphonate addition during bone repair. The goal of this study was to address the bone formation capacity of different interventions, and therefore a static condition (a lack of direct mechanical loading on the callus) was used. The use of a critical-sized defect model will include dynamic mechanical loading conditions similar to those received by regular bones, which is expected to further stimulate bone growth due to the positive effect of shear stresses on bone cells, including the encouragement

of osteogenic differentiation and mineral deposition(Marin et al., 2017; Melke et al., 2020). This will better mimic the conditions in which the scaffolds are intended to be used clinically, and provide more information about the usefulness of slower callus resorption in a fracture model. Further research should also take the concentration of the bisphosphonate into account. Zoledronate may have a different optimal concentration than was used in this study, and OX14 could very well have the desired effect at a higher concentration.

To summarize, HA/CC is a suitable material for bone regeneration and both its enhancement via cell-seeding and via bisphosphonate addition are promising avenues for the production of HA/CC scaffolds to be used for the repair of critical-sized defects in humans. Even so, many areas still need to be explored to optimize the osteogenicity. For one, the scaffold design and properties should be further investigated to improve cell attachment and penetration as well as nutrient flow. In cell-seeded scaffolds the effect of varying cell seeding densities and culture conditions on cell proliferation and differentiation should be assessed. Moreover, the growth factor deposition by MSCs can still be increased through various methods, such as changes in the cell culture environment and additions to the culture medium. After this, retaining those growth factors during decellularization and sterilisation will be a priority before finally moving on to in vivo testing.

The use of bisphosphonates to enhance HA/CC scaffolds is promising, showing an increase in callus size formation and reduced bone resorption. First, the dosage must be further investigated to achieve maximum therapeutic effect while minimizing potential side effects. Further research should focus on assessing the effect of rapid callus formation in a critical-sized bone defect model so as to determine its usefulness for critical-sized bone defects in humans and test the materials under dynamic mechanical loading. Additionally, the long-term effects of bisphosphonate-enhanced scaffolds on bone remodeling and bone quality must be studied to ensure safety and efficacy.

Ultimately, the success of scaffolds enhanced through either method depends on their osteogenic capacity, resorption rate, safety, and their practical application in

clinical settings. Both methods are plausible pathways for the enhancement of HA/CC scaffolds that, if successful, could lead to better availability of high-quality bone scaffolds and faster patient recovery time.

Appendix 1

ABClonal	*500 W Cummings Park Ste. 6500, Woburn, MA 01801*
Agar Scientific Ltd	*Unit 7, M11 Business Link, Parsonage Lane, Stansted, Essex CM24 8GF United Kingdom*
Baxter	*1 Baxter Pkwy, Deerfield, IL 60015, USA*
Corning	*One Riverfront Plaza, Corning, NY 14831 USA*
Eppendorf	Eppendorf SE Barkhausenweg 1 22339 Hamburg Germany
Gibco	*1001 S 24th St W Ste 302 Billings, MT 59102, USA*
Hitachi High-Tech	*22610 Gateway Center Drive Suite 100 Clarksburg, Maryland 20871, U.S.A.*
Invitrogen	*168 Third Avenue. Waltham, MA UgSA 02451*
The Jackson Laboratory	600 Main Street, Bar Harbor, ME USA 04609
Matexcel.	*SUITE 210, 17 Ramsey Road, Shirley, NY 11967, USA*
Perkin-Elmer	*940 Winter Street Waltham, MA 02451, USA*
Qiagen	*19300 Germantown Rd Germantown MD 20874 USA*
Quorum	*1 Thomas Cir NW 6th Floor, Washington, DC 20005*
Sigma-Aldrich.	*3050 Spruce St Saint Louis, MO, 63103-2530, USA*
TaKaRa	*2560 and 2570 Orchard Parkway in San Jose, CA*
Thermo Fisher Scientific.	*168 Third Avenue. Waltham, MA USA 02451*

Appendix 2

Linked to	Gene	Forward (5' to 3')	Reverse (5' to 3')
Household	GAPDH	CATCACTGCCACCCAGAAGACTG	ATGCCAGTGAGCTTCCCGTTCAG
Osteoblasts	TGFβ	CCACCTGCAAGACCATCGAC	CTGGCGAGCCTTAGTTTGGAC
	BMP2	GGGACCCGCTGTCTTCTAGT	TCAACTCAAATTCGCTGAGGAC
Vascularization	Pdgfbb	CATCCGCTCCTTTGATGATCTT	GTGCTCGGGTCATGTTCAAGT
	Angiogenin	CCAGGCCCGTTGTTCTTGAT	GCAAACCATTCTCACAGGCAATA
Osteoclast differentiation	CSFR	GTGTCAGAACACTGTAGCCAC	TCAAAGGCAATCTGGCATGAAG
	CSK	CCGAGCGGCTTCTTTACCC	GCATGATACATGATGCGGTAGT
Osteoclast fusion	CCR2	ATCCACGGCATACTATCAACATC	TCGTAGTCATACGGTGTGGTG
	OCSTAMP	CTGTAACGAACTACTGACCCAGC	CCAGGCTTAGGAAGACGAAGA
	CD47	TGGTGGGAAACTACACTTGCG	CGTGCGGTTTTTCAGCTCTAT
	OSTM1	GAGCTGACCGCCTGTATGG	ATGTTTCGGCTGATGTTGTCC
Nerve markers	Netrin1	CAGCCTGATCCTTGCTCGG	GCGGGTTATTGAGGTCGGTG
	PGP9.5	AGGGACAGGAAGTTAGCCCTA	AGCTTCTCCGTTTCAGACAGA
Netrin1 receptor	DCC	CAAGCTGGCTTTTGTACTCTTCG	GAACTCCTCGGTCGGACTCT
Osteoblast differentiation	Osterix	ATGGCGTCCTCTCTGCTTG	TGAAAGGTCAGCGTATGGCTT
	Osteocalcin	CAGACACCATGAGGACCATC	GGACTGAGGCTCTGTGAGGT
	Col1a1	GCTCCTCTTAGGGGCCACT	CCACGTCTCACCATTGGGG

Glossary

Carboxylation	A chemical conversion in which CO2 is added to a compound to create a carboxylic acid
Glial scarring	Scarring of the nervous system, involving astrocyte accumulation
Osteoconductivity	bone formation along the surface of an implanted bone graft scaffold by bone-forming cells, specifically osteoblasts and their progenitors, that migrate from nearby bone tissue
Osteoinductivity	bone formation through the recruitment and stimulation of immature cells
Osteomyelitis	An infection of the bone
Radiculitis	Pain radiating along a nerve caused by inflammation, nerve pinching, or other reasons

References

Abdullah, A., Herdenberg, C., & Hedman, H. (2021). Netrin-1 functions as a suppressor of bone morphogenetic protein (BMP) signaling. *Scientific Reports*, *11*(1). https://doi.org/10.1038/s41598-021-87949-7

Adamzyk, C., Kachel, P., Hoss, M., Gremse, F., Modabber, A., Holzle, F., Tolba, R., Neuss, S., & Lethaus, B. (2016). Bone tissue engineering using polyetherketoneketone scaffolds combined with autologous mesenchymal stem cells in a sheep calvarial defect model. *J Craniomaxillofac Surg*, *44*(8), 985-994. https://doi.org/10.1016/j.jcms.2016.04.012

Ahmed, M., El-Sayed, A., Chen, H., Zhao, R., Yusuf, M., Zuo, Q., Zhang, Y., & Li, B. (2019). Comparison between curcumin and all-trans retinoic acid in the osteogenic differentiation of mouse bone marrow mesenchymal stem cells. *Experimental and Therapeutic Medicine*. https://doi.org/10.3892/etm.2019.7414

Babensee, J. E., McIntire, L. V., & Mikos, A. G. (2000). *Pharmaceutical Research*, *17*(5), 497-504. https://doi.org/10.1023/a:1007502828372

Bae, H. W., Zhao, L., Kanim, L. E. A., Wong, P., Delamarter, R. B., & Dawson, E. G. (2006). Intervariability and Intravariability of Bone Morphogenetic Proteins in Commercially Available Demineralized Bone Matrix Products. *Spine*, *31*(12). https://journals.lww.com/spinejournal/Fulltext/2006/05200/Intervariability_and_Intravariability_of_Bone.4.aspx

Balkan, W., Rodríguez-Gonzalez, M., Pang, M., Fernandez, I., & Troen, B. R. (2011). Retinoic acid inhibits NFATc1 expression and osteoclast differentiation. *J Bone Miner Metab*, *29*(6), 652-661. https://doi.org/10.1007/s00774-011-0261-0

Beck, L. S., Amento, E. P., Xu, Y., Deguzman, L., Lee, W. P., Nguyen, T., & Gillett, N. A. (1993). TGF-beta 1 induces bone closure of skull defects: temporal dynamics of bone formation in defects exposed to rhTGF-beta 1. *J Bone Miner Res*, *8*(6), 753-761. https://doi.org/10.1002/jbmr.5650080614

Ben-David, D., Srouji, S., Shapira-Schweitzer, K., Kossover, O., Ivanir, E., Kuhn, G., Müller, R., Seliktar, D., & Livne, E. (2013). Low dose BMP-2 treatment for bone repair using a PEGylated fibrinogen hydrogel matrix. *Biomaterials*, *34*(12), 2902-2910. https://doi.org/https://doi.org/10.1016/j.biomaterials.2013.01.035

Bergsma, E. J., Rozema, F. R., Bos, R. R. M., & Bruijn, W. C. D. (1993). Foreign body reactions to resorbable poly(l-lactide) bone plates and screws used for the fixation of unstable zygomatic fractures. *Journal of Oral and Maxillofacial Surgery*, *51*(6), 666-670. https://doi.org/https://doi.org/10.1016/S0278-2391(10)80267-8

Betsholtz, C., Lindblom, P., & Gerhardt, H. (2005). Role of pericytes in vascular morphogenesis. *Exs*(94), 115-125. https://doi.org/10.1007/3-7643-7311-3_8

Boyce, B. F. (2013). Advances in the Regulation of Osteoclasts and Osteoclast Functions. *Journal of Dental Research*, *92*(10), 860-867. https://doi.org/10.1177/0022034513500306

Brink, O. (2021). The choice between allograft or demineralized bone matrix is not unambiguous in trauma surgery. *Injury*, *52*, S23-S28. https://doi.org/10.1016/j.injury.2020.11.013

Brydone, A. S., Meek, D., & Maclaine, S. (2010). Bone grafting, orthopaedic biomaterials, and the clinical need for bone engineering. *Proc Inst Mech Eng H*, *224*(12), 1329-1343. https://doi.org/10.1243/09544119jeim770

Burova, I., Wall, I., & Shipley, R. J. (2019). Mathematical and computational models for bone tissue engineering in bioreactor systems. *Journal of Tissue Engineering*, *10*, 204173141982792. https://doi.org/10.1177/2041731419827922

Cahill, K. S., McCormick, P. C., & Levi, A. D. (2015). A comprehensive assessment of the risk of bone morphogenetic protein use in spinal fusion surgery and postoperative cancer diagnosis. *J Neurosurg Spine*, *23*(1), 86-93. https://doi.org/10.3171/2014.10.SPINE14338

Calabrese, G., Franco, D., Petralia, S., Monforte, F., Condorelli, G. G., Squarzoni, S., Traina, F., & Conoci, S. (2021). Dual-Functional Nano-Functionalized Titanium Scaffolds to Inhibit Bacterial Growth and Enhance Osteointegration. *Nanomaterials (Basel)*, *11*(10). https://doi.org/10.3390/nano11102634

Campana, V., Milano, G., Pagano, E., Barba, M., Cicione, C., Salonna, G., Lattanzi, W., & Logroscino, G. (2014). Bone substitutes in orthopaedic surgery: from basic science to clinical practice. *Journal of Materials Science: Materials in Medicine*, *25*(10), 2445-2461. https://doi.org/10.1007/s10856-014-5240-2

Cao, H., Ke, Y., Zhang, Y., Zhang, C. J., Qian, W., & Zhang, G. L. (2012). Icariin stimulates MC3T3-E1 cell proliferation and differentiation through up-regulation of bone morphogenetic protein-2. *Int J Mol Med*, *29*(3), 435-439. https://doi.org/10.3892/ijmm.2011.845

Cappellari, O., Benedetti, S., Innocenzi, A., Francesco, Moreno-Fortuny, A., Ugarte, G., Maria, Messina, G., & Cossu, G. (2013). Dll4 and PDGF-BB Convert Committed Skeletal Myoblasts to Pericytes without Erasing Their Myogenic Memory. *Developmental Cell*, *24*(6), 586-599. https://doi.org/10.1016/j.devcel.2013.01.022

Cartsos, V. M., Zhu, S., & Zavras, A. I. (2008). Bisphosphonate use and the risk of adverse jaw outcomes: a medical claims study of 714,217 people. *J Am Dent Assoc*, *139*(1), 23-30. https://doi.org/10.14219/jada.archive.2008.0016

Caterson, E. J., Nesti, L. J., Danielson, K. G., & Tuan, R. S. (2002). Human Marrow-Derived Mesenchymal Progenitor Cells. *Molecular Biotechnology*, *20*(3), 245-256. https://doi.org/10.1385/mb:20:3:245

Chappuis, V., Gamer, L., Cox, K., Lowery, J. W., Bosshardt, D. D., & Rosen, V. (2012). Periosteal BMP2 activity drives bone graft healing. *Bone*, *51*(4), 800-809. https://doi.org/10.1016/j.bone.2012.07.017

Charalambides, C., Beer, M., & Cobb, A. G. (2005). Poor results after augmenting autograft with xenograft (Surgibone) in hip revision surgery. *Acta Orthopaedica*, *76*(4), 544-549. https://doi.org/10.1080/17453670510041547

Cheng, B. H., Chu, T. M., Chang, C., Kang, H. Y., & Huang, K. E. (2013). Testosterone delivered with a scaffold is as effective as bone morphologic protein-2 in promoting the repair of critical-size segmental defect of femoral bone in mice. *PLOS ONE*, *8*(8), e70234. https://doi.org/10.1371/journal.pone.0070234

Choudhery, M. S., Badowski, M., Muise, A., Pierce, J., & Harris, D. T. (2014). Donor age negatively impacts adipose tissue-derived mesenchymal stem cell expansion and differentiation. *Journal of Translational Medicine*, *12*(1), 8. https://doi.org/10.1186/1479-5876-12-8

Clark, D., Nakamura, M., Miclau, T., & Marcucio, R. (2017). Effects of Aging on Fracture Healing. *Curr Osteoporos Rep*, *15*(6), 601-608. https://doi.org/10.1007/s11914-017-0413-9

Conrad, E. U., Gretch, D. R., Obermeyer, K. R., Moogk, M. S., Sayers, M., Wilson, J. J., & Strong, D. M. (1995). Transmission of the hepatitis-C virus by tissue transplantation. *J Bone Joint Surg Am*, *77*(2), 214-224. https://doi.org/10.2106/00004623-199502000-00007

Conway, J. D., Shabtai, L., Bauernschub, A., & Specht, S. C. (2014). BMP-7 versus BMP-2 for the treatment of long bone nonunion. *Orthopedics*, *37*(12), e1049-1057. https://doi.org/10.3928/01477447-20141124-50

Cowan, C. M., Aalami, O. O., Shi, Y. Y., Chou, Y. F., Mari, C., Thomas, R., Quarto, N., Nacamuli, R. P., Contag, C. H., Wu, B., & Longaker, M. T. (2005). Bone morphogenetic protein 2 and retinoic acid accelerate in vivo bone formation, osteoclast recruitment, and bone turnover. *Tissue Eng*, *11*(3-4), 645-658. https://doi.org/10.1089/ten.2005.11.645

Dacic, S., Kalajzic, I., Visnjic, D., Lichtler, A. C., & Rowe, D. W. (2001). Col1a1-Driven Transgenic Markers of Osteoblast Lineage Progression. *Journal of Bone and Mineral Research*, *16*(7), 1228-1236. https://doi.org/10.1359/jbmr.2001.16.7.1228

Daniel, Alexander, Jeffrey, Thorsten, Ian, Patrick, Thomas, Kerry, Cynthia, & Bethany. (2019). Investigating the Osteoinductive Potential of a Decellularized Xenograft Bone Substitute. *Cells Tissues Organs*, *207*(2), 97-113. https://doi.org/10.1159/000503280

Day, A. G. E., Francis, W. R., Fu, K., Pieper, I. L., Guy, O., & Xia, Z. (2018). Osteogenic Potential of Human Umbilical Cord Mesenchymal Stem Cells on Coralline Hydroxyapatite/Calcium Carbonate Microparticles. *Stem Cells International*, *2018*, 4258613. https://doi.org/10.1155/2018/4258613

Deng, F., Liu, L., Li, Z., & Liu, J. (2021). 3D printed Ti6Al4V bone scaffolds with different pore structure effects on bone ingrowth. *Journal of Biological Engineering*, *15*(1). https://doi.org/10.1186/s13036-021-00255-8

Descalzi Cancedda, F., Gentili, C., Manduca, P., & Cancedda, R. (1992). Hypertrophic chondrocytes undergo further differentiation in culture. *Journal of Cell Biology*, *117*(2), 427-435. https://doi.org/10.1083/jcb.117.2.427

Dimitriou, R., Jones, E., McGonagle, D., & Giannoudis, P. V. (2011). Bone regeneration: current concepts and future directions. *BMC Medicine*, *9*(1), 66. https://doi.org/10.1186/1741-7015-9-66

Distler, T., Fournier, N., Grünewald, A., Polley, C., Seitz, H., Detsch, R., & Boccaccini, A. R. (2020). Polymer-Bioactive Glass Composite Filaments for 3D Scaffold Manufacturing by Fused Deposition Modeling: Fabrication and Characterization. *Front Bioeng Biotechnol*, *8*, 552. https://doi.org/10.3389/fbioe.2020.00552

Dmitriev, A. E., Lehman, R. A., & Symes, A. J. (2011). Bone morphogenetic protein-2 and spinal arthrodesis: the basic science perspective on protein interaction with the nervous system. *The Spine Journal*, *11*(6), 500-505. https://doi.org/https://doi.org/10.1016/j.spinee.2011.05.002

Dun, X.-P., & Parkinson, D. (2017). Role of Netrin-1 Signaling in Nerve Regeneration. *International Journal of Molecular Sciences*, *18*(3), 491. https://doi.org/10.3390/ijms18030491

El Bialy, I., Jiskoot, W., & Reza Nejadnik, M. (2017). Formulation, Delivery and Stability of Bone Morphogenetic Proteins for Effective Bone Regeneration. *Pharmaceutical Research*, *34*(6), 1152-1170. https://doi.org/10.1007/s11095-017-2147-x

Enneking, W., & Campanacci, D. (2001). Retrieved Human Allografts: A Clinicopathological Study. *The Journal of bone and joint surgery. American volume*, *83-A*, 971-986. https://doi.org/10.2106/00004623-200107000-00001

Ford, L., Wolfinbarger, J., Lloyd, S., Jon C., M., Jr., & Laine (2003). *Textured bone allograft, method of making and using same* (United States Patent No. U. S. Patent.

Friedlaender, G. E., Perry, C. R., Cole, J. D., Cook, S. D., Cierny, G., Muschler, G. F., Zych, G. A., Calhoun, J. H., LaForte, A. J., & Yin, S. (2001a). Osteogenic protein-1 (bone morphogenetic protein-7) in the treatment of tibial nonunions. *J Bone Joint Surg Am*, *83-A Suppl 1*(Pt 2), S151-158.

Friedlaender, G. E., Perry, C. R., Cole, J. D., Cook, S. D., Cierny, G., Muschler, G. F., Zych, G. A., Calhoun, J. H., LaForte, A. J., & Yin, S. (2001b). Osteogenic protein-1 (bone morphogenetic protein-7) in the treatment of tibial nonunions. *The Journal of bone*

and joint surgery. American volume, *83-A Suppl 1*(Pt 2), S151-S158. https://pubmed.ncbi.nlm.nih.gov/11314793

https://www.ncbi.nlm.nih.gov/pmc/articles/PMC1425155/

Fu, K., Xu, Q., Czernuszka, J., Triffitt, J. T., & Xia, Z. (2013). Characterization of a biodegradable coralline hydroxyapatite/calcium carbonate composite and its clinical implementation. *Biomed Mater*, *8*(6), 065007. https://doi.org/10.1088/1748-6041/8/6/065007

Fujioka-Kobayashi, M., Kobayashi, E., Schaller, B., Mottini, M., Miron, R. J., & Saulacic, N. (2017). Effect of recombinant human bone morphogenic protein 9 (rhBMP9) loaded onto bone grafts versus barrier membranes on new bone formation in a rabbit calvarial defect model. *Journal of Biomedical Materials Research Part A*, *105*(10), 2655-2661. https://doi.org/10.1002/jbm.a.36125

Gao, T., Lindholm, T., Kommonen, B., Ragni, P., Paronzini, A., Lindholm, T., Jalovaara, P., & Urist, M. (1997). The use of coral composite implant containing bone morphogenetic protein to repair a segmental tibial defect in sheep. *International orthopaedics*, *21*, 194-200. https://doi.org/10.1007/s002640050149

Garg, P., Mazur, M. M., Buck, A. C., Wandtke, M. E., Liu, J., & Ebraheim, N. A. (2017). Prospective Review of Mesenchymal Stem Cells Differentiation into Osteoblasts. *Orthopaedic Surgery*, *9*(1), 13-19. https://doi.org/10.1111/os.12304

Geesink, R. G., de Groot, K., & Klein, C. P. (1988). Bonding of bone to apatite-coated implants. *J Bone Joint Surg Br*, *70*(1), 17-22. https://doi.org/10.1302/0301-620x.70b1.2828374

Gillman, C. E., & Jayasuriya, A. C. (2021). FDA-approved bone grafts and bone graft substitute devices in bone regeneration. *Materials Science and Engineering: C*, *130*, 112466. https://doi.org/https://doi.org/10.1016/j.msec.2021.112466

Gooch, K. J., Kwon, J. H., Blunk, T., Langer, R., Freed, L. E., & Vunjak-Novakovic, G. (2001). Effects of mixing intensity on tissue-engineered cartilage. *Biotechnology and Bioengineering*, *72*(4), 402-407. https://doi.org/10.1002/1097-0290(20000220)72:4<402::aid-bit1002>3.0.co;2-q

Govender, S., Csimma, C., Genant, H. K., Valentin-Opran, A., Amit, Y., Arbel, R., Aro, H., Atar, D., Bishay, M., Börner, M. G., Chiron, P., Choong, P., Cinats, J., Courtenay, B., Feibel, R., Geulette, B., Gravel, C., Haas, N., Raschke, M., . . . Wisniewski, T. (2002). Recombinant human bone morphogenetic protein-2 for treatment of open tibial fractures: a prospective, controlled, randomized study of four hundred and fifty patients. *J Bone Joint Surg Am*, *84*(12), 2123-2134. https://doi.org/10.2106/00004623-200212000-00001

Govindan, R., Kumar, G. S., & Girija, E. K. (2015). Polymer coated phosphate glass/hydroxyapatite composite scaffolds for bone tissue engineering applications [10.1039/C5RA09258B]. *RSC Advances*, *5*(74), 60188-60198. https://doi.org/10.1039/C5RA09258B

Grayson, W. L., Bhumiratana, S., Cannizzaro, C., & Vunjak-Novakovic, G. (2011). Bioreactor Cultivation of Functional Bone Grafts. In (pp. 231-241). Humana Press. https://doi.org/10.1007/978-1-60761-999-4_18

Groeneveld, E., & Burger, E. (2000). Bone morphogenetic proteins in human bone regeneration. *European Journal of Endocrinology*, *142*(1), 9-21. https://doi.org/10.1530/eje.0.1420009

Gruskin, E., Doll, B. A., Futrell, F. W., Schmitz, J. P., & Hollinger, J. O. (2012). Demineralized bone matrix in bone repair: History and use. *Advanced Drug Delivery Reviews*, *64*(12), 1063-1077. https://doi.org/10.1016/j.addr.2012.06.008

Gupta, M., & Gupta, N. (2022). Bisphosphonate Related Jaw Osteonecrosis. In *StatPearls*. StatPearls Publishing

Hall, J., Sorensen, R. G., Wozney, J. M., & Wikesjö, U. M. (2007). Bone formation at rhBMP-2-coated titanium implants in the rat ectopic model. *J Clin Periodontol*, *34*(5), 444-451. https://doi.org/10.1111/j.1600-051X.2007.01064.x

Harada, Y., Itoi, T., Wakitani, S., Irie, H., Sakamoto, M., Zhao, D., Nezu, Y., Yogo, T., Hara, Y., & Tagawa, M. (2012). Effect of Escherichia coli-produced recombinant human bone morphogenetic protein 2 on the regeneration of canine segmental ulnar defects. *Journal of Bone and Mineral Metabolism*, *30*(4), 388-399. https://doi.org/10.1007/s00774-011-0329-x

Hart, N. H., Nimphius, S., Rantalainen, T., Ireland, A., Siafarikas, A., & Newton, R. U. (2017). Mechanical basis of bone strength: influence of bone material, bone structure and muscle action. *J Musculoskelet Neuronal Interact*, *17*(3), 114-139.

Hasegawa, T., Miwa, M., Sakai, Y., Niikura, T., Lee, S. Y., Oe, K., Iwakura, T., Kurosaka, M., & Komori, T. (2010). Efficient Cell-seeding into Scaffolds Improves Bone Formation. *Journal of Dental Research*, *89*(8), 854-859. https://doi.org/10.1177/0022034510370022

He, W., Wu, Z., Wu, Y., Zhong, Z., & Hong, Y. (2021). Construction of the Gypsum-Coated Scaffolds for In Situ Bone Regeneration. *ACS Appl Mater Interfaces*, *13*(27), 31527-31541. https://doi.org/10.1021/acsami.1c08372

Herliansyah, M. K., Hamdi, M., Ide-Ektessabi, A., Wildan, M. W., & Toque, J. A. (2009). The influence of sintering temperature on the properties of compacted bovine hydroxyapatite. *Materials Science and Engineering: C*, *29*(5), 1674-1680. https://doi.org/10.1016/j.msec.2009.01.007

Hess, L. M., Jeter, J. M., Benham-Hutchins, M., & Alberts, D. S. (2008). Factors associated with osteonecrosis of the jaw among bisphosphonate users. *Am J Med*, *121*(6), 475-483.e473. https://doi.org/10.1016/j.amjmed.2008.01.047

Hisada, K., Hata, K., Ichida, F., Matsubara, T., Orimo, H., Nakano, T., Yatani, H., Nishimura, R., & Yoneda, T. (2013). Retinoic acid regulates commitment of undifferentiated mesenchymal stem cells into osteoblasts and adipocytes. *J Bone Miner Metab*, *31*(1), 53-63. https://doi.org/10.1007/s00774-012-0385-x

Hollinger, J. O., Schmitt, J. M., Buck, D. C., Shannon, R., Joh, S.-P., Zegzula, H. D., & Wozney, J. (1998). Recombinant human bone morphogenetic protein-2 and collagen for bone regeneration. *Journal of Biomedical Materials Research*, *43*(4), 356-364. https://doi.org/10.1002/(sici)1097-4636(199824)43:4<356::aid-jbm3>3.0.co;2-7

Honsawek, S., Powers, R. M., & Wolfinbarger, L. (2005). Extractable bone morphogenetic protein and correlation with induced new bone formation in an in vivo assay in the athymic mouse model. *Cell and Tissue Banking*, *6*(1), 13-23. https://doi.org/10.1007/s10561-005-1445-4

Hooper, L. V., Stappenbeck, T. S., Hong, C. V., & Gordon, J. I. (2003). Angiogenins: a new class of microbicidal proteins involved in innate immunity. *Nat Immunol*, *4*(3), 269-273. https://doi.org/10.1038/ni888

Huang, W. (2007). Signaling and transcriptional regulation in osteoblast commitment and differentiation. *Frontiers in Bioscience*, *12*(8-12), 3068. https://doi.org/10.2741/2296

Ishii, T., Ruiz-Torruella, M., Ikeda, A., Shindo, S., Movila, A., Mawardi, H., Albassam, A., Kayal, R. A., Al-Dharrab, A. A., Egashira, K., Wisitrasameewong, W., Yamamoto, K., Mira, A. I., Sueishi, K., Han, X., Taubman, M. A., Miyamoto, T., & Kawai, T. (2018). OC-STAMP promotes osteoclast fusion for pathogenic bone resorption in periodontitis via up-regulation of permissive fusogen CD9. *The FASEB Journal*, *32*(7), 4016-4030. https://doi.org/10.1096/fj.201701424r

John Martin, T., Kong Wah, N., & Nicholson, G. C. (1988). 1 Cell biology of bone. *Baillière's Clinical Endocrinology and Metabolism*, *2*(1), 1-29. https://doi.org/10.1016/s0950-351x(88)80006-5

Kara, A., Gunes, O. C., Albayrak, A. Z., Bilici, G., Erbil, G., & Havitcioglu, H. (2020). Fish scale/poly(3-hydroxybutyrate-co-3-hydroxyvalerate) nanofibrous composite scaffolds for bone regeneration. *Journal of Biomaterials Applications*, *34*(9), 1201-1215. https://doi.org/10.1177/0885328220901987

Kern, S., Eichler, H., Stoeve, J., Klüter, H., & Bieback, K. (2006). Comparative Analysis of Mesenchymal Stem Cells from Bone Marrow, Umbilical Cord Blood, or Adipose Tissue. *Stem Cells*, *24*(5), 1294-1301. https://doi.org/10.1634/stemcells.2005-0342

Khan, U. A., Hashimi, S. M., Bakr, M. M., Forwood, M. R., & Morrison, N. A. (2016). CCL2 and CCR2 are Essential for the Formation of Osteoclasts and Foreign Body Giant Cells. *Journal of Cellular Biochemistry*, *117*(2), 382-389. https://doi.org/10.1002/jcb.25282

Kim, C.-S., Kim, J.-I., Kim, J., Choi, S.-H., Chai, J.-K., Kim, C.-K., & Cho, K.-S. (2005). Ectopic bone formation associated with recombinant human bone morphogenetic proteins-2 using absorbable collagen sponge and beta tricalcium phosphate as carriers. *Biomaterials*, *26*(15), 2501-2507. https://doi.org/https://doi.org/10.1016/j.biomaterials.2004.07.015

Kim, H. K. W., Oxendine, I., & Kamiya, N. (2013). High-concentration of BMP2 reduces cell proliferation and increases apoptosis via DKK1 and SOST in human primary periosteal cells. *Bone*, *54*(1), 141-150. https://doi.org/https://doi.org/10.1016/j.bone.2013.01.031

Kisiel, M., Ventura, M., Oommen, O. P., George, A., Walboomers, X. F., Hilborn, J., & Varghese, O. P. (2012). Critical assessment of rhBMP-2 mediated bone induction: An in vitro and in vivo evaluation. *Journal of Controlled Release*, *162*(3), 646-653. https://doi.org/https://doi.org/10.1016/j.jconrel.2012.08.004

Kjaer, I., & Nolting, D. (2008). Immunohistochemical PGP 9.5 positivity in human osteoblasts may indicate that compensatory and dysplastic craniofacial growth are under control by peripheral nerves. *Orthod Craniofac Res*, *11*(4), 196-200. https://doi.org/10.1111/j.1601-6343.2008.00430.x

Koëter, S., Tigchelaar, S. J., Farla, P., Driessen, L., Van Kampen, A., & Buma, P. (2008). Coralline hydroxyapatite is a suitable bone graft substitute in an intra-articular goat defect model. *Journal of Biomedical Materials Research Part B: Applied Biomaterials*, *90B*(1), 116-122. https://doi.org/10.1002/jbm.b.31260

Koons, G. L., Diba, M., & Mikos, A. G. (2020). Materials design for bone-tissue engineering. *Nature Reviews Materials*, *5*(8), 584-603. https://doi.org/10.1038/s41578-020-0204-2

Lange, S., Heger, J., Euler, G., Wartenberg, M., Piper, H. M., & Sauer, H. (2009). Platelet-derived growth factor BB stimulates vasculogenesis of embryonic stem cell-derived endothelial cells by calcium-mediated generation of reactive oxygen species. *Cardiovascular Research*, *81*(1), 159-168. https://doi.org/10.1093/cvr/cvn258

Lawson, M. A., Ebetino, F. H., Mazur, A., Chantry, A. D., Paton-Hough, J., Evans, H. R., Lath, D., Tsoumpra, M. K., Lundy, M. W., Dobson, R. L., Quijano, M., Kwaasi, A. A., Dunford, J. E., Duan, X., Triffitt, J. T., Jeans, G., & Russell, R. G. G. (2017). The Pharmacological Profile of a Novel Highly Potent Bisphosphonate, OX14 (1-Fluoro-2-(Imidazo-[1,2-α]Pyridin-3-yl)-Ethyl-Bisphosphonate). *Journal of Bone and Mineral Research*, *32*(9), 1860-1869. https://doi.org/10.1002/jbmr.3138

Lechtzier, V., Hutoran, M., Levy, T., Kotler, M., Brenner, T., & Steinitz, M. (2002). Sodium dodecyl sulphate-treated proteins as ligands in ELISA. *J Immunol Methods*, *270*(1), 19-26. https://doi.org/10.1016/s0022-1759(02)00214-4

Li, R. H., & Wozney, J. M. (2001). Delivering on the promise of bone morphogenetic proteins. *Trends in Biotechnology*, *19*(7), 255-265. https://doi.org/https://doi.org/10.1016/S0167-7799(01)01665-1

Li, Z., Gu, X., Lou, S., & Zheng, Y. (2008). The development of binary Mg–Ca alloys for use as biodegradable materials within bone. *Biomaterials*, *29*(10), 1329-1344. https://doi.org/https://doi.org/10.1016/j.biomaterials.2007.12.021

Liang, X., & Song, E. (2020). The role of bone marrow stromal cells in blood diseases and clinical significance as a crucial part of the hematopoietic microenvironment. *Annals of Blood*, *5*, 2-2. https://doi.org/10.21037/aob.2019.12.03

Liu, Y., Liu, Y., Zhang, R., Wang, X., Huang, F., Yan, Z., Nie, M., Huang, J., Wang, Y., Wang, Y., Chen, L., Yin, L., He, B., & Deng, Z. (2014). All-trans retinoic acid modulates bone morphogenic protein 9-induced osteogenesis and adipogenesis of preadipocytes through BMP/Smad and Wnt/β-catenin signaling pathways. *The International Journal of Biochemistry & Cell Biology*, *47*, 47-56. https://doi.org/https://doi.org/10.1016/j.biocel.2013.11.018

Lode, A., Bernhardt, A., & Gelinsky, M. (2008). Cultivation of human bone marrow stromal cells on three-dimensional scaffolds of mineralized collagen: influence of seeding density on colonization, proliferation and osteogenic differentiation. *Journal of Tissue Engineering and Regenerative Medicine*, *2*(7), 400-407. https://doi.org/10.1002/term.110

Lomas, R., Chandrasekar, A., & Board, T. N. (2013). Bone allograft in the U.K.: perceptions and realities. *Hip Int*, *23*(5), 427-433. https://doi.org/10.5301/hipint.5000018

Loozen, L. D., Vandersteen, A., Kragten, A. H., Oner, F. C., Dhert, W. J., Kruyt, M. C., & Alblas, J. (2018). Bone formation by heterodimers through non-viral gene delivery of BMP-2/6 and BMP-2/7. *Eur Cell Mater*, *35*, 195-208. https://doi.org/10.22203/eCM.v035a14

Luo, G., Hofmann, C., Bronckers, A. L., Sohocki, M., Bradley, A., & Karsenty, G. (1995). BMP-7 is an inducer of nephrogenesis, and is also required for eye development and skeletal patterning. *Genes Dev*, *9*(22), 2808-2820. https://doi.org/10.1101/gad.9.22.2808

Luo, X., Chang, H.-M., Yi, Y., Sun, Y., & Leung, P. C. K. (2021). Bone morphogenetic protein 2 inhibits growth differentiation factor 8-induced cell signaling via upregulation of gremlin2 expression in human granulosa-lutein cells. *Reproductive Biology and Endocrinology*, *19*(1), 173. https://doi.org/10.1186/s12958-021-00854-6

Luther, G., Wagner, E. R., Zhu, G., Kang, Q., Luo, Q., Lamplot, J., Bi, Y., Luo, X., Luo, J., Teven, C., Shi, Q., Kim, S. H., Gao, J. L., Huang, E., Yang, K., Rames, R., Liu, X., Li, M., Hu, N., . . . He, T. C. (2011). BMP-9 induced osteogenic differentiation of mesenchymal stem cells: molecular mechanism and therapeutic potential. *Curr Gene Ther*, *11*(3), 229-240. https://doi.org/10.2174/156652311795684777

Lyons, K. M., Hogan, B. L. M., & Robertson, E. J. (1995). Colocalization of BMP 7 and BMP 2 RNAs suggests that these factors cooperatively mediate tissue interactions during murine development. *Mechanisms of Development*, *50*(1), 71-83. https://doi.org/https://doi.org/10.1016/0925-4773(94)00326-I

Maile, L. A., Demambro, V. E., Wai, C., Aday, A. W., Capps, B. E., Beamer, W. G., Rosen, C. J., & Clemmons, D. R. (2011). An essential role for the association of CD47 to SHPS-1 in skeletal remodeling. *Journal of Bone and Mineral Research*, *26*(9), 2068-2081. https://doi.org/10.1002/jbmr.441

Malladi, P., Xu, Y., Yang, G. P., & Longaker, M. T. (2006). Functions of vitamin D, retinoic acid, and dexamethasone in mouse adipose-derived mesenchymal cells. *Tissue Eng*, *12*(7), 2031-2040. https://doi.org/10.1089/ten.2006.12.2031

Mankani, M. H., Kuznetsov, S. A., Fowler, B., Kingman, A., & Gehron Robey, P. (2001). In vivo bone formation by human bone marrow stromal cells: Effect of carrier particle size and shape. *Biotechnology & Bioengineering*, *72*(1), 96-107. https://doi.org/10.1002/1097-0290(20010105)72:1<96::aid-bit13>3.0.co;2-a

Marijanovic, I., Antunovic, M., Matic, I., Panek, M., & Ivkovic, A. (2016). Bioreactor-Based Bone Tissue Engineering. In. InTech. https://doi.org/10.5772/62546

Marín, A. C., Brunelli, M., & Lacroix, D. (2018). Flow perfusion rate modulates cell deposition onto scaffold substrate during cell seeding. *Biomechanics and Modeling in Mechanobiology*, *17*(3), 675-687. https://doi.org/10.1007/s10237-017-0985-4

Marin, A. C., Grossi, T., Bianchi, E., Dubini, G., & Lacroix, D. (2017). µ-Particle tracking velocimetry and computational fluid dynamics study of cell seeding within a 3D porous scaffold. *Journal of the Mechanical Behavior of Biomedical Materials*, *75*, 463-469. https://doi.org/10.1016/j.jmbbm.2017.08.003

Markarian, C. F., Frey, G. Z., Silveira, M. D., Chem, E. M., Milani, A. R., Ely, P. B., Horn, A. P., Nardi, N. B., & Camassola, M. (2014). Isolation of adipose-derived stem cells: a comparison among different methods. *Biotechnology Letters*, *36*(4), 693-702. https://doi.org/10.1007/s10529-013-1425-x

Martin, I., Wendt, D., & Heberer, M. (2004). The role of bioreactors in tissue engineering. *Trends in Biotechnology*, *22*(2), 80-86. https://doi.org/10.1016/j.tibtech.2003.12.001

Maruotti, N., Corrado, A., Neve, A., & Cantatore, F. P. (2012). Bisphosphonates: effects on osteoblast. *European Journal of Clinical Pharmacology*, *68*(7), 1013-1018. https://doi.org/10.1007/s00228-012-1216-7

Maruyama, K., Kawasaki, T., Hamaguchi, M., Hashimoto, M., Furu, M., Ito, H., Fujii, T., Takemura, N., Karuppuchamy, T., Kondo, T., Kawasaki, T., Fukasaka, M., Misawa, T., Saitoh, T., Suzuki, Y., Martino, M. M., Kumagai, Y., & Akira, S. (2016). Bone-protective Functions of Netrin 1 Protein. *Journal of Biological Chemistry*, *291*(46), 23854-23868. https://doi.org/10.1074/jbc.m116.738518

Matsuura, T., Hashimoto, Y., Kinoshita, T., Nishino, K., Nishida, Y., Takigami, J., Katsuda, H., & Shimada, N. (2019). Donor Site Evaluation After Osteochondral Autograft Transplantation for Capitellar Osteochondritis Dissecans. *The American Journal of Sports Medicine*, *47*(12), 2836-2843. https://doi.org/10.1177/0363546519871064

McNamara, I. R. (2010). Impaction bone grafting in revision hip surgery: past, present and future. *Cell Tissue Bank*, *11*(1), 57-73. https://doi.org/10.1007/s10561-009-9147-y

Mediero, A., Ramkhelawon, B., Perez-Aso, M., Moore, K. J., & Cronstein, B. N. (2015). Netrin-1 Is a Critical Autocrine/Paracrine Factor for Osteoclast Differentiation. *Journal of Bone and Mineral Research*, *30*(5), 837-854. https://doi.org/10.1002/jbmr.2421

Mehlen, P., & Furne, C. (2005). Netrin-1: when a neuronal guidance cue turns out to be a regulator of tumorigenesis. *Cellular and Molecular Life Sciences*, *62*(22), 2599-2616. https://doi.org/10.1007/s00018-005-5191-3

Melke, J., Zhao, F., Ito, K., & Hofmann, S. (2020). Orbital seeding of mesenchymal stromal cells increases osteogenic differentiation and bone-like tissue formation. *Journal of Orthopaedic Research*, *38*(6), 1228-1237. https://doi.org/10.1002/jor.24583

Mennan, C., Garcia, J., Roberts, S., Hulme, C., & Wright, K. (2019). A comprehensive characterisation of large-scale expanded human bone marrow and umbilical cord mesenchymal stem cells. *Stem Cell Research & Therapy*, *10*(1). https://doi.org/10.1186/s13287-019-1202-4

Mennan, C., Wright, K., Bhattacharjee, A., Balain, B., Richardson, J., & Roberts, S. (2013). Isolation and Characterisation of Mesenchymal Stem Cells from Different Regions

of the Human Umbilical Cord. *BioMed Research International*, *2013*, 1-8. https://doi.org/10.1155/2013/916136

Mera, P., Ferron, M., & Mosialou, I. (2018). Regulation of Energy Metabolism by Bone-Derived Hormones. *Cold Spring Harbor Perspectives in Medicine*, *8*(6), a031666. https://doi.org/10.1101/cshperspect.a031666

Miyazaki, T., Tanaka, S., Sanjay, A., & Baron, R. (2006). The role of c-Src kinase in the regulation of osteoclast function. *Mod Rheumatol*, *16*(2), 68-74. https://doi.org/10.1007/s10165-006-0460-z

Mohamed-Ahmed, S., Fristad, I., Lie, S. A., Suliman, S., Mustafa, K., Vindenes, H., & Idris, S. B. (2018). Adipose-derived and bone marrow mesenchymal stem cells: a donor-matched comparison. *Stem Cell Research & Therapy*, *9*(1). https://doi.org/10.1186/s13287-018-0914-1

Moonga, B. S., & Dempster, D. W. (2009). Zinc is a potent inhibitor of osteoclastic bone resorption in vitro. *Journal of Bone and Mineral Research*, *10*(3), 453-457. https://doi.org/10.1002/jbmr.5650100317

Mroz, T. E., Wang, J. C., Hashimoto, R., & Norvell, D. C. (2010). Complications related to osteobiologics use in spine surgery: a systematic review. *Spine (Phila Pa 1976)*, *35*(9 Suppl), S86-104. https://doi.org/10.1097/BRS.0b013e3181d81ef2

Murphy, C. M., & O'Brien, F. J. (2010). Understanding the effect of mean pore size on cell activity in collagen-glycosaminoglycan scaffolds. *Cell adhesion & migration*, *4*(3), 377-381. https://doi.org/10.4161/cam.4.3.11747

Myllylä, R. M., Haapasaari, K.-M., Lehenkari, P., & Tuukkanen, J. (2014). Bone morphogenetic proteins 4 and 2/7 induce osteogenic differentiation of mouse skin derived fibroblast and dermal papilla cells. *Cell and Tissue Research*, *355*(2), 463-470. https://doi.org/10.1007/s00441-013-1745-0

Nakashima, K., Zhou, X., Kunkel, G., Zhang, Z., Deng, J. M., Behringer, R. R., & De Crombrugghe, B. (2002). The Novel Zinc Finger-Containing Transcription Factor Osterix Is Required for Osteoblast Differentiation and Bone Formation. *Cell*, *108*(1), 17-29. https://doi.org/10.1016/s0092-8674(01)00622-5

Nevins, M., Kirker-Head, C., Nevins, M., Wozney, J. A., Palmer, R., & Graham, D. (1996). Bone formation in the goat maxillary sinus induced by absorbable collagen sponge implants impregnated with recombinant human bone morphogenetic protein-2. *Int J Periodontics Restorative Dent*, *16*(1), 8-19.

Nguyen, H., Morgan, D. A. F., & Forwood, M. R. (2007). Sterilization of allograft bone: effects of gamma irradiation on allograft biology and biomechanics. *Cell and Tissue Banking*, *8*(2), 93-105. https://doi.org/10.1007/s10561-006-9020-1

Niinomi, M., Liu, Y., Nakai, M., Liu, H., & Li, H. (2016). Biomedical titanium alloys with Young's moduli close to that of cortical bone. *Regen Biomater*, *3*(3), 173-185. https://doi.org/10.1093/rb/rbw016

Nirmala, F. S., Lee, H., Kim, J. S., Ha, T., Jung, C. H., & Ahn, J. (2020). Green Tomato Extract Prevents Bone Loss in Ovariectomized Rats, a Model of Osteoporosis. *Nutrients*, *12*(10). https://doi.org/10.3390/nu12103210

O'Dea, R., Byrne, H., & Waters, S. (2012). Continuum Modelling of In Vitro Tissue Engineering: A Review. In (pp. 229-266). Springer Berlin Heidelberg. https://doi.org/10.1007/8415_2012_140

Panda, S., Biswas, C. K., & Paul, S. (2021). A comprehensive review on the preparation and application of calcium hydroxyapatite: A special focus on atomic doping methods for bone tissue engineering. *Ceramics International*, *47*(20), 28122-28144. https://doi.org/https://doi.org/10.1016/j.ceramint.2021.07.100

Park, Y. J., Ku, Y., Chung, C. P., & Lee, S. J. (1998). Controlled release of platelet-derived growth factor from porous poly(l-lactide) membranes for guided tissue

regeneration. *Journal of Controlled Release*, *51*(2), 201-211. https://doi.org/https://doi.org/10.1016/S0168-3659(97)00169-7
Pata, M., & Vacher, J. (2018). Ostm1 Bifunctional Roles in Osteoclast Maturation: Insights From a Mouse Model Mimicking a Human OSTM1 Mutation. *Journal of Bone and Mineral Research*, *33*(5), 888-898. https://doi.org/10.1002/jbmr.3378
Pereira, H. F., Cengiz, I. F., Silva, F. S., Reis, R. L., & Oliveira, J. M. (2020). Scaffolds and coatings for bone regeneration. *Journal of Materials Science: Materials in Medicine*, *31*(3). https://doi.org/10.1007/s10856-020-06364-y
Perić Kačarević, Z., Kavehei, F., Houshmand, A., Franke, J., Smeets, R., Rimashevskiy, D., Wenisch, S., Schnettler, R., Jung, O., & Barbeck, M. (2018). Purification processes of xenogeneic bone substitutes and their impact on tissue reactions and regeneration. *The International Journal of Artificial Organs*, *41*(11), 789-800. https://doi.org/10.1177/0391398818771530
Pietrzak, W. S., Woodell-May, J., & McDonald, N. (2006). Assay of bone morphogenetic protein-2, -4, and -7 in human demineralized bone matrix. *J Craniofac Surg*, *17*(1), 84-90. https://doi.org/10.1097/01.scs.0000179745.91165.73
Pobloth, A.-M., Checa, S., Razi, H., Petersen, A., Weaver, J. C., Schmidt-Bleek, K., Windolf, M., Tatai, A. Á., Roth, C. P., Schaser, K.-D., Duda, G. N., & Schwabe, P. (2018). Mechanobiologically optimized 3D titanium-mesh scaffolds enhance bone regeneration in critical segmental defects in sheep. *Science Translational Medicine*, *10*(423), eaam8828. https://doi.org/10.1126/scitranslmed.aam8828
Prasad, A. (2021). State of art review on bioabsorbable polymeric scaffolds for bone tissue engineering. *Materials Today: Proceedings*, *44*, 1391-1400. https://doi.org/https://doi.org/10.1016/j.matpr.2020.11.622
Pyatibratov, M. G., & Kostyukova, A. S. (2012). New Insights into the Role of Angiogenin in Actin Polymerization. In (pp. 175-198). Elsevier. https://doi.org/10.1016/b978-0-12-394306-4.00011-3
Qi, L., Liu, Y., Li, H., & Zhang, Y. (2014). Results of 10-year follow-up of the iliac donor site of graft patients. *J Int Med Res*, *42*(6), 1348-1352. https://doi.org/10.1177/0300060514550351
Ray, S., Thormann, U., Eichelroth, M., Budak, M., Biehl, C., Rupp, M., Sommer, U., El Khassawna, T., Alagboso, F. I., Kampschulte, M., Rohnke, M., Henß, A., Peppler, K., Linke, V., Quadbeck, P., Voigt, A., Stenger, F., Karl, D., Schnettler, R., . . . Alt, V. (2018). Strontium and bisphosphonate coated iron foam scaffolds for osteoporotic fracture defect healing. *Biomaterials*, *157*, 1-16. https://doi.org/10.1016/j.biomaterials.2017.11.049
Rebelatto, C. K., Aguiar, A. M., Moretão, M. P., Senegaglia, A. C., Hansen, P., Barchiki, F., Oliveira, J., Martins, J., Kuligovski, C., Mansur, F., Christofis, A., Amaral, V. F., Brofman, P. S., Goldenberg, S., Nakao, L. S., & Correa, A. (2008). Dissimilar Differentiation of Mesenchymal Stem Cells from Bone Marrow, Umbilical Cord Blood, and Adipose Tissue. *Experimental Biology and Medicine*, *233*(7), 901-913. https://doi.org/10.3181/0712-rm-356
Rezwan, K., Chen, Q. Z., Blaker, J. J., & Boccaccini, A. R. (2006). Biodegradable and bioactive porous polymer/inorganic composite scaffolds for bone tissue engineering. *Biomaterials*, *27*(18), 3413-3431. https://doi.org/https://doi.org/10.1016/j.biomaterials.2006.01.039
Ripamonti, U. (1996). Osteoinduction in porous hydroxyapatite implanted in heterotopic sites of different animal models. *Biomaterials*, *17*(1), 31-35. https://doi.org/10.1016/0142-9612(96)80752-6

Ripamonti, U., Crooks, J., Khoali, L., & Roden, L. (2009). The induction of bone formation by coral-derived calcium carbonate/hydroxyapatite constructs. *Biomaterials*, *30*(7), 1428-1439. https://doi.org/10.1016/j.biomaterials.2008.10.065

Roa, L. A., Bloemen, M., Carels, C. E. L., Wagener, F. A. D. T. G., & Von den Hoff, J. W. (2019). Retinoic acid disrupts osteogenesis in pre-osteoblasts by down-regulating WNT signaling. *The International Journal of Biochemistry & Cell Biology*, *116*, 105597. https://doi.org/https://doi.org/10.1016/j.biocel.2019.105597

Rogers, M. J., Gordon, S., Benford, H. L., Coxon, F. P., Luckman, S. P., Monkkonen, J., & Frith, J. C. (2000). Cellular and molecular mechanisms of action of bisphosphonates. *Cancer*, *88*(12 Suppl), 2961-2978. https://doi.org/10.1002/1097-0142(20000615)88:12+<2961::aid-cncr12>3.3.co;2-c

Rogers, M. J., Mönkkönen, J., & Munoz, M. A. (2020). Molecular mechanisms of action of bisphosphonates and new insights into their effects outside the skeleton. *Bone*, *139*, 115493. https://doi.org/https://doi.org/10.1016/j.bone.2020.115493

Roohani-Esfahani, S.-I., Newman, P., & Zreiqat, H. (2016). Design and Fabrication of 3D printed Scaffolds with a Mechanical Strength Comparable to Cortical Bone to Repair Large Bone Defects. *Scientific Reports*, *6*(1), 19468. https://doi.org/10.1038/srep19468

Roosa, S. M. M., Kemppainen, J. M., Moffitt, E. N., Krebsbach, P. H., & Hollister, S. J. (2010). The pore size of polycaprolactone scaffolds has limited influence on bone regeneration in anin vivomodel. *Journal of Biomedical Materials Research Part A*, *92A*(1), 359-368. https://doi.org/10.1002/jbm.a.32381

Santhanam, L., Liu, G., Jandu, S., Su, W., Wodu, B. P., Savage, W., Poe, A., Liu, X., Alexander, L. M., Cao, X., & Wan, M. (2021). Skeleton-secreted PDGF-BB mediates arterial stiffening. *J Clin Invest*, *131*(20). https://doi.org/10.1172/jci147116

Sato, T., Kokabu, S., Enoki, Y., Hayashi, N., Matsumoto, M., Nakahira, M., Sugasawa, M., & Yoda, T. (2017). Functional Roles of Netrin-1 in Osteoblast Differentiation. *In Vivo*, *31*(3), 321-328. https://doi.org/10.21873/invivo.11062

Savolainen, S., Usenius, J. P., & Hernesniemi, J. (1994). Iliac crest versus artificial bone grafts in 250 cervical fusions. *Acta Neurochirurgica*, *129*(1-2), 54-57. https://doi.org/10.1007/bf01400873

Schmitt, J. M., Hwang, K., Winn, S. R., & Hollinger, J. O. (1999). Bone morphogenetic proteins: An update on basic biology and clinical relevance. *Journal of Orthopaedic Research*, *17*(2), 269-278. https://doi.org/10.1002/jor.1100170217

Schneider, S., Unger, M., Van Griensven, M., & Balmayor, E. R. (2017). Adipose-derived mesenchymal stem cells from liposuction and resected fat are feasible sources for regenerative medicine. *European Journal of Medical Research*, *22*(1). https://doi.org/10.1186/s40001-017-0258-9

Schwartz, Z., Somers, A., Mellonig, J. T., Carnes, D. L., Jr., Dean, D. D., Cochran, D. L., & Boyan, B. D. (1998). Ability of commercial demineralized freeze-dried bone allograft to induce new bone formation is dependent on donor age but not gender. *J Periodontol*, *69*(4), 470-478. https://doi.org/10.1902/jop.1998.69.4.470

Seebach, C., Schultheiss, J., Wilhelm, K., Frank, J., & Henrich, D. (2010). Comparison of six bone-graft substitutes regarding to cell seeding efficiency, metabolism and growth behaviour of human mesenchymal stem cells (MSC) in vitro. *Injury*, *41*(7), 731-738. https://doi.org/https://doi.org/10.1016/j.injury.2010.02.017

Servin-Trujillo, M. A., Reyes-Esparza, J. A., Garrido, F., Ntilde, A, G., Flores-Gazca, E., Osuna-Martinez, U., & Rodriguez-Fragoso, L. (2011). Use of a Graft of Demineralized Bone Matrix Along with TGF-β1 Leads to an Early Bone Repair in Dogs. *Journal of Veterinary Medical Science*, *73*(9), 1151-1161. https://doi.org/10.1292/jvms.10-0155

Shao, J., Wang, Z., Yang, T., Ying, H., Zhang, Y., & Liu, S. (2015). Bone Regulates Glucose Metabolism as an Endocrine Organ through Osteocalcin. *International Journal of Endocrinology*, *2015*, 1-9. https://doi.org/10.1155/2015/967673

Shestenko, O. P., Nikonov, S. D., & Mertvetsov, N. P. (2001). [Angiogenin and its role in angiogenesis]. *Mol Biol (Mosk)*, *35*(3), 349-371. (Angiogenin i ego rol' v angiogeneze.)

Shi, Y. (2017). *Allografts combined with tissue derived stem cells for bone healing* (United States Patent No. U. S. Patent.

Shi, Y., He, R., Deng, X., Shao, Z., Deganello, D., Yan, C., & Z., X. (2020). Three-dimensional biofabrication of an aragoniteenriched self-hardening bone graft substitute and assessment of its osteogenicity in vitro and in vivo. *Biomaterials Translational*, *1*(1), 69-81. https://doi.org/10.3877/cma.j.issn.2096-112X.2020.01.007

Simonds, R. J., Holmberg, S. D., Hurwitz, R. L., Coleman, T. R., Bottenfield, S., Conley, L. J., Kohlenberg, S. H., Castro, K. G., Dahan, B. A., Schable, C. A., & et al. (1992). Transmission of human immunodeficiency virus type 1 from a seronegative organ and tissue donor. *N Engl J Med*, *326*(11), 726-732. https://doi.org/10.1056/nejm199203123261102

Sinha, K. M., & Zhou, X. (2013). Genetic and molecular control of osterix in skeletal formation. *Journal of Cellular Biochemistry*, *114*(5), 975-984. https://doi.org/10.1002/jcb.24439

Siqueira, E. B., & Kranzler, L. I. (1982). Cervical interbody fusion using calf bone. *Surgical Neurology*, *18*(1), 37-39. https://doi.org/10.1016/0090-3019(82)90010-6

Skillington, J., Choy, L., & Derynck, R. (2002). Bone morphogenetic protein and retinoic acid signaling cooperate to induce osteoblast differentiation of preadipocytes. *J Cell Biol*, *159*(1), 135-146. https://doi.org/10.1083/jcb.200204060

Squillaro, T., Peluso, G., & Galderisi, U. (2016). Clinical Trials with Mesenchymal Stem Cells: An Update. *Cell Transplantation*, *25*(5), 829-848. https://doi.org/10.3727/096368915x689622

Steijvers, E., Ghei, A., & Xia, Z. (2022). Manufacturing artificial bone allografts: a perspective. *Biomater Transl*, *3*(1), 65-80. https://doi.org/10.12336/biomatertransl.2022.01.007

T, A., & C, J. (2001). Osteoinduction, osteoconduction and osseointegration. *European Spine Journal*, *10*(0), S96-S101. https://doi.org/10.1007/s005860100282

Takizawa, T., Nakayama, N., Haniu, H., Aoki, K., Okamoto, M., Nomura, H., Tanaka, M., Sobajima, A., Yoshida, K., Kamanaka, T., Ajima, K., Oishi, A., Kuroda, C., Ishida, H., Okano, S., Kobayashi, S., Kato, H., & Saito, N. (2018). Titanium Fiber Plates for Bone Tissue Repair. *Advanced Materials*, *30*(4), 1703608. https://doi.org/10.1002/adma.201703608

Tello-Montoliu, A., Patel, J. V., & Lip, G. Y. H. (2006). Angiogenin: a review of the pathophysiology and potential clinical applications. *Journal of Thrombosis and Haemostasis*, *4*(9), 1864-1874. https://doi.org/10.1111/j.1538-7836.2006.01995.x

Temple, J. P., Yeager, K., Bhumiratana, S., Vunjak-Novakovic, G., & Grayson, W. L. (2013). Bioreactor Cultivation of Anatomically Shaped Human Bone Grafts. In (pp. 57-78). Springer New York. https://doi.org/10.1007/7651_2013_33

Tenkumo, T., Vanegas Sáenz, J. R., Nakamura, K., Shimizu, Y., Sokolova, V., Epple, M., Kamano, Y., Egusa, H., Sugaya, T., & Sasaki, K. (2018). Prolonged release of bone morphogenetic protein-2 in vivo by gene transfection with DNA-functionalized calcium phosphate nanoparticle-loaded collagen scaffolds. *Mater Sci Eng C Mater Biol Appl*, *92*, 172-183. https://doi.org/10.1016/j.msec.2018.06.047

Tsuji, K., Bandyopadhyay, A., Harfe, B. D., Cox, K., Kakar, S., Gerstenfeld, L., Einhorn, T., Tabin, C. J., & Rosen, V. (2006). BMP2 activity, although dispensable for bone

formation, is required for the initiation of fracture healing. *Nat Genet*, *38*(12), 1424-1429. https://doi.org/10.1038/ng1916

Tsuruga, E., Takita, H., Itoh, H., Wakisaka, Y., & Kuboki, Y. (1997). Pore Size of Porous Hydroxyapatite as the Cell-Substratum Controls BMP-Induced Osteogenesis. *Journal of Biochemistry*, *121*(2), 317-324. https://doi.org/10.1093/oxfordjournals.jbchem.a021589

Vantler, M., Karikkineth, B. C., Naito, H., Tiburcy, M., Didié, M., Nose, M., Rosenkranz, S., & Zimmermann, W. H. (2010). PDGF-BB protects cardiomyocytes from apoptosis and improves contractile function of engineered heart tissue. *J Mol Cell Cardiol*, *48*(6), 1316-1323. https://doi.org/10.1016/j.yjmcc.2010.03.008

Vetsch, J. R., Müller, R., & Hofmann, S. (2015). The evolution of simulation techniques for dynamic bone tissue engineering in bioreactors. *J Tissue Eng Regen Med*, *9*(8), 903-917. https://doi.org/10.1002/term.1733

Vunjak-Novakovic, G., Obradovic, B., Martin, I., Bursac, P. M., Langer, R., & Freed, L. E. (1998). Dynamic Cell Seeding of Polymer Scaffolds for Cartilage Tissue Engineering. *Biotechnology Progress*, *14*(2), 193-202. https://doi.org/10.1021/bp970120j

Wang, A., Ding, X., Sheng, S., & Yao, Z. (2008). Retinoic acid inhibits osteogenic differentiation of rat bone marrow stromal cells. *Biochem Biophys Res Commun*, *375*(3), 435-439. https://doi.org/10.1016/j.bbrc.2008.08.036

Warren, G. L., Hulderman, T., Mishra, D., Gao, X., Millecchia, L., O'Farrell, L., Kuziel, W. A., & Simeonova, P. P. (2005). Chemokine receptor CCR2 involvement in skeletal muscle regeneration. *Faseb j*, *19*(3), 413-415. https://doi.org/10.1096/fj.04-2421fje

Weber, F. E. (2019). Reconsidering Osteoconduction in the Era of Additive Manufacturing. *Tissue Eng Part B Rev*, *25*(5), 375-386. https://doi.org/10.1089/ten.TEB.2019.0047

Weng, Z., Wang, C., Zhang, C., Xu, J., Chai, Y., Jia, Y., Han, P., & Wen, G. (2019). All-Trans Retinoic Acid Promotes Osteogenic Differentiation and Bone Consolidation in a Rat Distraction Osteogenesis Model. *Calcified Tissue International*, *104*(3), 320-330. https://doi.org/10.1007/s00223-018-0501-6

Werner, M., Petersen, A., Kurniawan, N. A., & Bouten, C. V. C. (2019). Cell‐Perceived Substrate Curvature Dynamically Coordinates the Direction, Speed, and Persistence of Stromal Cell Migration. *Advanced Biosystems*, *3*(10), 1900080. https://doi.org/10.1002/adbi.201900080

Westas, E., Gillstedt, M., Lonn-Stensrud, J., Bruzell, E., & Andersson, M. (2014). Biofilm formation on nanostructured hydroxyapatite-coated titanium. *J Biomed Mater Res A*, *102*(4), 1063-1070. https://doi.org/10.1002/jbm.a.34757

Wilson, C. E., Dhert, W. J. A., Van Blitterswijk, C. A., Verbout, A. J., & De Bruijn, J. D. (2002). **Evaluating 3D bone tissue engineered constructs with different seeding densities using the alamarBlue™ assay and the effect on in vivo bone formation**. *Journal of Materials Science: Materials in Medicine*, *13*(12), 1265-1269. https://doi.org/10.1023/a:1021139415528

Xia, Z., Shi, Y., He, H., Pan, Y., & Liu, C. (2018). Development of Biodegradable Bone Graft Substitutes Using 3D Printing. In (pp. 517-545). Springer Singapore. https://doi.org/10.1007/978-981-10-5975-9_13

Yamashita, T., Kollmannsberger, P., Mawatari, K., Kitamori, T., & Vogel, V. (2016). Cell sheet mechanics: How geometrical constraints induce the detachment of cell sheets from concave surfaces. *Acta Biomaterialia*, *45*, 85-97. https://doi.org/https://doi.org/10.1016/j.actbio.2016.08.044

Yang, N., Zhong, Q., Zhou, Y., Kundu, S. C., Yao, J., & Cai, Y. (2016). Controlled degradation pattern of hydroxyapatite/calcium carbonate composite microspheres. *Microsc Res Tech*, *79*(6), 518-524. https://doi.org/10.1002/jemt.22661

Yuan, H., Kurashina, K., de Bruijn, J. D., Li, Y., de Groot, K., & Zhang, X. (1999). A preliminary study on osteoinduction of two kinds of calcium phosphate ceramics. *Biomaterials*, *20*(19), 1799-1806. https://doi.org/10.1016/s0142-9612(99)00075-7

Zeddou, M., Briquet, A., Relic, B., Josse, C., Malaise, M. G., Gothot, A., Lechanteur, C., & Beguin, Y. (2010). The umbilical cord matrix is a better source of mesenchymal stem cells (MSC) than the umbilical cord blood. *Cell Biology International*, *34*(7), 693-701. https://doi.org/10.1042/cbi20090414

Zhang, J., Liu, H., Ding, J.-X., Wu, J., Zhuang, X.-L., Chen, X.-S., Wang, J.-C., Yin, J.-B., & Li, Z.-M. (2016). High-Pressure Compression-Molded Porous Resorbable Polymer/Hydroxyapatite Composite Scaffold for Cranial Bone Regeneration. *ACS Biomaterials Science & Engineering*, *2*(9), 1471-1482. https://doi.org/10.1021/acsbiomaterials.6b00202

Zhang, J. M., Feng, F. E., Wang, Q. M., Zhu, X. L., Fu, H. X., Xu, L. P., Liu, K. Y., Huang, X. J., & Zhang, X. H. (2016). Platelet-Derived Growth Factor-BB Protects Mesenchymal Stem Cells (MSCs) Derived From Immune Thrombocytopenia Patients Against Apoptosis and Senescence and Maintains MSC-Mediated Immunosuppression. *Stem Cells Transl Med*, *5*(12), 1631-1643. https://doi.org/10.5966/sctm.2015-0360

Zhang, S., Chen, X., Hu, Y., Wu, J., Cao, Q., Chen, S., & Gao, Y. (2016). All-trans retinoic acid modulates Wnt3A-induced osteogenic differentiation of mesenchymal stem cells via activating the PI3K/AKT/GSK3β signalling pathway. *Mol Cell Endocrinol*, *422*, 243-253. https://doi.org/10.1016/j.mce.2015.12.018

Zhang, W., Deng, Z. L., Chen, L., Zuo, G. W., Luo, Q., Shi, Q., Zhang, B. Q., Wagner, E. R., Rastegar, F., Kim, S. H., Jiang, W., Shen, J., Huang, E., Gao, Y., Gao, J. L., Zhou, J. Z., Luo, J., Huang, J., Luo, X., . . . He, B. C. (2010). Retinoic acids potentiate BMP9-induced osteogenic differentiation of mesenchymal progenitor cells. *PLOS ONE*, *5*(7), e11917. https://doi.org/10.1371/journal.pone.0011917

Zhang, Z. Y., Teoh, S. H., Chong, M. S., Schantz, J. T., Fisk, N. M., Choolani, M. A., & Chan, J. (2009). Superior osteogenic capacity for bone tissue engineering of fetal compared with perinatal and adult mesenchymal stem cells. *Stem Cells*, *27*(1), 126-137. https://doi.org/10.1634/stemcells.2008-0456

Zhao, J., Ohba, S., Shinkai, M., Chung, U. I., & Nagamune, T. (2008). Icariin induces osteogenic differentiation in vitro in a BMP- and Runx2-dependent manner. *Biochem Biophys Res Commun*, *369*(2), 444-448. https://doi.org/10.1016/j.bbrc.2008.02.054

Zhou, Y. F., Sae-Lim, V., Chou, A. M., Hutmacher, D. W., & Lim, T. M. (2006). Does seeding density affectin vitro mineral nodules formation in novel composite scaffolds? *Journal of Biomedical Materials Research Part A*, *78A*(1), 183-193. https://doi.org/10.1002/jbm.a.30685

Zuo, W., Yu, L., Lin, J., Yang, Y., & Fei, Q. (2021). Properties improvement of titanium alloys scaffolds in bone tissue engineering: a literature review. *Annals of Translational Medicine*, *9*(15), 1259-1259. https://doi.org/10.21037/atm-20-8175